3D hydrological simulation of a forested headwater catchment: Spatio-temporal validation and scale dependent parameterization

Dissertation

zur

Erlangung des Doktorgrades (Dr. rer. nat.)

der

Mathematisch-Naturwissenschaftlichen Fakultät

der

Rheinischen Friedrich-Wilhelms-Universität Bonn

vorgelegt von

Zhufeng Fang

aus

Shenyang, China

Bonn 2016

Angefertigt mit Genehmigung der Mathematisch-Naturwissenschaftlichen

Fakultät der Rheinischen Friedrich-Wilhelms-Universität Bonn

1. Gutachter: Prof. Harry Vereecken
2. Gutachter: Prof. Bernd Diekkrüger

Tag der Promotion: September 14, 2016

Erscheinungsjahr: 2016

Abstract

Soil moisture plays a key role in the water and energy balance in soil, vegetation and atmosphere systems. There is a grand need to increase global-scale hyper-resolution water-energy-biogeochemistry land surface modelling capabilities. High reliability simulation of soil water content using various kinds of numerical modeling tools has been studied in recent years. Multiple methods have been applied for more accurate parameterizations. In distributed hydrological modelling one often faces the problem that input data need to be aggregated to match the model resolution. However, aggregated data may be too coarse for the parametrization of the processes represented. This dilemma can be circumvented by the adjustment of certain model parameters. Unfortunately, it is not clear how to parameterize hydrological processes as a function of scale, and how to test deterministic models with regard to epistemic uncertainties.

In this study, high resolution long-term simulations were conducted in the highly instrumented TERENO hydrological observatory of the Wüstebach catchment. Soil hydraulic parameters were derived using inverse modeling with the Hydrus-1D model using the global optimization scheme SCE-UA and soil moisture data from a wireless soil moisture sensor network. The estimated parameters were then used for 3D simulations of water transport using the integrated parallel simulation platform ParFlow-CLM. The simulated soil moisture dynamics, as well as evapotranspiration (ET) and runoff, were compared with long-term field observations to illustrate how well the model was able to reproduce the water budget dynamics. Different anisotropies of hydraulic conductivity were investigated to analyze how fast lateral flow processes above the underlying bedrock affect the simulation results. For a detail investigation of the model results the empirical orthogonal function (EOF) and wavelet coherence methods were applied. The EOF analysis of temporal-spatial patterns of simulated

and observed soil moisture revealed that introduction of heterogeneity in the soil porosity effectively improves estimates of soil moisture patterns. The wavelet coherence analysis indicates that wet and dry seasons have significant effect on temporal correlation between observed and simulated soil moisture and ET. This study demonstrates the usefulness of the EOF and wavelet coherence methods for a more in-depth validation of spatially highly resolved hydrological 3D models.

To further investigate how the reduction of local hydraulic gradients due to spatial aggregation can be partially compensated by increasing soil hydraulic conductivity. Information entropy concept was employed for the scale dependent parameterization of soil hydraulic conductivity. The loss of information content of terrain curvature as consequence of spatial aggregation was used to determine an amplification factor for soil hydraulic conductivity to compensate the resulting retardation of water flow. To test the usefulness of this approach, continuous 3D hydrological simulations were conducted with different spatial resolutions in the highly instrumented Wüstebach catchment. The results indicated that the introduction of an amplification factor can effectively improve model performances both in terms of soil moisture and runoff simulation. However, comparing simulated soil moisture pattern with observation indicated that uniform application of an amplification factor can lead to local overcorrection of soil hydraulic conductivity. This problem could be circumvented by applying the amplification factor only to model grid cells that suffer from high information loss. To this end, two schemes were developed to define appropriate location-specific correction factors. Both schemes led to improved model performance both in terms of soil water content and runoff simulation. Thus, the proposed scaling approach is useful for the application of next-generation hyper-resolution global land surface models.

Then the output of Parflow-CLM simulated pressure was put into a particle tracking simulation platform SLIM-FAST to investigate the water particle migration and transit time distribution (TTD) at the Wüstebach testing site. Different model scenarios were conducted to investigate the effect of number of initial particles, dispersion parameters and hydraulic parameter upscaling schemes. A stable isotope tracer model TRANSEP was used in simulation of TTD for comparison purpose. Our results indicate that: 1) the initial number of water particles has no effect on TTD, unless the initial number exceeds a very high amount. 2) Higher α_L leads to higher TTD, a 0.002 m α_L gives best agreement with model TRANSEP. 3) Global and localized amplification factor applications lead to mixed results in estimates of transit time distribution and central location of particles plume. TTD estimation using particle tracking codes like SLIM-FAST can provide insight of the evaluation of 3D hydrological models like Parflow-CLM with respect to the correct parametrization of hydrological properties and the representation of water flow pathways.

Kurzzusammenfassung

Die Bodenfeuchte spielt eine wichtige Rolle im Bereich der Wasser- und Energiebilanz im System Boden-Vegetation-Atmosphäre. Es gibt einen großen Bedarf globale Landoberflächenmodelle in Bezug auf die räumliche Auflösung zu verbessern. In den vergangenen Jahren wurde die Zuverlässigkeit von numerischen Modellen zur Simulation der Bodenfeuchtedynamik untersucht. Hierbei wurde unterschiedliche Verfahren zur genaueren Parametrisierungen angewendet. Bei der verteilten hydrologischen Modellierung besteht oft das Problem, dass Eingangsdaten aggregiert werden müssen, um diese der Modellauflösung zu entsprechen. Hierbei besteht das Problem, dass die aggregierte Daten zu grob für die Parametrisierung der zu simulierenden Prozesse sein können. Dieses Dilemma kann durch die Anpassung bestimmter Modellparameter umgangen werden. Leider ist es nicht klar, wie in Abhängigkeit der Skala hydrologischen Prozesse zu parametrisieren sind und wie deterministische Modelle hinsichtlich epistemischer Unsicherheiten zu überprüfen sind.

In dieser Studie wurden Langzeitsimulationen mit hoher Auflösung des hoch-instrumentierten TERENO hydrologischen Observatorium Wüstebach Einzugsgebiet durchgeführt. Bodenhydraulische Parameter wurden unter Verwendung von inverser Modellierung mit dem Hydrus-1D-Modell abgeleitet, unter Verwendung des globalen Optimierungsalgorithmus SCE-UA und Bodenfeuchtedaten aus einem drahtlosen Bodenfeuchtesensor-Netzwerk. Die geschätzten Parameter wurden dann für 3D-Simulationen von Wassertransport mit der Simulationsplattform ParFlow-CLM verwendet. Die simulierte Bodenfeuchtedynamik, sowie Evapotranspiration (ET) und Abfluss, wurden mit den langfristigen Beobachtungen verglichen, um zu testen wie gut das Modell in der Lage war, den Wasserhaushalt Dynamik zu reproduzieren. Hierbei wurden verschiedene Anisotropien der hydraulischen Leitfähigkeit daraufhin untersucht, wie schnelle laterale Fließprozesse über

das verdichtete Grundgestein die Simulationsergebnisse beeinflussen. Für die Detailuntersuchung der Modellergebnisse wurden die empirische orthogonalen Funktion (EOF) und Wavelet-Kohärenz-Methoden angewendet. Die EOF Analyse von räumlich-zeitlichen Muster der simulierten und beobachteten Bodenfeuchte ergab, dass die Einführung von Heterogenität in der Bodenporosität zu einer verbesserten Simulation der Bodenfeuchte-Muster führte. Die Wavelet-Kohärenz-Analyse zeigte, dass Regen- und Trockenzeiten erhebliche Auswirkungen auf die zeitliche Korrelation zwischen den beobachteten und simulierten Bodenfeuchte und ET haben. Diese Ergebnisse zeigen den Nutzen von EOF und Wavelet-Kohärenz Methoden für eine weitergehende Validierung von räumlich hochaufgelösten hydrologischen 3D-Modellen.

Im Weiteren wurde untersucht, inwieweit die Verringerung der lokalen hydraulischen Gradienten aufgrund der räumlichen Aggregation teilweise durch zunehmende hydraulische Leitfähigkeit kompensiert werden kann. Hierbei wurde das Informationsentropie-Konzept für die maßstabsabhängige Parametrisierung der Bodenwasserleitfähigkeit verwendet. Der Verlust an Informationsgehalt in Bezug auf Oberflächenkrümmung als Folge der räumlichen Aggregation wurde verwendet, um einen Verstärkungsfaktor für die bodenhydraulische Leitfähigkeit zu bestimmen. Dieser Verstärkungsfaktor soll die aufgrund der Aggregation resultierenden Verzögerung des Wasserflusses kompensieren. Um den Nutzen dieses Ansatzes zu testen, wurden kontinuierliche 3D-hydrologische Simulationen mit unterschiedlichen räumlichen Auflösungen im Wüstebach Einzugsgebiet durchgeführt. Die Ergebnisse zeigen, dass die Einführung eines Verstärkungsfaktors die Modellierungsgüte sowohl in Bezug auf die Bodenfeuchte und Abflusssimulation verbessern kann. Jedoch zeigte der Vergleich der simulierten mit beobachteten Bodenfeuchtemuster, dass die einheitliche Anwendung eines Verstärkungsfaktors zu lokalen Überkorrektion bodenhydraulischen

Leitfähigkeit führen kann. Dieses Problem konnte dadurch umgangen werden, dass die Anwendung des Verstärkungsfaktors nur auf Modellgitterzellen erfolgte, wo ein hohen Informationsverlust aufgrund der Aggregation erfolgt war. Zu diesem Zweck wurden zwei Schemata getestet, die entsprechende ortsspezifischen Korrekturfaktoren nutzten. Beide Schemata führten zu einer verbesserten Modellleistung, sowohl in Bezug auf die Simulation der Bodenwasserdynamik als auch des Abflusses. Der vorgeschlagene Skalierungsansatz kann auch für die Anwendung von globalen Landoberflächenmodelle der nächsten Generation mit hyper-Auflösung nützlich sein.

Weiterhin wurde die Laufzeitverteilungen (transit time distribution, TTD) der Wassermoleküle im Wüstebach Einzugsgebiet mittels der Partikel-Tracking Modells SLIM-FAST untersucht. Hierzu wurden die mit dem Modell Parflow-CLM simulierten 3D Druckverteilungen aus den verschiedenen Modellläufen als Grundlage verwendet. Im Besonderen wurden folgende Fragestellungen untersucht: Wie wirkt sich die Anzahl der angenommen Teilchen die TTD aus? Welcher Wert für die Dispersion kann für das Wüstebach Einzugsgebiet angenommen werden? Und wie wirken sich unterschiedliche Skalierungsverfahren für die hydraulische Leitfähigkeit auf die TTD aus?

Als Referenz wurde die TTD für das Wüstebach Einzugsgebiet mittels kontinuierlich gemessener stabiler Isotopendaten und dem Tracermodell TRANSEP bestimmt und für Vergleichszwecke verwendet. Unsere Ergebnisse zeigen, dass: 1) die anfängliche Anzahl von Wasserteilchen keinen Effekt auf die TTD hat es sei denn, dass die Anfangszahl einen sehr hohen Betrag übersteigt; 2) Höhere Dispersionswerte führen zu einer höheren TTD, wobei ein Wert von 0.002 m beste Übereinstimmung mit der Referenz TTD ergibt; und 3) Globale und lokale Verstärkungsfaktor-Anwendungen führen zu unterschiedlichen Ergebnissen bei

den Schätzungen der Laufzeitverteilung und der Lage der Teilchenausbreitung im Einzugsgebiet. Es kann festgehalten werden, dass die TTD-Analyse mittels Partikel Tracking-Verfahren wie SLIM-FAST eine tiefergehende Auswertung von Simulationsergebnissen hydrologischen 3D Modelle wie Parflow-CLM ermöglich, sowohl in Bezug auf die korrekte Parametrisierung der hydrologischen Eigenschaften als auch in der korrekten Darstellung von Wasserfließwegen.

Contents

List of Abbreviations and Symbols

CH	constant head
CLM	community land model
DEM	digital elevation model
EMI	electromagnetic imaging
EOF	empirical orthogonal function
Eq.	equation
FD	free drainage
LAI	leaf area index
NSE	Nash-Sutcliffe efficiency
PTFs	pedotransfer functions
RMSD	root mean square deviation
RMSE	root mean square error
SF	seepage face
STD	standard deviation
SWC	soil water content
TFG	terrain following grid
TTD	transit time distribution
κ_p	terrain curvature
I	information content
τ	amplification factor
γ	partitioning parameter
E	evaporation
T	transpiration

ET	actual evapotranspiration
ET_0	potential evapotranspiration
k	canopy parameter
P	precipitation
R	Pearson linear correlation
R_f	runoff
S	slope
K_s	saturated hydraulic conductivity
S_e	effective saturation
θ	volumetric moisture
θ_r	residual water content
θ_s	saturated water content
ψ	hydraulic head
α and n	van Genuchten parameters
φ^*	complex conjugate of the mother wavelet
$\overline{W}^2$	global wavelet power
W_n^{xy}	cross wavelet spectrum
c_j	aqueous concentration of primary species *j* in solution
c_j^{im}	immobile concentration of primary species *j* sorbed onto the solid phase
c_j^T	total concentration of species *j*
C	stream water isotope concentration
$\emptyset$	medium porosity
$\mathbf{v}$	groundwater flow velocity
$\mathbf{D}$	hydrodynamic dispersion tensor

α_L	longitudinal dispersivities
α_T	transverse dispersivities
D_e	effective molecular diffusivity
τ_T	particles travel time
λ_j	radioactive decay rate of species j
R_j^{min}	rate of loss or gain of aqueous mass from mineral dissolution or precipitation reactions
s_j^{fm}	rate of loss or gain of aqueous mass in a fracture regime to and from the matrix regime from matrix diffusion
Q_w	volumetric rate of pumping from a well
δ	Dirac function

List of Tables

List of Figures

1 General Introduction

1.1 Background and Motivation

Water flow and solute transport in the surface and subsurface medium play a key role in agriculture, environmental, catastrophe flooding, climate prediction, and natural resource management problems [Sudduth et al., 2001; Zhang et al., 2002; Seneviratne et al., 2010; Castillo et al., 2003; Smith et al., 2002; Wang and Zhu, 2003]. Flow in unsaturated subsurface zone is complex and non-linear and cannot be observed directly. As a result, more reliable weather and climate models for the prediction of water, energy and CO_2 transport are needed. For the improvement and validation of such models, a better and more comprehensive understanding of the processes and interdependencies within and between soil, vegetation and the atmosphere are urgently needed [Wood et al., 2011]. In recent years distributed hydrological models are becoming increasingly realistic through the availability of high performance computing and integrated field observations [Kollet et al., 2010]. While boundary conditions, such as evaporation, infiltration and groundwater level, can often be specified with sufficient accuracy, system properties such as water retention and hydraulic conductivity are often unknown. Access to hydraulic properties is often limited due to the complex measurement techniques, budget constraints, long measurement times, or simply the difficulty of obtaining good quality samples from deep vadose zones. On the other hand, it is generally easier to obtain such data as moisture content, runoff, evapotranspiration and meteorological forcing data. In such situations, both inverse and forward methods have been developed to use limited measurements to predict surface and subsurface water flow. The inverse methods estimate soil hydraulic properties generally by calibrating soil hydraulic

parameters to achieve the best fitting between model predictions and actual soil moisture dynamics observations in the site [Wang et al., 2003; Liu et al., 2004; Zhang et al., 2004; Ward et al., 2006]. Inverse methods can give reliable estimates [Li et al., 1999; Hughson et al., 2000] of soil hydraulic parameters and subsequently improved predictions of subsurface water flow, however, inverse modeling requires solving Richards' Equation iteratively, requiring considerable computational time, especially for the large scale experiment describe in this dissertation.

Soil moisture is the most significant variable in the soil-vegetation-atmosphere continuum due to its important role in the exchange of water and energy at the soil surface. Fast lateral flow under gravitational forces (interflow) can facilitate fast redistribution of soil water in hillslopes during intensive precipitation events (e.g. Hopp et al. [2011]; Zhang et al. [2011]). However, this important hydrological flux is still poorly understood, because it is difficult to measure and quantify [Weiler and McDonnell, 2007; Bachmair and Weiler, 2012]. Recently, it was recognized that interflow is also very important for understanding the spatial and temporal variability of biogeochemical fluxes and trace gas emissions [Groffman et al., 2009; Tang et al., 2014]. According to Ghasemizade and Schirmer [2013], interflow processes are mainly controlled by factors depending on topography, geology, soil properties, rainfall, and vegetation. Previous modelling studies suggest that interflow processes are governed by hillslope characteristics, such as the depth to bedrock and the presence and connectivity of preferential flow pathways [Freer et al., 2002; Tromp-van Meerveld and McDonnell, 2006; Weiler and McDonnell, 2007; Bachmair and Weiler, 2012]. Recently, Cornelissen et al. [2014] conducted a 3D simulation of the Wüstebach catchment, located in the Eifel mountain range in Germany, using the hydrological model HydroGeoSphere with the aim to explore forest catchment spatiotemporal soil moisture variability. They showed that sharply rising

discharge peaks resulting from fast lateral subsurface flow could not be reproduced, because of simplified spatially homogeneous soil and bedrock properties. This demonstrates the need for considering the effect of heterogeneity and anisotropy of soil hydraulic parameters better simulate the mass and energy dynamics in mountainous forest catchment. Recently, an analysis of preferential flow occurrences in the Wüstebach catchment was presented [Wiekenkamp et al., 2015]. According to this study, fast interflow can occur in Wüstebach especially after strong precipitation events. In addition, the study of Stockinger et al. [2014] suggests, that during times of high catchment wetness, hillslopes are getting connected to the riparian zone via interflow processes. In this study, we investigated how these interflow processes can be represented in the framework of numerical modeling.

Another aspect, which is often overlooked in hydrological modelling studies, is the litter layer in forest ecosystems, mainly due to limitations in the direct measurement of forest floor processes. An exception is the study of Schaap et al. [1997], who investigated the moisture dynamics of a coniferous forest floor and derived hydraulic properties of the litter layer. Recently, Bogena et al. [2013] used these hydraulic properties to simulate temporal water dynamics in the litter layer of the forest catchment Wüstebach demonstrating its importance for soil moisture assessment.

In recent times numerical hydrological models for the prediction of fluid transport are increasingly used to support the management of surface and ground water. To this end, parallel simulation platforms have been developed in the past decade to enable detailed estimations of long-term dynamics of hydrological fluxes and storages (e.g. soil moisture, runoff discharge, evapotranspiration), e.g. STOMP [White and Oostrom, 2006], PFLOTRAN [Lichtner et al., 2015], MODFLOW [Harbaugh, 2005], HYDRUS [Simunek et al., 2012], and

HydroGeoSphere (HGS) [Therrien et al., 2010]. A parallel, three-dimensional, variably saturated water transport code ParFlow [Ashby and Falgout, 1996; Maxwell et al., 2010] was developed for simulating large-scale, high-resolution flow problems. The ParFlow platform was extended to consider energy and mass balance at the land surface by incorporating the Common Land Model (CLM; [Dai et al., 2003]) into ParFlow [Kollet and Maxwell, 2007; Maxwell and Miller, 2005]. However, due to the limitation of availability of in-situ dataset measurement, it was usually difficult to validate the results of long-term, high-resolution surface-subsurface flow problems, especially for the forested catchments.

Spatial and temporal patterns of fluxes and states in the soil-vegetation-atmosphere continuum are inseparably intertwined, resulting in complex feedbacks and system responses on different spatial and temporal scales [Simmer et al., 2015]. One useful way to investigate the spatiotemporal relations between water budget components and soil moisture is applying the method of empirical orthogonal functions (EOF) [Graf et al., 2014; Kim and Barros, 2002; Liu, 2003; Syed et al., 2004; Jawson and Niemann, 2007; Schmidt et al., 2008]. However, the EOF analysis has not yet been used for the spatio-temporal validation of a 3D simulation of soil moisture patterns. Very recently, Koch et al [2015] applied the EOF-analysis in a novel manner for the spatial validation of a distributed hydrological model with observed satellite based land surface temperature data and Mascaro et al. [2015] utilized EOFs to analyze results from a high-resolution distributed hydrologic simulation. Wavelet analysis has been applied in catchment studies [Lauzon et al., 2004], model validation [Schaefli and Zehe, 2009], field-scale time series [Vargas et al., 2010], and also in combination with EOF analysis [Parent et al., 2006]. To our knowledge, a combined EOF and wavelet analysis to explore modelled spatiotemporal patterns of soil water content, runoff and evapotranspiration has not been applied so far on catchment scale.

On the other hand, the reliable consideration of the impacts of small scale heterogeneity on the simulation of water fluxes at larger spatial scales is still a critical issue in hydrological modelling [Clark et al., 2015]. Topography is one of the main factors governing hydrological dynamics and a change of scale (grid size) in topographic discretization means that hydraulic parameters, such as saturated soil hydraulic conductivity (K_s) must be upscaled/recalibrated [Grayson and Blöschl, 2000]. Many modelling studies demonstrated the importance of correct parametrization of K_s and preferential flow on the simulation of soil moisture, evapotranspiration, groundwater dynamics, runoff, solute transport and erosion [Bogena et al., 2002; Simunek et al., 2003; Weiler, 2005; Maxwell and Kollet, 2008 and Yu et al., 2014].

Several studies investigated the effect of model resolution on simulation of hydrological processes [e.g. Geza and McCary, 2008; Kumar et al., 2009; Ye et al., 2010]. Very recently, Cornelissen et al. [2014] investigated the influence of spatial and temporal resolution on 3D simulation of hydrological processes. They studied the scale dependency of water balance and discharge simulation using different spatio-temporal resolutions and found that process-based scaling is a promising way to increase model accuracy at coarse resolutions.

Previous studies showed that entropy theory could be used to quantify the loss of information content and the effect of aggregation of topographical data and model parameters [Singh, 1997; Vieux, 1993; Mendicino and Sole, 1997; Kuo et al., 1999; Krebs et al., 2015]. Niedda [2004] utilized the entropy concept in a 2D modelling framework. He introduced an amplification factor for the upscaling of K_s by related its value to the loss of terrain curvature information. This information driven upscaling of K_s led to a much better agreement between observed and simulated runoff.

In order to enable realistic distributed soil moisture simulations, the model domain of numerical models needs to be informed with appropriate soil hydraulic parameters. Numerous methods have been applied in recent studies to obtain appropriate model parameterizations, including inverse calibration [Burbey and Zhang, 2015; Simunek and van Genuchten, 1996], linear regression [Arshad et al., 2013], pedotransfer functions (PTFs) [Schaap et al., 2001], upscaling techniques [Zhu and Mohanty, 2002; Zhang et al., 2004] to name a few. Recently, terrain information entropy concept was introduced for soil hydraulic parameters estimation [Niedda, 2004; Fang et al., 2016]. Another challenge is the appropriate validation of distributed hydrological models. Recently, Fang et al. [2015] and Koch et al. [2016] used data from a soil moisture sensor network to validate 3D numerical water transport models with respect to correct simulation soil moisture pattern. However, even if the models are accurately reproducing the spatial soil moisture pattern, this no guarantee for the correct representation of water particles movement in the catchment. An effective way to evaluate the model performance with respect to water transport is the analysis of water transit time distribution (TTD). Typically, TTD are estimated from stable isotope data using simple model assumption [Kirchner, 2016]. For instance, Stockinger et al. [2014] used the tracer-aided conceptual model TRANSEP and continuous measurements of stable isotope of water as tracers to estimate the spatial heterogeneity of TTDs of the Wüstebach catchment. In addition, TTD analysis were also performed in the framework of 2D and 3D modeling studies using particle tracking, e.g. Marçais et al., [2015]; Green et al., [2014]; Woolfenden and Ginn, [2009]. Such particle tracking schemes were commonly applied with physically-based models in the framework of groundwater flow and contaminant transport study, e.g. Suk, [2012]; Cadini et al., [2012]; Salamon et al., [2006]; Goode, [1990]; Binning and Celia, [2002]. Recently, the particle tracking code SLIM-FAST in conjunction with the ParFlow-

CLM numerical model was successfully applied to different catchment and with varying spatial resolutions [Kollet and Maxwell, 2008; de Rooij et al., 2013]. As one of the most significant factors of particle migration in soil and aquifers, longitude and transverse dispersivity were widely studied in recent studies by either experimental methods or numerical modeling [Gelhar et al., 1992; Vanderborght and Vereecken, 2007; Kollet and Maxwell, 2008; Chou and Wyseure, 2009; Perfect et al., 2002]. The correct dispersivity estimation is an important requisite to achieve realistic estimates of TTDs using particle transport modelling. However, different researches based on different testing methods and materials often revealed quite different longitude dispersivity for aquifers and soils [Schulze-Makuch, 2005].

1.2 Research Objectives

The objective of this research is developing an accurate, reliable and comprehensive 3D large-scale modeling system of parameterization, simulation, prediction, and validation model in a forested catchment in western Germany. We selected the Wüstebach catchment as the study area for this study to utilize the comprehensive validation data sets from atmospheric, pedological and hydrological monitoring equipment installed in the framework of the TERENO and SFB/TR32 projects [Bogena et al., 2010] [Bogena et al., 2015]. This integrated data ideally suited for the analysis of pattern in soil-vegetation-atmosphere systems [Simmer et al., 2015] and of the linkage between hydrological and atmospheric processes in complex environments such as forest ecosystems.

The following questions are being tried to answer:

1. How can fast lateral flow above the bedrock be represented in a 3D Richards-equation based model?
2. How will different representations of heterogeneity and anisotropy of soil properties affect the performance of a 3D hydrological model?
3. What is the value of EOF and wavelet coherence analysis for the spatiotemporal validation of hydrological models?
4. How can the terrain curvature information from different resolution Digital Elevation Models (DEMs) of the Wüstebach catchment be represented using the information entropy concept?
5. Which upscaling scheme is the best strategy to compensate the information loss in terms of estimated soil water content, runoff, and transit time distribution of water particles?
6. Can spatial aggregation of a three-dimensional hydrological model be compensated by parameter upscaling using the information entropy concept?
7. How many particles are needed to achieve reliable estimates of TTD in a forested headwater catchment?
8. How strong is the TTD estimation influenced by the dispersivity parametrization?
9. How well compare TTD estimated from stable isotopes as tracers with those derived from 3D hydrological modelling?

1.3 Methodology

In this study, we used HYDRUS+SCEUA to inversely estimated hydraulic parameters. We used ParFlow-CLM to run all the simulations for soil water content, runoff, and

evapotranspiration. We used SAGA-GIS to calculate the terrain curvature information. We used SLIM-FAST to track water particles migration and estimate TTD.

The model domain used for the Wüstebach catchment has a size of 1180 m × 740 m and a uniform depth of 1.6 m, which corresponds to the averaged measured soil depth. In addition, following Bogena et al. [2013] a litter layer was considered with a uniform depth of 0.05 m. We used the DEM of the Land Surveying Office of North Rhine-Westphalia with a spatial resolution of 10 m to spatially discretize the model domain and to assign slope values to each grid. The vertical resolution of the model domain was set to 0.025 m. The total number of spatially uniform grids in the model domain was 118 × 74 × 66. The flow direction grid was generated using GRASS software. We utilized the terrain following grid (TFG) method [Maxwell, 2013] to decrease the number of vertical grid cells.

The CLM model is used to define the top boundary of the ParFlow-CLM simulation platform. We used hourly information on global radiation, precipitation rate, air temperature, wind speed, air pressure, and specific humidity from the Kalterherberg climate station of the German Weather Service (located 9.6 km west of the Wüstebach catchment) to force the CLM model. This climate station is well representative for our test site as demonstrated in the study of Graf et al., [2014]. The lateral boundary condition was set as a constant head of -0.88 m, which corresponds to the average depth of observed water table in the area. No flux boundary condition was chosen for the bottom of the model domain since the bedrock of the Wüstebach catchment has a very low permeability, and deep drainage into the bedrock was found to be negligible [Graf et al., 2014].

The soil profile was differentiated into four different soil horizons with specific hydraulic properties following Bogena et al. [2013]: a soil covering litter layer (+0.05-0 m), a top A horizon (0-0.1 m), an intermediate B horizon (0.1-0-4 m), and a C horizon (0.4-1.6 m) overlaying the bedrock.

Detailed descriptions and illustrations of the proposed method will be discussed in Chapter 2 - 4.

1.4 Experiments and data

This research was conducted in the Wüstebach test site, which is a 38.5 ha large experimental catchment of the TERENO Eifel/Lower Rhine Valley Observatory [Zacharias et al., 2011] and the Collaborative Research Centre TR32 [Vereecken et al., 2010; Simmer et al., 2015] located in the national park Eifel. The altitude ranges from 595 m in the north to 628 m in the south and the average slope is 3.6 % with maximum values near the riparian zone (up to 10.4 %). The bedrock is mainly composed of fractured Devonian shales exhibiting very low hydraulic conductivity (10^{-9} to 10^{-7} m/s) [Graf et al, 2014]. The bedrock is overlain by a periglacial solifluction layer with an average thickness of 1.6 m. Cambisols and Planosols are mainly located on hillslope zone, whereas Gleysols and half-bogs have been developed in the riparian zone under the influence of groundwater [Bogena et al., 2015]. The prevailing soil texture is silty clay loam with a medium to high fraction of coarse material. The litter layer has a thickness about 5 cm [Richter, 2008]. More than 90% of the forest is comprised of Norway spruce trees planted in 1946 [Etmann, 2009], with a typical canopy height of about 25 m [Bogena et al., 2015]. The test site belongs to the temperate climate zone with a mean

temperature of about 7°C and exhibits a long-term mean annual precipitation amount of 1310 mm for the period 1981 to 2013.

We made use of long-term soil moisture data from a wireless senor network installed in the Wüstebach catchment consisting of 150 sensor nodes [Bogena et al., 2010]. Each node is equipped with four ECH2O EC-5 and two 5TE sensors (Decagon Devices, Inc.) measuring soil moisture in three depths (5, 20 and 50 cm) with a temporal resolution of 15 min. Calibration of the ECH2O sensors is explained in detail in Rosenbaum et al. [2012]. Representative sensor network locations were identified and outliers were removed using EMI (electromagnetic imaging) data [Cornelisson et al., 2014]. Accordingly, soil moisture observations at 104 sensor nodes were used in this study. Discharge is measured at the catchment outlet using a runoff station equipped with a combination of a V-notch weir for low flow measurements and a Parshall flume to measure mean to high flows [Bogena et al., 2015]. For the parameterization of atmospheric forcing we used hourly information on global radiation, precipitation rate, air temperature, wind speed, air pressure, and specific humidity from the Kalterherberg climate station of the German Weather Service (located 9.6 km west of the Wüstebach catchment).

1.5 Dissertation Overview

The present dissertation is structured into three main parts. In the first part, we obtained soil hydraulic parameters using inverse calibration HYDRUS and SCE-UA, conducted simulation of soil water content, runoff, and evapotranspiration of Wüstebach catchment, closed the water budget gap, investigated the effect of heterogeneity and anisotropy on soil moisture

distribution variation using EOF and wavelet coherence analysis. In the second part, we introduced information entropy concept to represent the loss of terrain curvature information due to spatial aggregation, calculated the amplification factor applied to hydraulic conductivity field to compensate the information loss, and compared four model scenarios of different upscaling schemes of amplification factor application. In the third part, we tracked water particles based on the simulated pressure of the four scenarios from ParFlow-CLM model, estimated transit time distribution using SLIM-FAST model, and compared the effect of number of particles and dispersion parameters on transit time distribution estimation. The results of this dissertation are presented in three chapters which correspond to published or submitted publications in international peer-reviewed journals Journal of Hydrology.

Chapter 2: Spatio-temporal validation of long-term 3D hydrological simulations of a forested catchment using empirical orthogonal functions and wavelet coherence analysis.
Chapter 3: Scale dependent parameterization of soil hydraulic conductivity in 3D simulation of hydrological processes in a forested headwater catchment.
Chapter 4: Evaluation of 3D model parameterizations using water transit time distributions.

These chapters feature their own objectives, introductions, methods and materials since the different issues highlight aspects of the overall research question in a different manner. The results are concluded and a brief outlook for further research is given in Chapter 5.

2 Spatio-temporal validation of long-term 3D hydrological simulations of a forested catchment using empirical orthogonal functions and wavelet coherence analysis

This chapter has been published as: Fang, Z., Bogena, H., Kollet, S., Koch, J., Vereecken, H., 2015. Spatio-temporal validation of long-term 3D hydrological simulations of a forested catchment using orthogonal functions and wavelet coherence analysis. Journal of Hydrology. 529, 1754-1767.

2.1 Abstract

Soil moisture plays a key role in the water and energy balance in soil, vegetation and atmosphere systems. According to Wood et al. (2011) there is a grand need to increase global-scale hyper-resolution water-energy-biogeochemistry land surface modelling capabilities. These modelling capabilities should also recognize epistemic uncertainties, as well as the nonlinearity and hysteresis in its dynamics. Unfortunately, it is not clear how to parameterize hydrological processes as a function of scale, and how to test deterministic models with regard to epistemic uncertainties. In this study, high resolution long-term simulations were conducted in the highly instrumented TERENO hydrological observatory of the Wüstebach catchment. Soil hydraulic parameters were derived using inverse modeling with the Hydrus-1D model using the global optimization scheme SCE-UA and soil moisture data from a wireless soil moisture sensor network. The estimated parameters were then used for 3D simulations of water transport using the integrated parallel simulation platform ParFlow-CLM. The simulated soil moisture dynamics, as well as evapotranspiration (ET) and runoff, were compared with long-term field observations to illustrate how well the model was able to reproduce the water budget dynamics. We investigated different anisotropies of hydraulic conductivity to analyze how fast lateral flow processes above the underlying bedrock affect the simulation results. For a detail investigation of the model results we applied the empirical orthogonal function (EOF) and wavelet coherence methods. The EOF analysis of temporal-spatial patterns of simulated and observed soil moisture revealed that introduction of heterogeneity in the soil porosity effectively improves estimates of soil moisture patterns. Our wavelet coherence analysis indicates that wet and dry seasons have significant effect on temporal correlation between observed and simulated soil moisture and

ET. Our study demonstrates the usefulness of the EOF and wavelet coherence methods for a more in-depth validation of spatially highly resolved hydrological 3D models.

2.2 Introduction

More reliable weather and climate models for the prediction of water, energy and CO_2 transport are needed to better support the management of natural resources. For the improvement and validation of such models, a better understanding of the processes and interdependencies within and between soil, vegetation and the atmosphere are urgently needed (Wood et al. [2011]). Soil moisture is the most significant variable in the soil-vegetation-atmosphere continuum due to its important role in the exchange of water and energy at the soil surface. Fast lateral flow under gravitational forces (interflow) can facilitate fast redistribution of soil water in hillslopes during intensive precipitation events (e.g. Hopp et al., 2011; Zhang et al., 2011). However, this important hydrological flux is still poorly understood, because it is difficult to measure and quantify (e.g. Weiler and McDonnell, 2007; Bachmair and Weiler, 2012). Recently, it was recognized that interflow is also very important for understanding the spatial and temporal variability of biogeochemical fluxes and trace gas emissions (e.g. Groffman et al., 2009; Tang et al., 2014). According to Ghasemizade and Schirmer [2013] interflow processes are mainly controlled by factors depending on topography, geology, soil properties, rainfall, and vegetation. Previous modelling studies suggest that interflow processes are governed by hillslope characteristics, such as the depth to bedrock and the presence and connectivity of preferential flow pathways (e.g. Freer et al., 2002; Tromp-van Meerveld and McDonnell, 2006; Weiler and McDonnell, 2007; Bachmair and Weiler, 2012). Cornelissen et al. [2014] conducted a 3D simulation of the Wüstebach

catchment, located in the Eifel mountain range in Germany, using the hydrological model HydroGeoSphere with the aim to explore forest catchment spatiotemporal soil moisture variability. They showed that sharply rising discharge peaks resulting from fast lateral subsurface flow could not be reproduced, because of simplified spatially homogeneous soil and bedrock properties. This demonstrates the need for considering the effect of heterogeneity and anisotropy of soil hydraulic parameters better simulate the mass and energy dynamics in mountainous forest catchment. Recently, an analysis of preferential flow occurrences in the Wüstebach catchment was presented [Wiekenkamp et al., 2015]. According to this study, fast interflow can occur in Wüstebach especially after strong precipitation events. In addition, the study of Stockinger et al. [2014] suggests, that during times of high catchment wetness, hillslopes are getting connected to the riparian zone via interflow processes. In this study, we investigated how these interflow processes can be represented in the framework of numerical modeling.

Another aspect, which is often overlooked in hydrological modelling studies, is the litter layer in forest ecosystems, mainly due to limitations in the direct measurement of forest floor processes. An exception is the study of Schaap et al. [1997], who investigated the moisture dynamics of a coniferous forest floor and derived hydraulic properties of the litter layer. Recently, Bogena et al. [2013] used these hydraulic properties to simulate temporal water dynamics in the litter layer of the forest catchment Wüstebach demonstrating its importance for soil moisture assessment.

A parallel, three-dimensional, variably saturated water transport code ParFlow [Ashby and Falgout, 1996; Maxwell et al., 2010] was developed for simulating large-scale, high-resolution flow problems. The ParFlow platform was extended to consider energy and mass

balance at the land surface by incorporating the Common Land Model (CLM; [Dai et al., 2003]) into ParFlow [Kollet and Maxwell, 2007; Maxwell and Miller, 2005]. However, due to the limitation of availability of in-situ dataset measurement, it was usually difficult to validate the results of long-term, high-resolution surface-subsurface flow problems, especially for the forested catchments.

Spatial and temporal patterns of fluxes and states in the soil-vegetation-atmosphere continuum are inseparably intertwined, resulting in complex feedbacks and system responses on different spatial and temporal scales [Simmer et al., 2015]. One useful way to investigate the spatiotemporal relations between water budget components and soil moisture is applying the method of empirical orthogonal functions (EOF) [Graf et al., 2014; Kim and Barros, 2002; Liu, 2003; Syed et al., 2004; Jawson and Niemann, 2007; Schmidt et al., 2008]. However, the EOF analysis has not yet been used for the spatio-temporal validation of a 3D simulation of soil moisture patterns. Very recently, Koch et al [2015] applied the EOF-analysis in a novel manner for the spatial validation of a distributed hydrological model with observed satellite based land surface temperature data and Mascaro et al. [2015] utilized EOFs to analyze results from a high-resolution distributed hydrologic simulation. Wavelet analysis has been applied in catchment studies [Lauzon et al., 2004], model validation [Schaefli and Zehe, 2009], field-scale time series [Vargas et al., 2010], and also in combination with EOF analysis [Parent et al., 2006]. To our knowledge, a combined EOF and wavelet analysis to explore modelled spatiotemporal patterns of soil water content, runoff and evapotranspiration has not been applied so far on catchment scale.

The objective of this study is to perform high resolution 3D water flow simulations of a forested headwater catchment using the Parflow-CLM model. We selected the Wüstebach

catchment as the study area for this study to utilize the comprehensive validation data sets from atmospheric, pedological and hydrological monitoring equipment installed in the framework of the TERENO and SFB/TR32 projects [Bogena et al., 2010] [Bogena et al., 2015]. This integrated data ideally suited for the analysis of pattern in soil-vegetation-atmosphere systems [Simmer et al., 2015] and of the linkage between hydrological and atmospheric processes in complex environments such as forest ecosystems. In our study, we conducted high-resolution hydrological simulations of a complex forest catchment using the Parflow-CLM model and evaluated different parameterization schemes. For the evaluation with employed a combination of EOF and wavelet analysis to enable a more in-depth analysis of the model performance. This study was to answer the following research questions: 1) how can fast lateral flow above the bedrock be represented in a 3D Richards-equation based model; 2) how will different representations of heterogeneity of soil properties affect the performance of a 3D hydrological model; and 3) what is the value of EOF and wavelet coherence analysis for the spatiotemporal validation of hydrological models.

2.3 Materials and methods

2.3.1 The experimental test site

This research was conducted in the Wüstebach catchment (Figure 2.1), a 38.5 ha large experimental test site of the TERENO Eifel/Lower Rhine Valley Observatory [Zacharias et al., 2011] located in the National park Eifel. The altitude ranges from 595 m in the north to 628 m in the south. The average slope is modest (3.6 %) with maximum values near the river (up to 10.4 %). The geology is dominated by fractured Devonian shales with occasional sandstone inclusions and a hydraulic conductivity on the order of 10^{-9} to 10^{-7} m/s [Graf et al,

2014]. The bedrock is overlain by a periglacial solifluction layer of about 1–2 m thickness, in which typical soil types have developed. Cambisols and Planosols are mainly located on hill slopes, whereas Gleysols and half-bogs have been developed in the riparian zone under the influence of groundwater (Figure 2.1). The prevailing soil texture is silty clay loam with a medium to high fraction of coarse material, and the litter layer has a thickness between 3 and 5 cm [Richter, 2008]. More than 90% of the forest is comprised of Norway spruce trees planted in 1946 [Etmann, 2009], with a typical canopy height of about 25 m. The test site belongs to the temperate climate zone with a mean temperature of about 7°C and a long-term mean precipitation rate of 1310 mm/a for the period 1981 to 2010.

We made use of long-term soil moisture data from a wireless senor network installed in the Wüstebach catchment consisting of 150 sensor nodes [Bogena et al., 2010], each equipped with four ECH2O EC-5 and two 5TE sensors (Decagon Devices, Inc.) To cover the test site area the sensor locations were distributed using a raster configuration with a resolution of 60 m. Additional locations were randomly located within each raster cell to achieve a wide range of distance classes. Soil moisture is measured in three depths (5, 20 and 50 cm) with a temporal resolution of 15 min [Bogena et al., 2010]. Calibration of the sensors is explained in detail in Rosenbaum et al. [2012]. We followed Cornelissen et al. [2014], who used EMI (electromagnetic imaging) data to identify representative sensor network locations and to remove outliers. Accordingly, soil moisture observations at 104 sensor nodes were used in the study for the inverse estimation of hydraulic parameters and for comparison with simulations results. The eddy covariance tower provided the actual ET data used for model validation, see [Bogena et al., 2015] for a detailed description of the measurement technique.

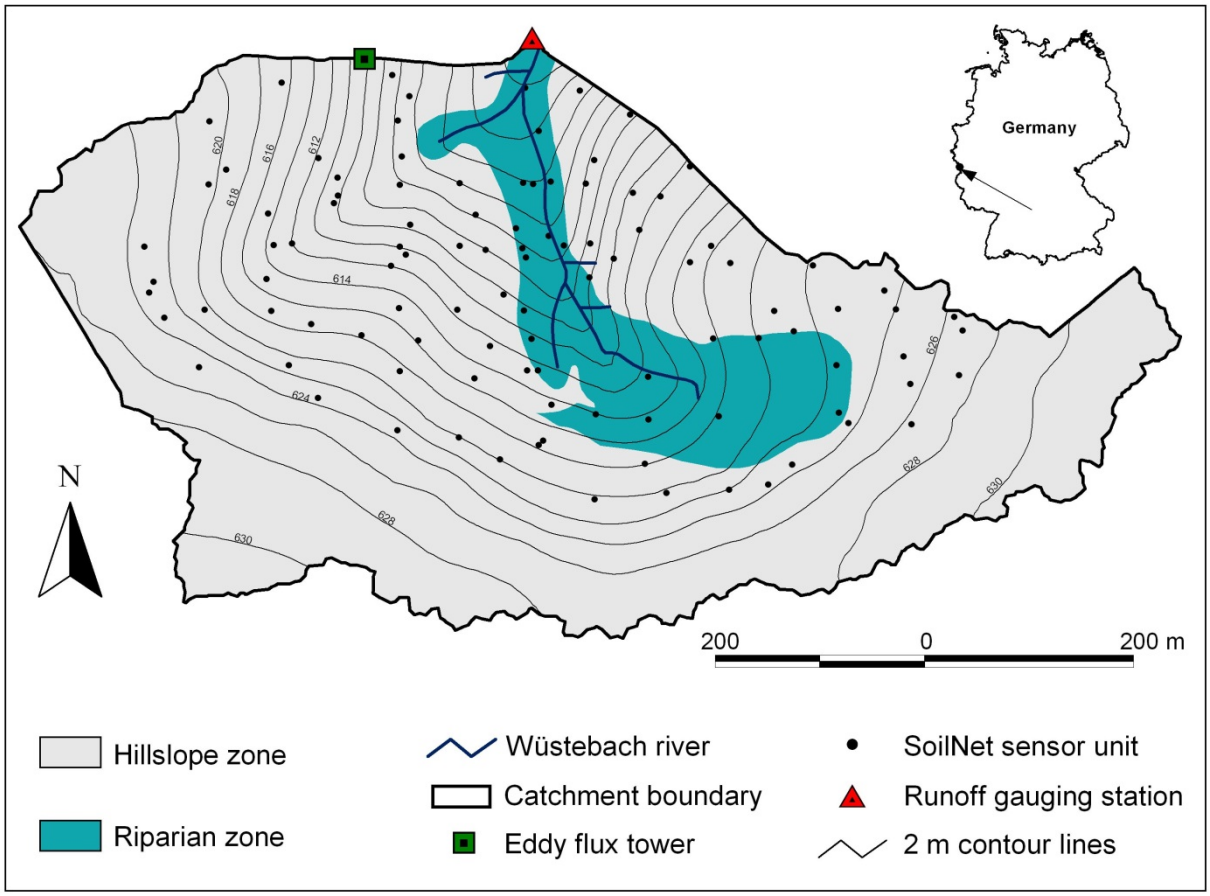

Figure 2.1: Map of the instrumentation of the Wüstebach experimental catchment.

2.3.2 The ParFlow-CLM Simulation Platform

The core of the ParFlow-CLM simulation platform used in this study is the ParFlow model [Ashby and Falgout, 1996], which is a parallel, three-dimensional, variably saturated water transport code that is especially suitable for large-scale, high-resolution flow problems. ParFlow makes use of advanced numerical solvers and multigrid preconditioners for massively parallel computer environments. It uses a sophisticated octree-space partitioning algorithm to depict complex structures in three-space, such as topography, different hydrologic facies, and watershed boundaries. ParFlow simulates the three-dimensional variably saturated subsurface flow by solving the Richards equation:

$$\frac{\partial \theta}{\partial t} = \nabla \cdot K(\psi)\nabla\psi + \frac{\partial K(\psi)}{\partial z} \quad (2.1)$$

where θ (-) is the volumetric moisture, K is hydraulic conductivity (L/T), and ψ is the hydraulic head (L).

Advanced boundary conditions, such as free-surface overland flow, afford the simulation of hillslope runoff and channel routing in an integrated fashion [Kollet and Maxwell, 2006]. Distributed surface roughness can be applied to honor different land cover types in the watershed.

The ParFlow platform was extended to consider energy and mass balance at the land surface by incorporating the Common Land Model (CLM; [Dai et al., 2003]) into ParFlow [Kollet and Maxwell, 2007; Maxwell and Miller, 2005]. This coupled ParFlow-CLM model can quantitatively exchange information between the land surface and the subsurface, such as plant interception, root uptake and evapotranspiration, in an operator splitting approach. For this study, we employed the version v693 of ParFlow-CLM released on July 28, 2014.

2.3.3 Model Setup

The model domain used for the Wüstebach catchment has a size of 1180 m × 740 m and a uniform depth of 1.6 m, which corresponds to the averaged measured soil depth. In addition, following Bogena et al. [2013] a litter layer was considered with a uniform depth of 0.05 m. We used the DEM of the Land Surveying Office of North Rhine-Westphalia with a spatial resolution of 10 m to spatially discretize the model domain and to assign slope values to each grid. The vertical resolution of the model domain was set to 0.025 m. The total number of

spatially uniform grids in the model domain was 118 × 74 × 66. The flow direction grid was generated using GRASS software. We utilized the terrain following grid (TFG) method [Maxwell, 2013] to decrease the number of vertical grid cells.

The CLM model is used to define the top boundary of the ParFlow-CLM simulation platform. We used hourly information on global radiation, precipitation rate, air temperature, wind speed, air pressure, and specific humidity from the Kalterherberg climate station of the German Weather Service (located 9.6 km west of the Wüstebach catchment) to force the CLM model. This climate station is well representative for our test site as demonstrated in the study of Graf et al., [2014]. The lateral boundary condition was set as a constant head of -0.88 m, which corresponds to the average depth of observed water table in the area. No flux boundary condition was chosen for the bottom of the model domain since the bedrock of the Wüstebach catchment has a very low permeability, and deep drainage into the bedrock was found to be negligible [Graf et al., 2014].

The soil profile was differentiated into four different soil horizons with specific hydraulic properties following Bogena et al. [2013]: a soil covering litter layer (+0.05-0 m), a top A horizon (0-0.1 m), an intermediate B horizon (0.1-0-4 m), and a C horizon (0.4-1.6 m) overlaying the bedrock (see Figure 2.2).

Soil hydraulic properties were parameterized using the van Genuchten - Mualem model (VGM):

$$\theta(h) = \begin{cases} \theta_r + \frac{\theta_s - \theta_r}{(1+|\alpha h^n|)^m}, & h < 0 \\ \theta_s, & h \geq 0 \end{cases} \qquad (2.2)$$

$$K(h) = K_s S_e^{0.5}[1 - \left(1 - S_e^{\frac{0.5}{m}}\right)^m]^2 \qquad (2.3)$$

$$S_e = \frac{\theta - \theta_r}{\theta_s - \theta_r} \qquad (2.4)$$

$$m = 1 - \frac{1}{n} \qquad (2.5)$$

where K_s is the saturated soil hydraulic conductivity (m day^{-1}), S_e is the effective saturation, θ_r and θ_s (m^{3}m^{-3}) represent the residual and saturated SWC, α (m^{-1}), n and m (both dimensionless) are parameters for fitting the soil water retention function. Due to lack of measurements, the hydraulic parameters θ_r, α, n, and K_s were estimated for each soil layer using inverse modelling, see section 2.3.4. The parameter θ_s was fixed to the maximum value of the observed soil moisture during the study period for each soil layer. This simple approach is valid, because high precipitation amounts have led to an observed saturation of the whole soil profile several times during the study period.

Following Bogena et al. [2013], we adopted the study of Schaap et al. [1997] to define appropriate values for the parameters θ_r, α, n and K_s of the litter layer. The paramter θ_s was estimated from the mean porosity of eight litter layer samples collected in the site [Bogena et al., 2013]. The corresponding hydraulic parameters used for the ParFlow-CLM simulation are as follows: K_s = 200.0 cm/day, θ_r = 0, θ_s = 0.87, α = 0.0264 cm^{-1}, and n = 1.286.

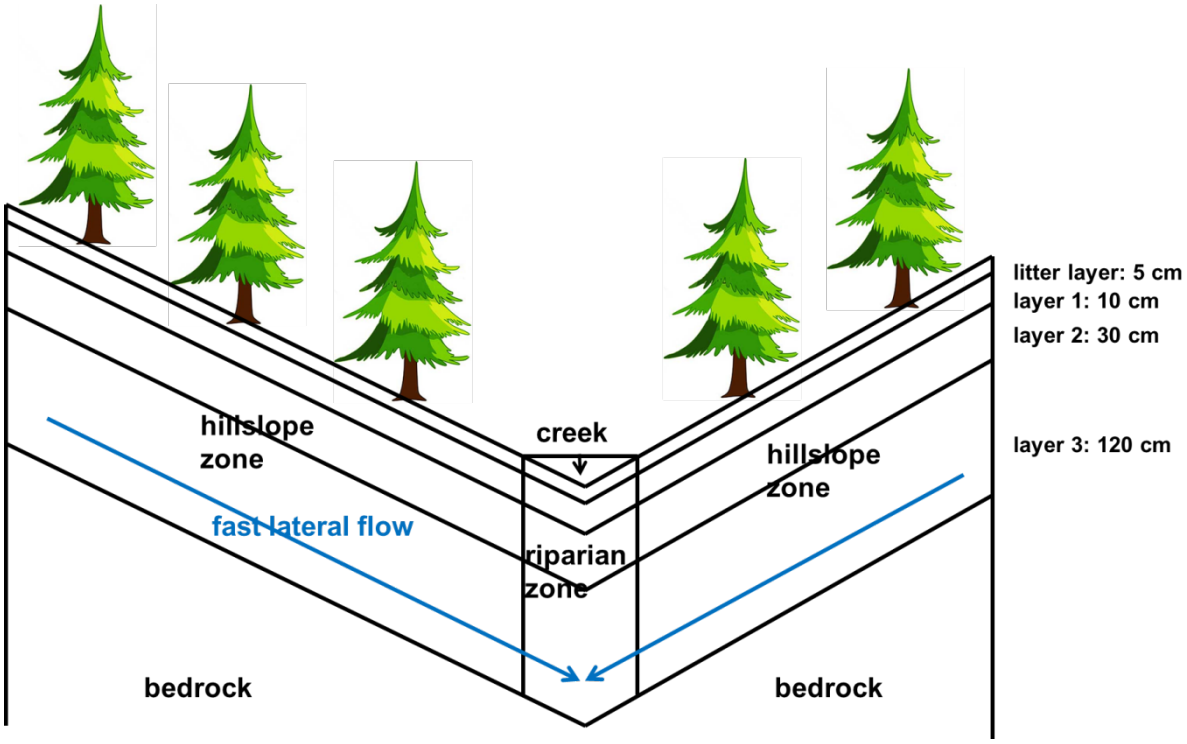

Figure 2.2: Schematic model of the Wüstebach catchment.

The simulation was conducted on hourly time steps for 1216 days from May 1 2010 to April 30 2013, before the deforestation work started [Bogena et al., 2015]. A spinup phase from January 1 to April 30, 2010 was conducted with an initial condition of constant head in -2.0 m. Actually, several testing simulation runnings indicated that the initial condition between -0.1 m to 5.0 m gave almost same results after one to two months running. Therefore the spinup phase was fairly effective. The simulations were performed on the high performance computer JUROPA in Centre for High-Performance Scientific Computing in Terrestrial Systems, HPSC TerrSys, Geoverbund ABC/J and clusters of the Forschungszentrum Jülich GmbH. It took around 40 – 60 hours for the 3-year simulations to complete. Considering its long term and the complicated interacted atmospheric-hydrological system in this study, such computational times are well accepted.

2.3.4 Inverse Estimation of Hydraulic Parameters

Soil hydraulic parameters can be determined either by direct or indirect methods. In case of direct methods, the hydraulic parameters are estimated by fitting the water retention and unsaturated hydraulic conductivity curve to experimental data obtained from soil cores in the laboratory. However, soil heterogeneity requires that a very large number of samples would be needed to adequately represent the variability of soil properties in the study area, which is very expensive and time consuming. Since measured time series of soil moisture at several depths are available as for this study, inverse modelling may be an appropriate alternative to obtain in-situ soil hydraulic parameter estimates [e.g. Vrugt et al., 2003; Zhang et al., 2004]. However, inverse modelling is computationally demanding and not feasible for 3D models based on the Richard's equation even in the presence of high performance computing facilities. Recently, Qu et al. [2014] showed that most of the spatial variability of soil moisture in the Wüstebach catchment can be described using a 1D vertical Richard's equation approach. Thus, we followed the approach of Bogena et al. [2013] and used an inverse HYDRUS-1D model [Simunek et al., 2008] to estimate the parameters of the Mualem-van Genuchten model.

The initial soil profile for HYDRUS 1-D was set to be saturated, and a 6-month spin up period with actual meteorological data was applied. Therefore, the simulation period was from 1 July 2009 to 30 April 2013. The reference potential evapotranspiration (ET_0) was computed by the Penman-Monteith equation [Allen et al., 1998]. Potential evaporation (E) and transpiration (T) were separated based on the leaf area index (LAI):

$$T = ET_0(1 - e^{-kLAI}) \quad (2.6)$$

$$E = ET_0 e^{-kLAI} \quad (2.7)$$

where *k* is a parameter (-) that governs the radiation extinction of the canopy. Given that the study area was homogenously covered by Norway spruce forest, it was found that a *k* value of 0.75 and a *LAI* value of 4 are appropriate [Bogena et al., 2013].

The root distribution was set to decrease linearly from maximum value at the soil surface to zero at 50 cm depth with a unit gradient. Root water uptake was computed by the Feddes approach [Feddes et al., 1976] implemented in HYDRUS-1D. The lower boundary was set to be three different types for comparison: free drainage (FD), constant head (CH), and seepage face (SF).

We discretized the soil profile in HYDRUS-1D in the same way the ParFlow-CLM model (three soil horizons plus a litter layer of organic material on top of the soil) and applied the global optimization algorithm SCE-UA [Duan et al., 1992] to estimate VGM parameters. We used spatially averaged SoilNet soil moisture data for three depths (5, 20 and 50 cm) from January 1 2009 and April 30 2013 to estimate soil hydraulic parameters for each of the three soil horizons (Figure 2.1). The litter layer was parameterized in the same way as the ParFlow-CLM model.

2.3.5 Model Scenarios

Two scenarios were simulated in order to illustrate how we can improve model performance by introducing anisotropy (different parameter values at different directions) and heterogeneity (different parameter values at different points) using Parflow-CLM. During strong precipitation events the soils in the study area often reached saturation, which

activated fast lateral water flow pathways above the impermeable bedrock [Rosenbaum et al., 2012; Stockinger et al., 2014]. We mimic the fast interflow process by assuming a strong horizontal anisotropy in the bottom soil layer (C horizon). Due to the high computational demand of ParFlow-CLM required for a 3-year simulation period, it was impossible to inversely estimate the optimal horizontal *Ks* value. Therefore, we investigated different scaling factors for the horizontal component of K_s to find the best representation of the interflow process in the Wüstebach catchment (modelling scenario SC1). We used a series of the scaling factors of anisotropy (10, 20, 40, and 80, respectively). During this study, the vertical *Ks* value was kept unchanged and isotropy in *Ks* in the upper two soil horizons was assumed because fast lateral flow typically occurs above the bedrock interface [e.g. Lin, 2005; Hopp and McDonnell, 2009; Uchida et al., 2005]. To evaluate the quality of the different scenarios we compared observed and simulated runoff, evapotranspiration, and soil moisture time series and used the root mean square error (RMSE) and Nash-Sutcliffe efficiency (NSE) as simulation quality criteria. The scaling factor that resulted in the best simulation results was used for all following simulations.

Table 2.1: Distributed porosity θ_s

Hillslope	Porosity_5cm	Porosity_20cm	Porosity_50cm
Low	0.52	0.44	0.36
Medium	0.59	0.49	0.41
High	0.65	0.55	0.52
Riparian	Porosity_5cm	Porosity_20cm	Porosity_50cm
Low	0.57	0.54	0.42
Medium	0.66	0.57	0.54
High	0.72	0.64	0.61

In a second modelling scenario (SC2), we investigated the effect of spatial heterogeneity of soil porosity on the simulation results. We considered a homogeneous case (SH1) and heterogeneous case SH2, in which soil porosity was fully distributed. The distributed porosity was determined from the maximum observed soil moisture at 104 monitoring locations, then interpolated to the whole domain using a Geographical Information System (ArcGIS, Esri, Redlands, CA), and subsequently clustered into 6 groups per layer (Figure 2.3, Table 2.1).

2.3.6 Validation Data

The validation of the simulation results was performed using observed states and fluxes in the Wüstebach catchment (i.e. soil moisture, runoff, and evapotranspiration) in daily resolution from January 2009 to May 2013. Using the same data, Graf et al. [2014] were able to close the local water balance of the Wüstebach catchment. Thus, this comprehensive data set is ideally suited for the validation of hydrological models like ParFlow-CLM.

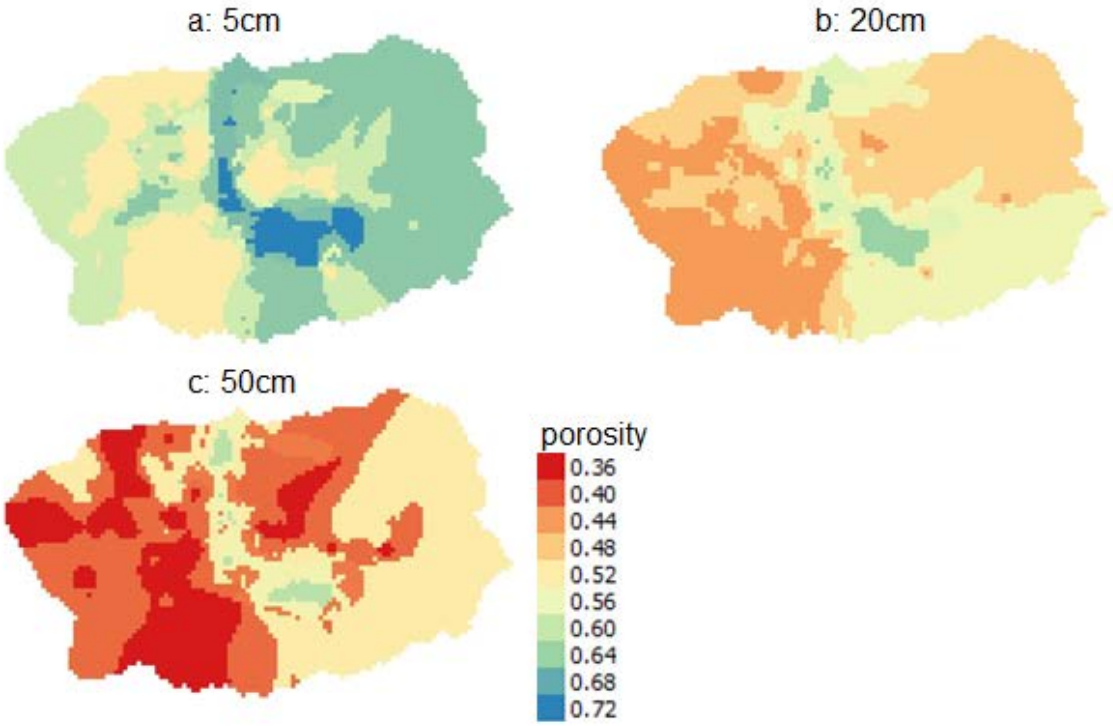

Figure 2.3: Estimated porosity distributions for three soil layers. (0 – 10 cm, 10 – 40 cm, and 40 -160 cm, respectively)

2.3.7 Empirical Orthogonal Function (EOF) Analysis

We employed the EOF method [Perry and Niemann, 2008] for a detailed analysis of the spatiotemporal pattern of simulated and observed soil moisture. Both observed and simulated soil moisture data sets contained 312 variables (104 monitoring points by 3 layers). Thus, we applied the EOF to the matrix of 312 measurement locations and 1096 days. This formed a 312 × 1096 matrix Y_0 with the soil moisture data, the rows representing the 312 measurement locations and the columns representing the 1096 measurement days. Then a new 312 × 1096 matrix Y was formed, each column of the matrix was average to zero with a prior removal of the means. Matrix Y can be expressed as a linear combination of new, statistically independent (orthogonal) columns Y' and their loadings (eigenvectors) E in matrix notation:

$$Y = Y' \times E^T \qquad (2.8)$$

where the superscript ^{T} indicates the matrix transpose. The matrix *Y'* contains the EOFs that can be used to create spatial patterns through interpolation. The first column of *Y'* describes as much as possible of the variance of *Y*, and can be used together with the first row of E^T as a memory-saving representation of a noise-reduced version of *Y*; the second and any further column of *Y'* describe as much as possible of the remaining variance.

As for the purpose of model validation, we followed the approach of Graf et al. [2014] and used only the first two EOF and loading time series. That means we only used the first two columns of *Y'*, Y'^*, with the largest two variance of *Y*, and the first two eigenvectors E^* to express a reconstructed 312 × 1096 matrix Y^* in Equation 2.9:

$$Y^* = Y'^* \times E^{*T} \qquad (2.9)$$

Then the reconstructed soil moisture matrix y^r was calculated using:

$$y_{ij}^r = y_{ij}^* + \overline{y_{0\iota}} \qquad (2.10)$$

where $\overline{y_{0\iota}}$ refers to the prior removal of the means.

The advantage of EOF analysis is that the spatiotemporal pattern of soil moisture can be represented by a largely reduced number of variables (from 312 × 1096 to 2 × 1096).

Following Graf et al. [2014], we focus in our validation analysis on the loadings EOF1 and EOF2 because they contain most of the soil moisture pattern information (see Chapter 2.4.6).

2.3.8 Wavelet Coherence Analysis

Wavelet analysis has been applied in catchment studies [Lauzon et al., 2004], model validation [Schaefli and Zehe, 2009], field-scale time series [Vargas et al., 2010], and in combination with EOF analysis [Parent et al., 2006]. The continuous wavelet transform of a time-dependent variable *y(t)* for a specific location along the time axis τ and a specific time scale s is given by Equation 2.11 [Si, 2008]:

$$W(s,\tau) = \int_{-\infty}^{\infty} y(t) \frac{1}{\sqrt{s}} \varphi^*\left(\frac{t-\tau}{s}\right) dt \qquad (2.11)$$

where φ^* is the complex conjugate of the mother wavelet φ which can be selected from a variety of functions. In this study we used the Morlet wavelet as the wavelet function. Two kinds of wavelet analysis were applied in our study: The global wavelet power spectrum analysis and the cross-wavelet spectrum analysis. The global wavelet power is calculated by averaging the wavelet powers over the localized time instances using:

$$\overline{W}^2(s) = \frac{1}{N} \sum_{n=0}^{N-1} |W_n(s)|^2 \qquad (2.12)$$

Similarly to Fourier analysis [e.g., Mauder et al., 2007], the wavelet transforms of two simultaneous samples variables can be used to compute the cross-wavelet spectrum. The cross-wavelet spectrum of two time series *x* and *y* can be calculated using:

$$W_n^{xy}(s) = W_n^x(s) W_n^y * (s) \qquad (2.13)$$

where $W_n^x(s)$ and $W_n^y(s)$ refer to the wavelet transform of time series *x* and *y*, respectively. Detailed descriptions of wavelet coherence methods are given in [Torrence and Compo, 1998], [Grinsted et al., 2004], [Si, 2008], and [Rahman et al., 2014].

As for the purpose of model validation, we followed the simplified setup as described in [Graf et al., 2014] to calculate the cross spectrum of simulated and observed variables such as averaged soil moisture, runoff, and evapotranspiration to illustrate the temporal variation in different seasons and time scales. In addition, global wavelet power was also calculated to provide comparison of temporal pattern between simulation and observation of soil moisture. The Matlab code for wavelet coherence analysis used in this study is described in detail in [Grinsted et al., 2004].

2.4 Results and Discussions

2.4.1 Estimation of Hydraulic Parameters

Using HYDRUS-1D and SCE-UA, soil hydraulic parameters for the whole model domain were inversely estimated. We tested two bottom boundary conditions: free drainage (FD) and seepage face (SF). The optimized parameters are listed in Table 2.2. Except for parameter α, both FD and SF boundary condition produced similar parameters. Both cases also produced similar soil moisture dynamics in 5 cm and 20 cm depth, indicated by the close RMSE and NSE values. However, we found that FD gives much better correspondence with observed soil moisture dynamics in 50 cm level compared to the SF boundary condition (RMSE and NSE increased from 0.021 to 0.032 and -0.475 to 0.342, respectively). This indicates that FD is the best boundary condition approximation, although the low permeability of the

underlying bedrock in the Wüstebach impedes deep drainage. Clearly, the simple HYDRUS-1D model cannot fully account for the complex soil-bedrock processes at the catchment scale. Nevertheless, given the reasonable simulation results of the HYDRUS-1D model, we selected the VGM parameters estimated using FD boundary condition for the ParFlow-CLM simulations. Further studies with more computational resources are needed to estimate heterogeneous hydraulic parameters from 3-D inverse calibration procedures with more differentiated boundary conditions.

Table 2.2: Estimated parameters of each layer of the whole domain under bottom boundary of FD and SF from HYDRUS inversion

5cm	θ_s	K_s(cm/d)	θ_r	α (1/cm)	n	RMSE	NSE
FD	0.57	803.35	0.122	0.010	1.26	0.0494	0.512
SF	0.55	1167.80	0.146	0.022	1.39	0.0483	0.533
20cm	θ_s	K_s(cm/d)	θ_r	α (1/cm)	n	RMSE	NSE
FD	0.49	1495.62	0.148	0.010	1.19	0.0277	0.521
SF	0.47	1494.36	0.149	0.031	1.22	0.0279	0.521
50cm	θ_s	K_s(cm/d)	θ_r	α (1/cm)	n	RMSE	NSE
FD	0.43	98.76	0.120	0.010	1.21	0.0211	0.3420
SF	0.40	138.52	0.075	0.027	1.27	0.0316	-0.475

2.4.2 Representation of the Interflow Process (SC1)

The results of our scenario analysis indicate that ET shows only very low sensitivity to the different Ks anisotropies (Table 2.3). In contrast, the soil moisture and runoff simulations are more strongly affected by the Ks scaling. For instance, a scaling factor of 20 provided much lower RMSE for soil moisture at both 5 cm and 50 cm depth (0.059 and 0.026, respectively). Increasing horizontal *Ks* also improved simulated runoff with RMSE reduced from 0.330 to

0.159. As a trade-off, we chose a scaling factor of 20 as a best compromise for the following ParFlow-CLM simulations.

Table 2.3: Statistical analysis of comparison of the five anisotropic simulation scenarios

RMSE	ET	Runoff	θ 5cm	θ 20cm	θ 50cm
isotropy	0.146	0.330	0.113	0.066	0.078
$10\times K_{sh}$	0.139	0.204	0.065	0.036	0.041
$20\times K_{sh}$	0.136	0.170	0.059	0.042	0.027
$40\times K_{sh}$	0.133	0.162	0.070	0.059	0.028
$80\times K_{sh}$	0.130	0.159	0.088	0.077	0.043

2.4.3 Effect of Heterogeneity

Based on the parameterization described above and the addition of the litter layer, we conducted three simulation cases with different spatial heterogeneity of soil porosity (see chapter 2.3.5). Figure 2.4 shows a comparison between average simulated and observed soil moisture of the two heterogeneity cases using the ParFlow-CLM model as well as the HYDRUS-1D simulation results. Whereas soil depths of 20 and 50 cm show mainly good correspondence between the simulations and observation, soil moisture simulations at 5 cm depth show distinct deviations from the observations. For instance, ParFlow-CLM overestimated in both cases soil moisture at 5 cm especially after strong precipitation events during the dry seasons. This bias is especially distinct for the dry spring season in 2011, which was also the driest spring season of the last 100 years. Interestingly, HYDRUS-1D was able to simulate this drying-up much better. One possible reason for the bias in the ParFlow-CLM simulations is that the drainage from the catchment is to some extent delayed due to the low topographic gradients in the riparian zone.

Another possible reason for the overestimation during drying phases is the presence of fast vertical bypass flow during strong precipitation events at the Wüstebach site as already suggested by [Cornelissen et al., 2014]. Recently, Wiekenkamp et al. [2015] analysed the preferential flow occurrence of the Wüstebach catchment in detail and found that bypass flow occurs especially during intensive rainfall and low antecedent soil moisture conditions induced by hydrophobicity. This finding supports our assumption that soil moisture overestimation is mainly caused by preferential in the topsoil especially during dry periods.

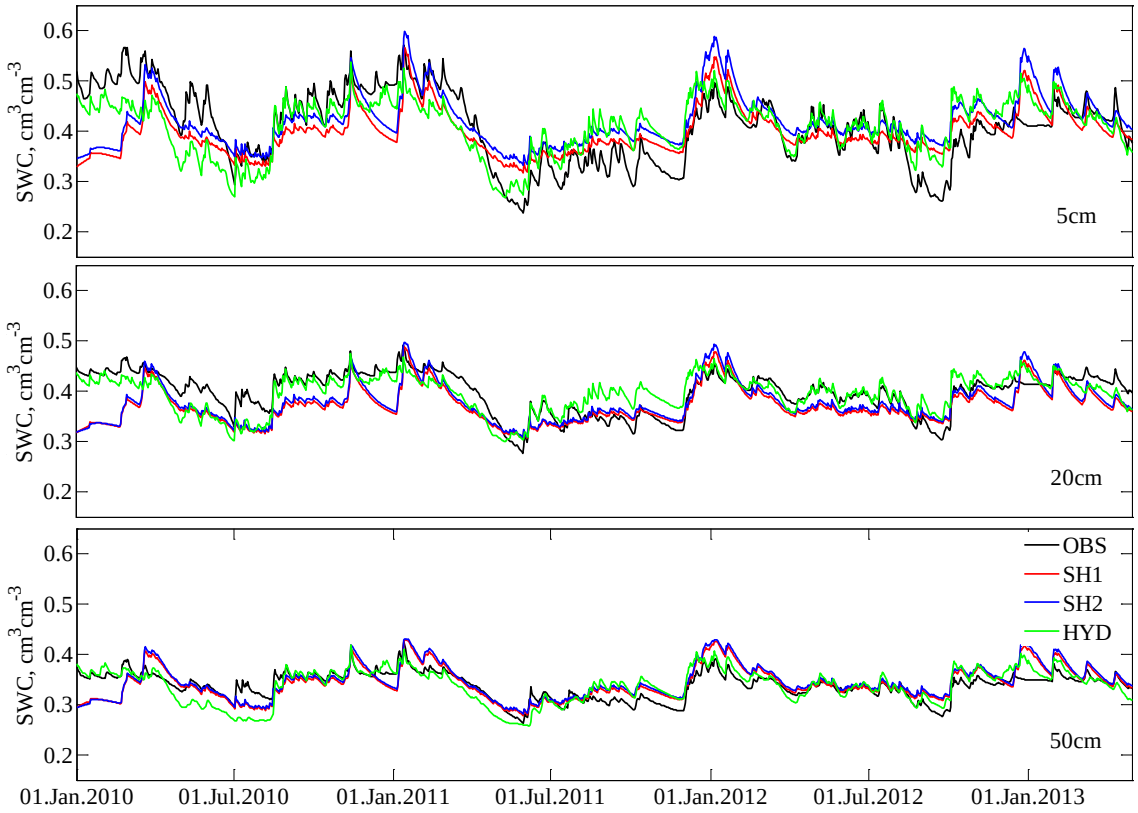

Figure 2.4: Observed and simulated daily soil moistures at depths of 5, 20 and 50 cm for different scenarios of spatial heterogeneity and the HYDRUS estimates.

Table 2.4: Statistical analysis of comparison of the simulation scenarios SH1 and SH2

	RMSE					NSE				
	ET	Runoff	θ 5cm	θ 20cm	θ 50cm	ET	Runoff	θ 5cm	θ 20cm	θ 50cm
SH1	0.142	0.173	0.064	0.035	0.025	-0.159	0.697	0.087	0.235	0206
SH2	0.141	0.173	0.052	0.032	0.022	-0.152	0.694	0.388	0.356	0.268

The simulation results of the two heterogeneity cases in terms of RMSE and NSE are presented in Table 2.4. We found that the ParFlow-CLM model was not very sensitive to the different cases of spatial heterogeneity in soil porosity in terms of ET and runoff. Whereas almost no difference in RMSE was found, NSE indicates that the simulation results were slightly worse in case of heterogeneous soil porosities. In contrast, the soil moisture simulation was clearly positively influenced by the application of heterogeneous soil porosities (the NSE value was 34% higher compared to SH1).

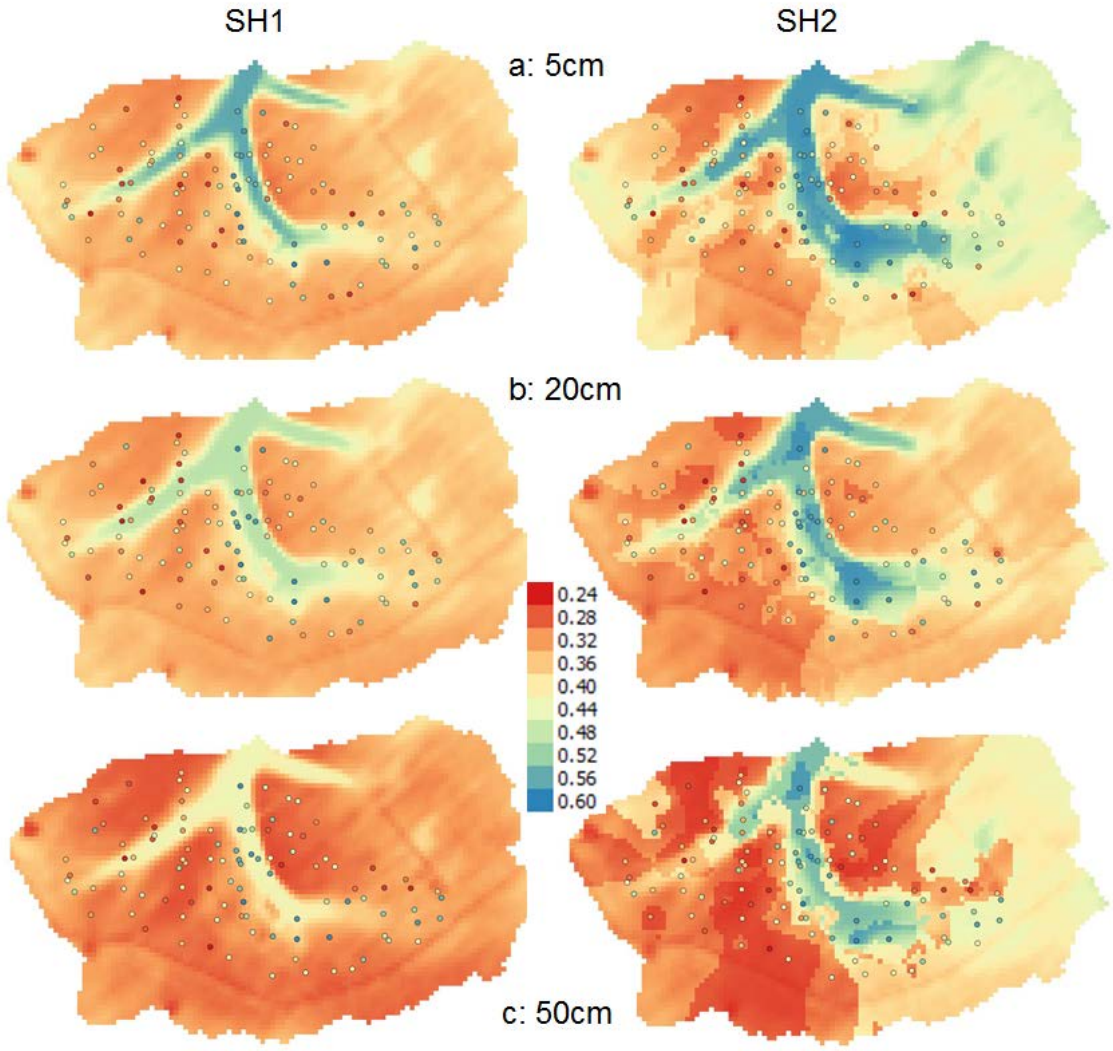

Figure 2.5: Observed and simulated soil moisture pattern at 5, 20, and 50 cm depth (3-year average between May 1, 2010 and April 30, 2013) of the two heterogeneity scenarios SH1 and SH2.

Figure 2.5 compares the simulated and observed soil moisture (average of the period between May 2010 and April 2013) for the three depths. The distributed case (SH2) better captures the main features of the observed soil moisture pattern, which is supported by the scatter plots shown in Figure 2.6. The Pearson linear correlation (R) increased considerable for all depths (Figure 2.6), but especially at 5 cm depth (R increased by ~60%). Clearly, this indicates that distributed information on porosity is important for an accurate simulation of soil moisture pattern.

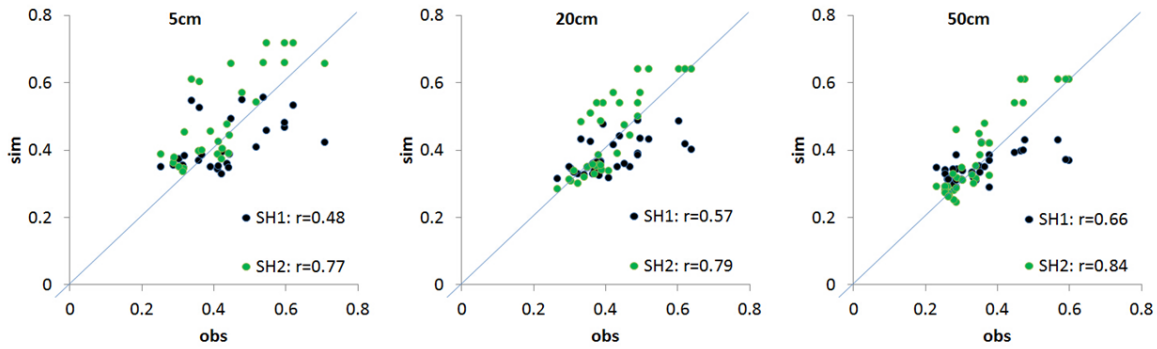

Figure 2.6: Scatter plot of observed and simulated 3-year averaged soil moisture of the two heterogeneity scenarios for the three soil depths.

2.4.4 Water Balance Closing

Figure 2.7 and Table 2.5 compare observed and simulated water budgets of the homogeneous and fully distributed cases for the three years simulation period. Both simulation cases gave very similar results. This was expected given the very similar runoff and ET simulation results of both cases (Table 5 shows results of SH2). The total simulated residual $r = P - ET - R_f$ of the three years period was -27.44 cm in SH1 and -27.10 cm in SH2, of which -18.91 (SH1) and -18.58 cm (SH2) is contributed by the first year. Since the *ET* measurements started on June 23 2010, this data gap had to be filled with a less reliable *ET* model [Graf et al, 2014], which is the main reason for the water budget discrepancy in the first year. In the latter two years, the annual residual of simulation is -3.7 cm and the annual residual percentage $r\% = r/P$ is -3.25%, which is lower than the SH1 case (~ -3.26%), and is acceptable compared to the residual of observation (~ -0.25%).

Table 2.5: Observed and simulated water budget elements (precipitation, ET, runoff, residual, and residual percentage) of the Wüstebach catchment for the total study period and annual sub-periods (case SH2)

unit in cm	P	Obs ET	Sim ET	Obs R	Sim R	obs r	obs r %	sim r	sim r %
May 2010 - April 2011	129.57	49.21	69.26	79.15	78.89	1.22	0.94%	-18.58	-14.34%
May 2011 - April 2012	130.32	62.11	64.54	59.58	66.40	8.62	6.62%	-0.62	-0.48%
May 2012 - April 2013	131.28	61.29	62.05	79.34	77.13	-9.35	-7.12%	-7.89	-6.01%
Sum	391.18	172.61	196.53	218.08	218.81	0.49	0.13%	-27.10	-6.93%

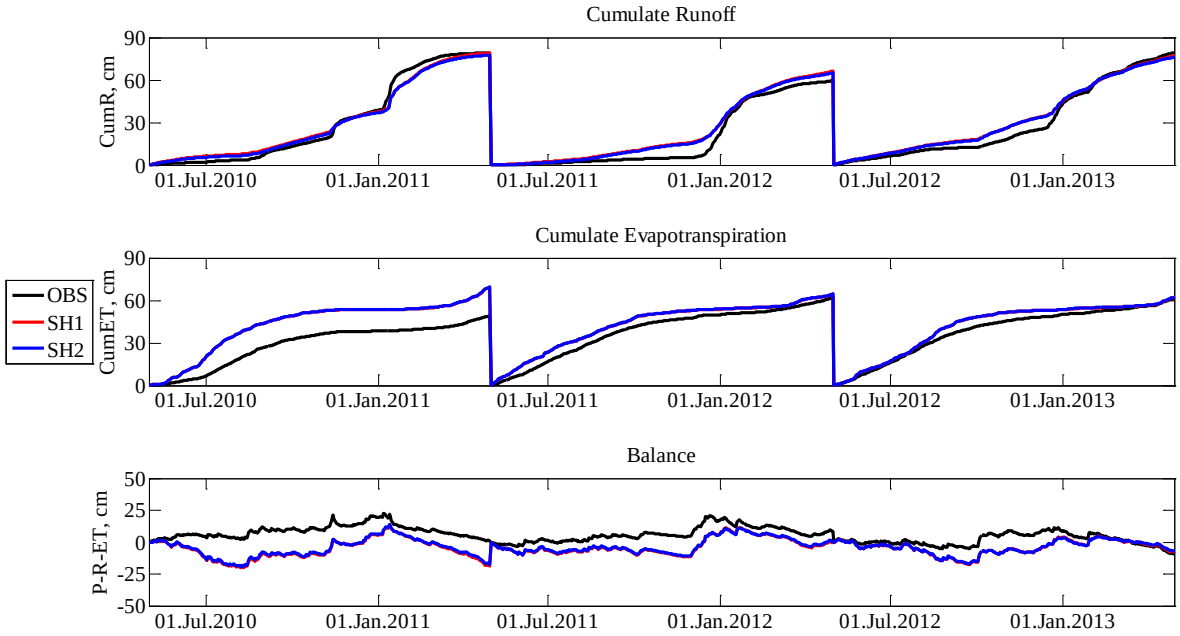

Figure 2.7: Observed and simulated water balance components for the period May 2010 – April 2013 using the two heterogeneity scenarios.

2.4.5 EOF Analysis

In the following we show results of our EOF analysis focusing on the loadings EOF1 and EOF2 which together describe more than 90% of the total variance of observed soil moisture pattern [Graf et al., 2014]. Figure 2.8 shows the loadings of EOF1 and EOF2 of the observed and simulated soil moisture time series plotted against spatially averaged soil moisture. From Figure 2.8 it becomes apparent that model case SH1 produced more scatter in the loadings of EOF1 as the heterogeneous cases SH2. EOF1 captures the most important spatial soil

moisture variation in the Wüstebach catchment, which is the soil moisture contrast between the hillslope and riparian zones (Figure 2.3). This contrast is mainly produced by the higher soil porosity in the riparian zone due to higher contents of organic matter (Figure 2.1).

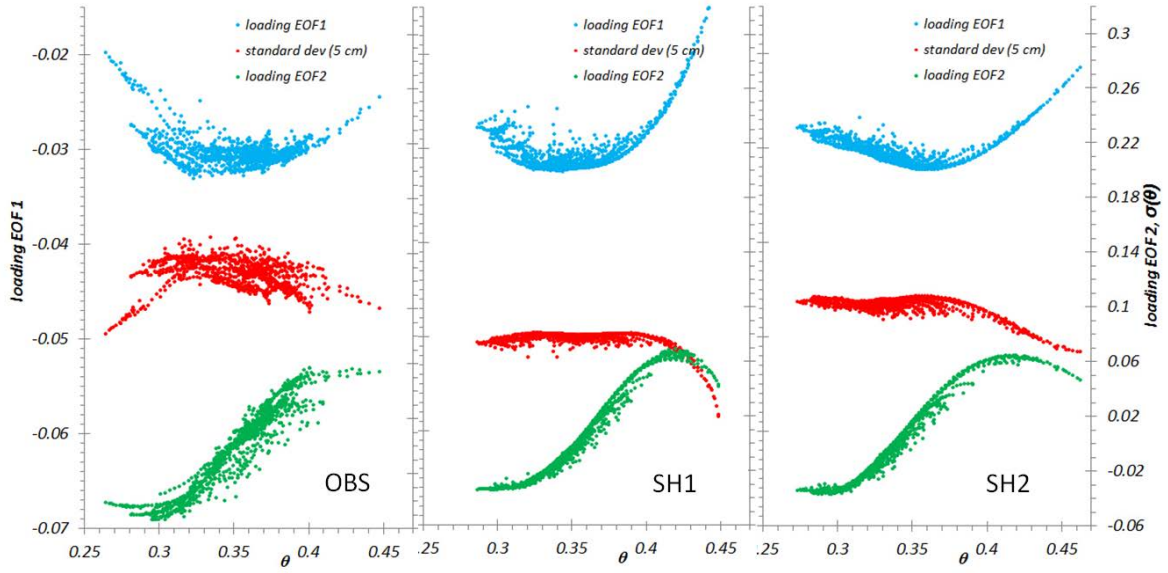

Figure 2.8: Loadings of the first two spatial soil moisture EOFs and spatial standard deviation at the 5 cm level against depth-averaged soil moisture θ for the soil moisture observation and ParFlow simulations using the three heterogeneity scenarios.

Both heterogeneity cases are able to reproduce the general pattern of the relationship between EOF2 loadings and mean soil moisture. In contrast to EOF1, the two cases did not produce strong differences in the EOF2 loadings. As the EOF2 loadings represent the second important spatial soil moisture variation, this indicates that the different heterogeneity in porosity did not produced further distinct differences in soil moisture patterns.

The EOFs of the soil moisture simulations also indicate the existence of a turning point θ_t as already found in the study by Graf et al. [2014] suggesting different spatial soil moisture pattern for mean soil moisture below and above θ_t. For example, the loadings of EOF1 show

a decreasing trend below θ_t and an increasing trend above θ_t for all cases. In contrast, EOF2 shows an increasing trend below and above θ_t . The value of θ_t case SH1 corresponds with the observations (~0.35). Introduction of heterogeneity θ_t is shifted very slightly to the wetter part that is negligible.

Figure 2.8 also shows the relationship between standard deviation of soil moisture and spatially averaged soil moisture. Clearly, both modelling cases produced less spatial variability in soil moisture compared to the observations. Standard deviation (STD) of scenario case SH1 is 32.0 % lower and STD of scenario case SH2 is 14.8 % lower compared to STD of the observations (~0.14). This is not surprising given the fact that the heterogeneity of the vegetation cover is not represented in the modelling. Interestingly, both cases did not reproduce the decrease in spatial variability towards the dry end. The main reason for this discrepancy is a generally longer lasting wetness contrast between the hillslope and riparian zones in the soil moisture simulations. For instance, the soil moisture observations indicated a dry-out of the riparian zone during the extremely dry spring season 2011, which was not reproduced by the ParFlow-CLM model (see Figure 2.4).

The ParFlow-CLM simulation also produced less scatter in the STD versus mean soil moisture relationship. As discussed by Rosenbaum et al. [2012] this scattering is the result of complex hysteresis loops at the event scale. After strong rainfall events, STD increases sharply indicating strong spatial variability in infiltration intensity due to small scale heterogeneities in soil properties and vegetation density. Since both soil and vegetation properties are homogeneous (expect for soil porosity for case SH2), it is not surprising that the STD versus mean soil moisture relationship shows less scattering.

2.4.6 Wavelet Coherence Analysis

In the following we present the results of the cross-wavelet coherence analysis using observed and simulated runoff, ET and soil moisture time series. Since both heterogeneity cases produced similar temporal dynamics in terms of catchment scale states and fluxes we focus on case SH2. Figure 2.9 presents the time series and the cross wavelet coherence plot of observed and simulated runoff. For the wavelet coherence plot it become apparent that good agreement between observed and simulated runoff exist especially for longer time scales, i.e. larger than one month, with R^2 being mostly larger than 0.9 throughout all the three years periods. Some breakdowns in coherence can be especially observed for shorter time scales less than 15 days. High coherence exists during very wet seasons, e.g. from October 2010 to January 2011 and from January to March 2012, and during distinct runoff events. Taking January 1 2012 as an example for a wetting period, high correlation exists for time scales larger than 15 days indicating that simulated and observed runoff are in good agreement. This is also confirmed by the almost uniform rightward arrowheads indicating delayless correlation.

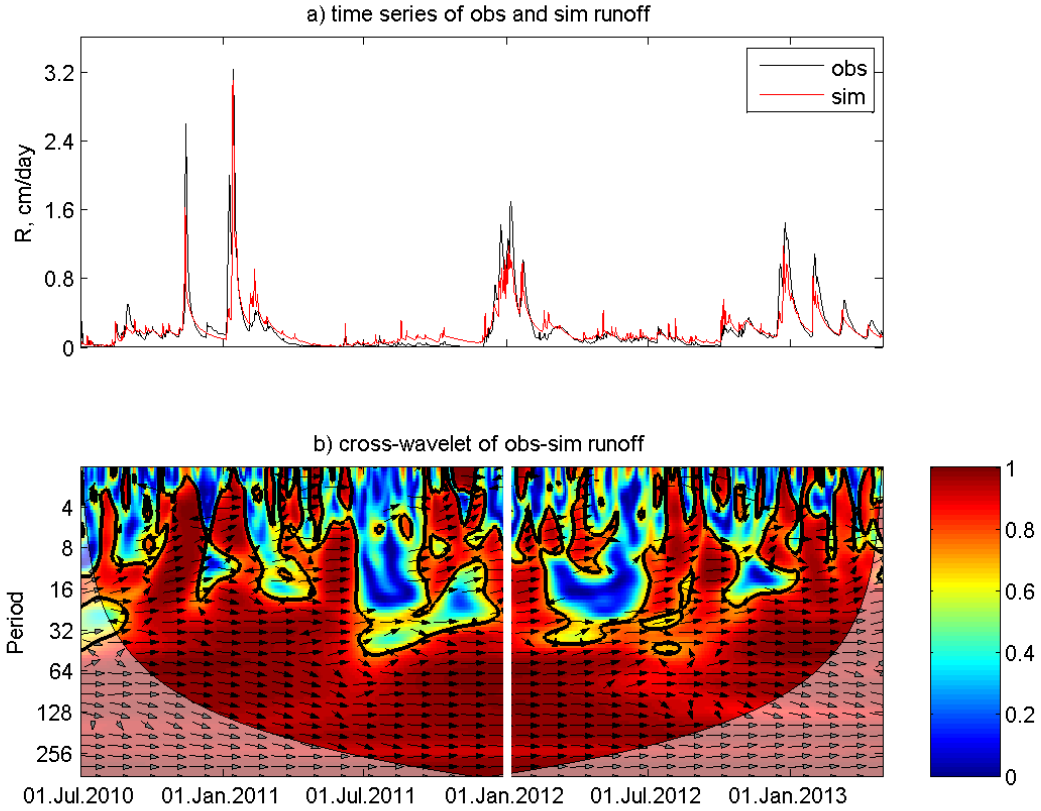

Figure 2.9: Cross wavelet coherence analysis for scenario SH2 for runoff. Phase arrows indicate the relative phase relationship between the series (pointing right: delayless correlation; left: anti-correlation; down: observation leading simulation by 90°).

The cross-wavelet coherence plot shown in Figure 2.10 reveals generally lower coherence between observed and simulated evapotranspiration compared to runoff. For the dry season from March to June 2011, coherence is especially low and with presence of anti-correlation (leftward arrow) with a time scale around 30 days. On the other hand, during the wet season from April to December 2012, zones of high coherence exist with time scales larger than 60 days. These findings indicate seasonality of ET simulation accuracy. During wet seasons, the ParFlow-CLM model provides reasonable simulation results, while during dry seasons, delays and anti-correlation in the coherence plots indicate the model is not able to reproduce short-term fluctuations in evapotranspiration.

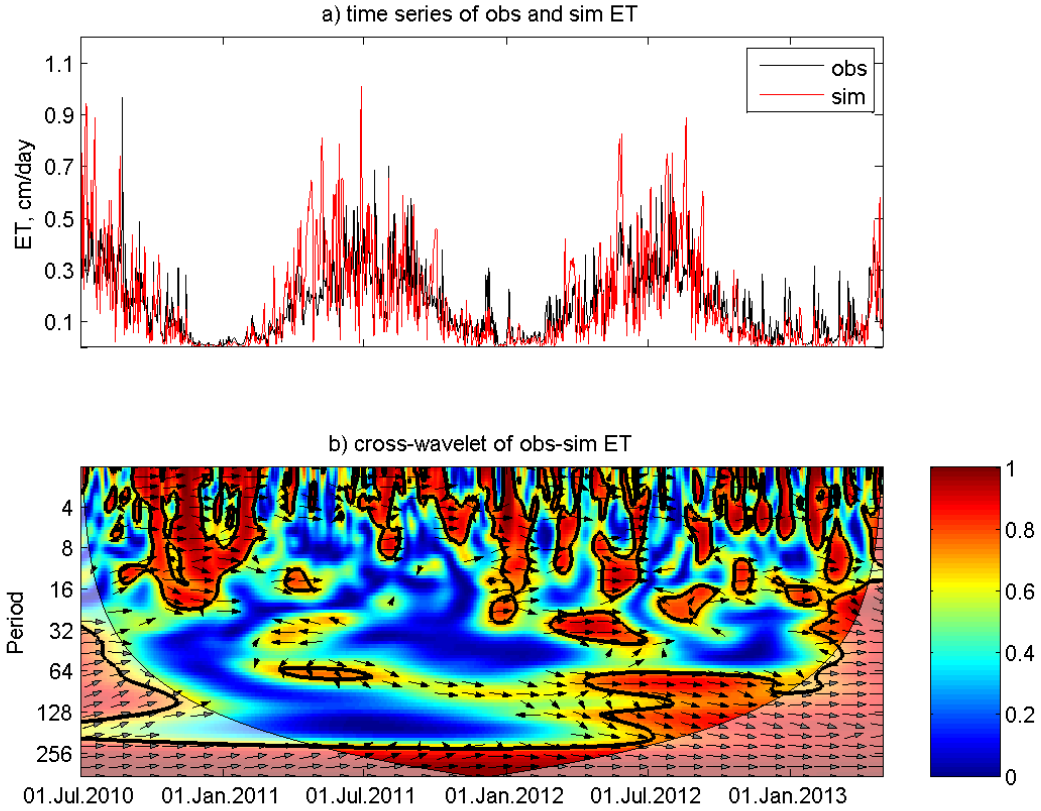

Figure 2.10: Cross wavelet coherence analysis for scenario SH2 for ET. Phase arrows indicate the relative phase relationship between the series (pointing right: delayless correlation; left: anti-correlation; down: observation leading simulation by 90°).

Figures 2.11, 2.12 and 2.13 show cross-wavelet coherence plots of observed and simulated soil moisture at 5, 20 and 50 cm depth, respectively. In general, the wavelet coherence plots show similar pattern for all depths. For instance, the plots reveal breakdowns in coherence for shorter time scales (i.e. less than 15 days) for all three depths. Higher coherence exists mainly for time scales larger than 30 days with few delays and anti-correlations. Interestingly, for time scales between 64 and 128 days two distinctive zones of low coherence exist for all soil depths (between January to June 2011, and between August to December 2012, respectively). Both zones of low coherence are coincident with dry periods. The first zone coincident with

the extraordinary dry period between March to June 2011 with only 0.24 cm of precipitation during that time.

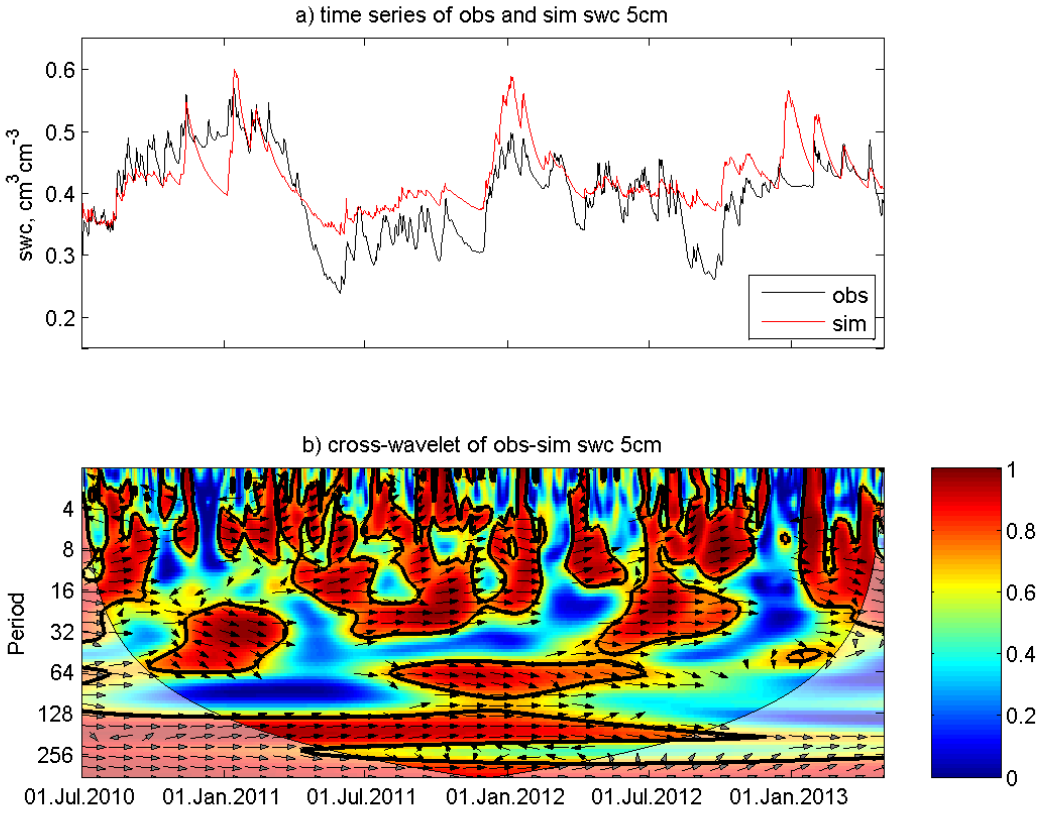

Figure 2.11: Cross wavelet coherence analysis for observed and simulated soil moisture at 5 cm depth (case SH2). Phase arrows indicate the relative phase relationship between the series (pointing right: delayless correlation; left: anti-correlation; down: observation leading simulation by 90°).

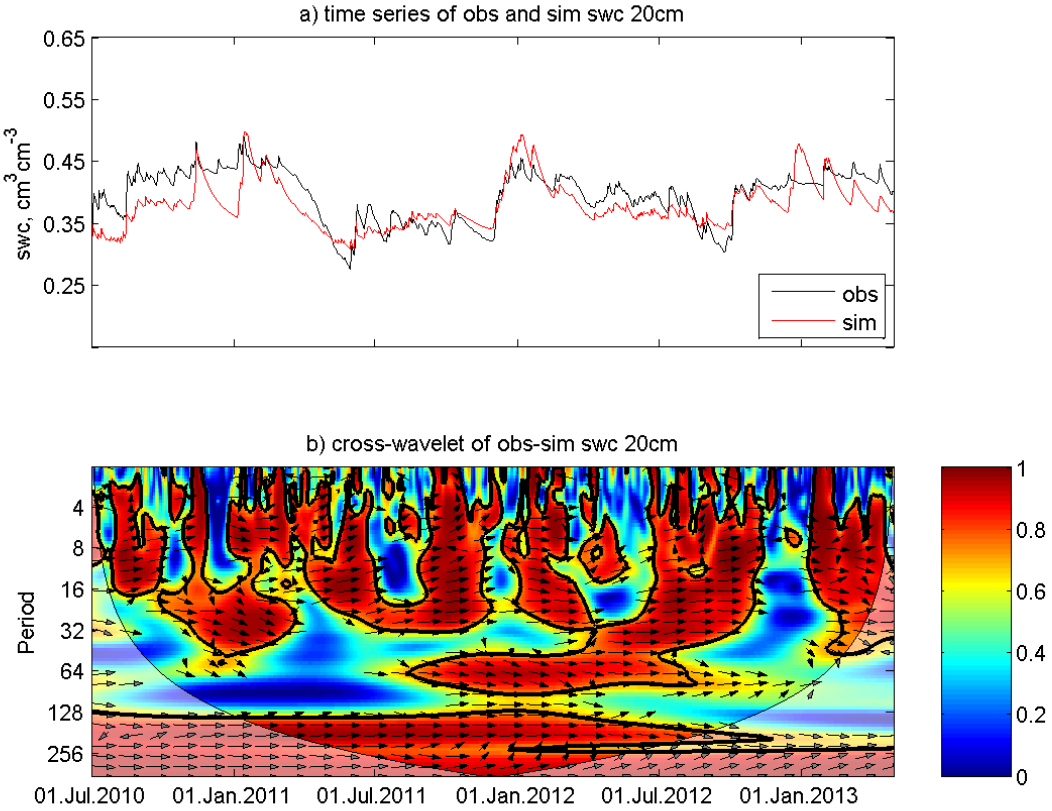

Figure 2.12: Cross wavelet coherence analysis for observed and simulated soil moisture at 20 cm depth (case SH2). Phase arrows indicate the relative phase relationship between the series (pointing right: delayless correlation; left: anti-correlation; down: observation leading simulation by 90°).

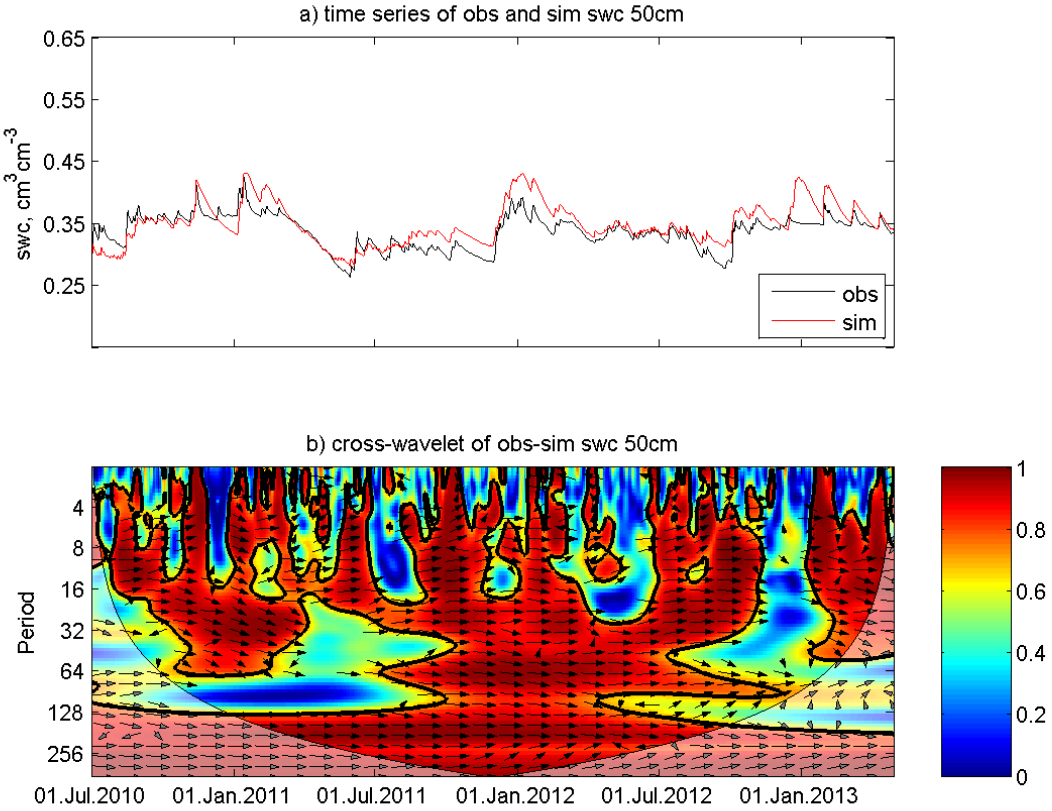

Figure 2.13: Cross wavelet coherence analysis for scenario SH2 for soil moisture at 50 cm. Phase arrows indicate the relative phase relationship between the series (pointing right: delayless correlation; left: anti-correlation; down: observation leading simulation by 90°).

To further analyze the reason for these breakdowns in coherence, we also present time localized powers wavelet plots taking the soil moisture times series at 20 cm as an example (Figure 2.14). In the first period, two distinct zones at time scale of about 64 days are noticeable in the power spectrum of the simulation results, which are not present in observational data. This indicates that the ParFlow-CLM model produced artefacts in the soil moisture simulation at a time scale of about 64 days. These artefacts are coincident with the dry periods as already discussed in Chapter 2.4.4.

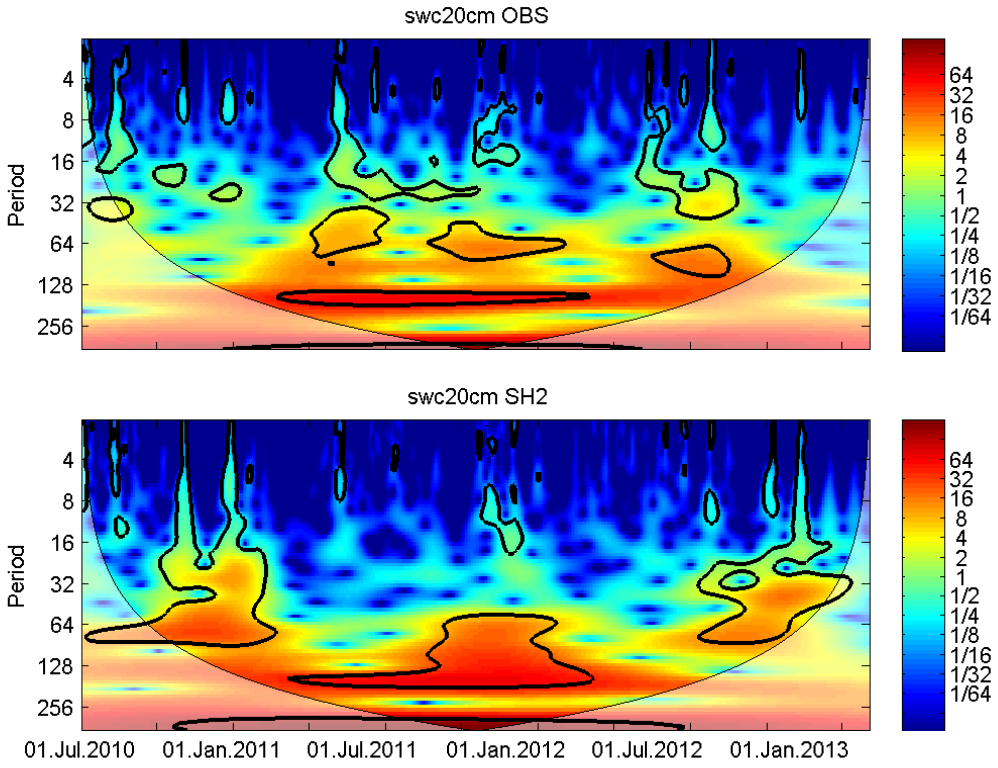

Figure 2.14: Power spectrum of observed and simulated (case SH2) soil moisture at 20 cm.

At all depths, soil moisture was simulated by ParFlow-CLM with high coherence between August 2011 to June 2012 at a time scale of 64 days as well as 128 days almost without delay (Figures 2.11, 2.12 and 2.13). Also for the period from July 2011 to March 2012, which is characterized by generally higher soil saturations, good agreement between simulated and observed soil moisture time series can be found (R^2: ~0.9). This indicates that the ParFlow-CLM model was better able to reproduce soil moisture dynamics during wet conditions.

2.5 Conclusions

We applied the 3-D hydrological model Parflow-CLM to the forested headwater catchment Wüstebach. We tested different parameterization strategies with respect to soil properties taking the anisotropy of Ks and the heterogeneity of soil porosity as examples. Finally, we

explored the methods of EOF and cross-wavelet coherence for an in-depth analysis of our model results.

We found that scaling factor of 20 for the horizontal K_s of the soil layer that overlies the impermeable bedrock increased the model performance in terms of runoff and soil moisture dynamics, but not for ET. This indicates that the interflow process plays an important role for the generation of runoff in the Wüstebach catchment. Furthermore, we could show that spatial information on porosity can significantly improve the simulation of spatial pattern of soil moisture using a 3D hydrological model.

Our EOF analysis showed that the spatial pattern of observed soil moisture content is better reproduced by the ParFlow-CLM model with distributed soil porosity information used. However, given the limited heterogeneity in the input parameters, the spatial variability of simulated soil moisture was clearly lower compared to the observations. Nevertheless, the EOF analysis indicated the ParFlow-CLM model was able to reproduce a characteristic turning point θ_t as already found in the study by Graf et al. [2014], suggesting different spatial soil moisture pattern for mean soil moisture below and above θ_t.

Using the cross-wavelet coherence analysis we were able to analyze the model results in more detail. For instance, the analyses revealed that the ParFlow-CLM model can reproduce the soil moisture observations better during wet seasons. Dry seasons were suffered from delays of correlation and even anti-correlation between simulated and observed soil moisture. Our detailed analysis of the ParFlow-CLM model results reveals a general overestimated of soil moisture content during dry seasons. We attribute this shortcoming to the low topographic gradients of the riparian zone that may have led to an underestimation of lateral

drainage and thus overestimation of riparian zone wetness. Another possible reason is the presence of fast vertical bypass flow during strong precipitation events at the Wüstebach catchment, which cannot be considered by ParFlow-CLM.

Future studies should consider heterogeneous hydraulic parameters to increase the model performance. Such information could be generated by 3-D inverse calibration, which is, however, not feasible at the moment because of computational constraints. In addition, higher spatial resolution could help to reduce low topographic gradients effect in flat area like riparian zones. The effect of terrain on ParFlow simulation results was not regarded in this study and but should be investigated in future studies. Finally, by enhancing the ParFlow-CLM to consider by-pass flow during infiltration, a better agreement of the soil moisture simulation during dry periods could be achieved.

3 Scale dependent parameterization of soil hydraulic conductivity in 3D simulation of hydrological processes in a forested headwater catchment

This chapter has been published as: Fang, Z., Bogena, H., Kollet, S., Vereecken, H., 2016. Scale dependent parameterization of soil hydraulic conductivity in 3D simulation of hydrological processes in a forested headwater catchment. Journal of Hydrology. 536, 365-375.

3.1 Abstract

In distributed hydrological modelling one often faces the problem that input data need to be aggregated to match the model resolution. However, aggregated data may be too coarse for the parametrization of the processes represented. This dilemma can be circumvented by the adjustment of certain model parameters. For instance, the reduction of local hydraulic gradients due to spatial aggregation can be partially compensated by increasing soil hydraulic conductivity. In this study, we employed the information entropy concept for the scale dependent parameterization of soil hydraulic conductivity. The loss of information content of terrain curvature as consequence of spatial aggregation was used to determine an amplification factor for soil hydraulic conductivity to compensate the resulting retardation of water flow. To test the usefulness of this approach, continuous 3D hydrological simulations were conducted with different spatial resolutions in the highly instrumented Wüstebach catchment, Germany. Our results indicated that the introduction of an amplification factor can effectively improve model performances both in terms of soil moisture and runoff simulation. However, comparing simulated soil moisture pattern with observation indicated that uniform application of an amplification factor can lead to local overcorrection of soil hydraulic conductivity. This problem could be circumvented by applying the amplification factor only to model grid cells that suffer from high information loss. To this end, we tested two schemes to define appropriate location-specific correction factors. Both schemes led to improved model performance both in terms of soil water content and runoff simulation. Thus, we anticipate that our proposed scaling approach is useful for the application of next-generation hyper-resolution global land surface models.

3.2 Introduction

In recent years distributed hydrological models are becoming increasingly realistic through the availability of high performance computing and integrated field observations [Kollet et al., 2010; Wood et al., 2011]. However, the reliable consideration of the impacts of small scale heterogeneity on the simulation of water fluxes at larger spatial scales is still a critical issue in hydrological modelling [Clark et al., 2015]. Topography is one of the main factors governing hydrological dynamics and a change of scale (grid size) in topographic discretization means that hydraulic parameters, such as saturated soil hydraulic conductivity (K_s) must be upscaled/recalibrated [Grayson and Blöschl, 2000]. Many modelling studies demonstrated the importance of correct parametrization of K_s and preferential flow on the simulation of soil moisture, evapotranspiration, groundwater dynamics, runoff, solute transport and erosion [Bogena et al., 2002; Simunek et al., 2003; Weiler, 2005; Maxwell and Kollet, 2008 and Yu et al., 2014].

Several studies investigated the effect of model resolution on simulation of hydrological processes [e.g. Geza and McCary, 2008; Kumar et al., 2009; Ye et al., 2010]. Very recently, Cornelissen et al. [2014] investigated the influence of spatial and temporal resolution on 3D simulation of hydrological processes. They studied the scale dependency of water balance and discharge simulation using different spatio-temporal resolutions and found that process-based scaling is a promising way to increase model accuracy at coarse resolutions.

Several studies showed that entropy theory could be used to quantify the loss of information content and the effect of aggregation of topographical data and model parameters [Singh, 1997; Vieux, 1993; Mendicino and Sole, 1997; Kuo et al., 1999; Krebs et al., 2015]. Niedda

[2004] utilized the entropy concept in a 2D modelling framework. He introduced an amplification factor for the upscaling of K_s by related its value to the loss of terrain curvature information. This information driven upscaling of K_s led to a much better agreement between observed and simulated runoff.

In this study, we employed the approach of [Niedda, 2004] to test whether information driven upscaling of K_s is also useful for the simulation of soil water content dynamics in a 3D modelling framework. The modelling of soil water content dynamics was accomplished using the three-dimensional, variably saturated water transport code ParFlow-CLM [Maxwell et al., 2014]. We selected the Wüstebach catchment as a case study area utilizing the comprehensive validation data sets from atmospheric, pedological and hydrological monitoring equipment [Bogena et al., 2010; Bogena et al., 2015] for the analysis of pattern in soil-vegetation-atmosphere systems [Simmer et al., 2015].

In our study, we focused on the following research questions:

1) How can the terrain curvature information from different resolution Digital Elevation Models (DEMs) of the Wüstebach catchment be represented using the information entropy concept?

2) Which is the best strategy to compensate the information loss in terms of estimated soil water content and runoff?

3) Can spatial aggregation of a three-dimensional hydrological model be compensated by parameter upscaling using the information entropy concept?

3.3 The experimental setup

3.3.1 The experimental test site Wüstebach

This research was conducted in the Wüstebach test site (Figure 3.1), which is a 38.5 ha large experimental catchment of the TERENO Eifel/Lower Rhine Valley Observatory [Zacharias et al., 2011] and the Collaborative Research Centre TR32 [Vereecken et al., 2010; Simmer et al., 2015] located in the national park Eifel. The altitude ranges from 595 m in the north to 628 m in the south and the average slope is 3.6 % with maximum values near the riparian zone (up to 10.4 %). The bedrock is mainly composed of fractured Devonian shales exhibiting very low hydraulic conductivity (10^{-9} to 10^{-7} m/s) [Graf et al, 2014]. The bedrock is overlain by a periglacial solifluction layer with an average thickness of 1.6 m. Cambisols and Planosols are mainly located on hillslope zone, whereas Gleysols and half-bogs have been developed in the riparian zone under the influence of groundwater [Bogena et al., 2015]. The prevailing soil texture is silty clay loam with a medium to high fraction of coarse material. The litter layer has a thickness about 5 cm [Richter, 2008]. More than 90% of the forest is comprised of Norway spruce trees planted in 1946 [Etmann, 2009], with a typical canopy height of about 25 m [Bogena et al., 2015]. The test site belongs to the temperate climate zone with a mean temperature of about 7°C and exhibits a long-term mean annual precipitation amount of 1310 mm for the period 1981 to 2013.

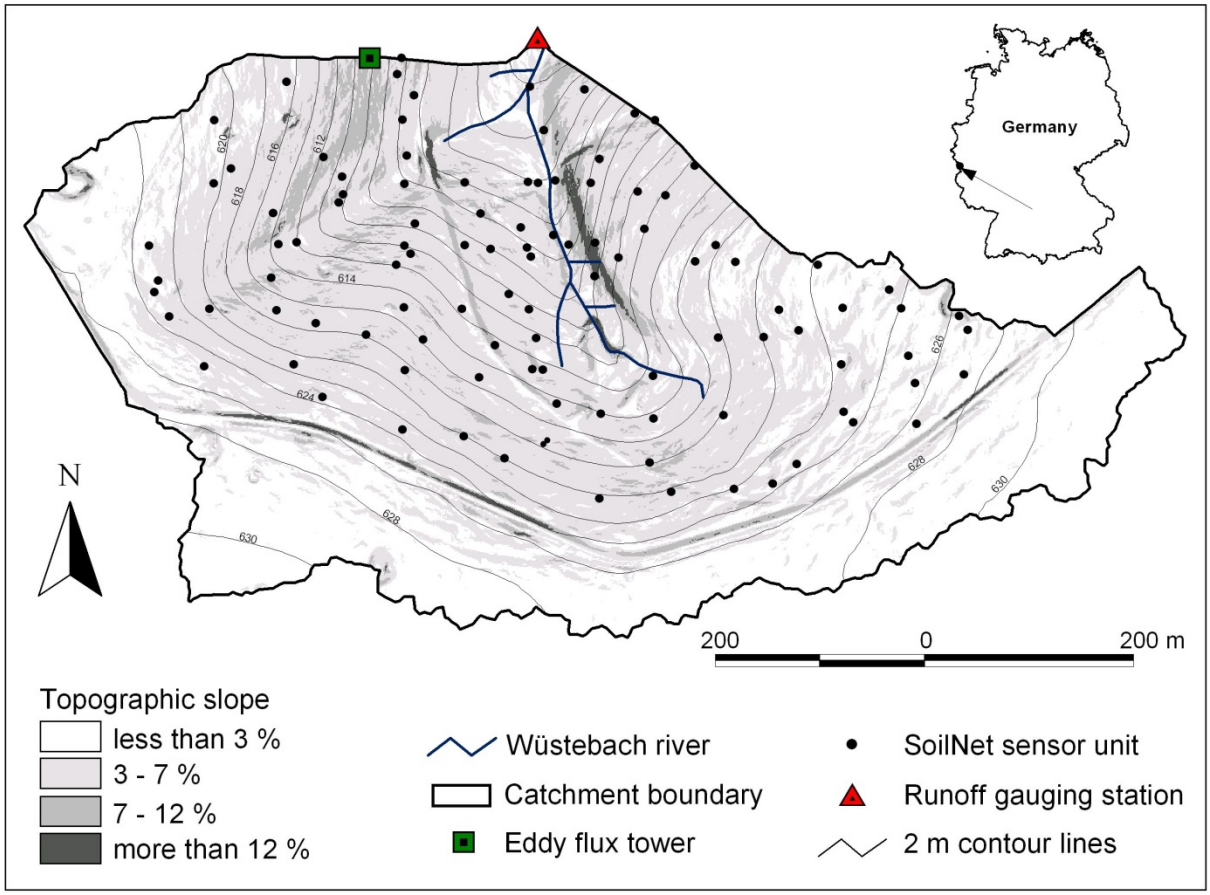

Figure 3.1: Map of the Wüstebach experimental catchment including instrumentations and topographic slope distribution.

3.3.2 Hydrology data collections

We made use of long-term soil moisture data from a wireless senor network installed in the Wüstebach catchment consisting of 150 sensor nodes [Bogena et al., 2010]. Each node is equipped with four ECH2O EC-5 and two 5TE sensors (Decagon Devices, Inc.) measuring soil moisture in three depths (5, 20 and 50 cm) with a temporal resolution of 15 min. Calibration of the ECH2O sensors is explained in detail in Rosenbaum et al. [2012]. Representative sensor network locations were identified and outliers were removed using EMI (electromagnetic imaging) data [Cornelisson et al., 2014]. Accordingly, soil moisture observations at 104 sensor nodes were used in this study. Discharge is measured at the

catchment outlet using a runoff station equipped with a combination of a V-notch weir for low flow measurements and a Parshall flume to measure mean to high flows [Bogena et al., 2015]. For the parameterization of atmospheric forcing we used hourly information on global radiation, precipitation rate, air temperature, wind speed, air pressure, and specific humidity from the Kalterherberg climate station of the German Weather Service (located 9.6 km west of the Wüstebach catchment).

3.4 Model and methods

3.4.1 The ParFlow-CLM model

ParFlow-CLM is a grid based, fully integrated water transport model that solves the Richards' equation in 3D [Ashby and Falgout, 1996]. The coupled land surface model CLM simulates the land surface energy mass balance components [Dai et al., 2003]. ParFlow-CLM simulates 2D surface flow by solving the kinematic wave equation. See Maxwell et al. [2014] and Fang et al. [2015] for a detailed description and a recent application of the ParFlow-CLM model at the Wüstebach catchment. In this research, we applied the newest version v693 of Parflow-CLM for numerical simulation.

3.4.2 Model Setup

We used a similar model setup as Fang et al. [2015]. The model domain used for the Wüstebach catchment has a total size of 1180 m × 740 m and a uniform depth of 1.6 m, which corresponds to the averaged measured soil depth. In addition, following Bogena et al. [2013] a litter layer was considered with a uniform depth of 0.05 m. We used a 1 m DEM of the Land Surveying Office of North Rhine-Westphalia to spatially discretize the model

domain and to assign slope values to each grid. The vertical resolution of the model domain was set to 0.025m.

The soil profile was differentiated into four different soil horizons with specific hydraulic properties following Bogena et al. [2013] to represent the vertical heterogeneity: a soil covering litter layer (+0.05-0 m), a top A horizon (0-0.1 m), an intermediate B horizon (0.1-0-4 m), and a C horizon (0.4-1.6 m) overlaying the bedrock. Soil hydraulic properties were parameterized using the van Genuchten - Mualem model [van Genuchten, 1980]. Parameters θ_r, α and n were assumed homogeneous within each soil horizon. We assumed no vertical leakage into the bedrock due to its extremely low permeability [Graf et al., 2014].

The simulation was conducted on hourly time steps for 365 days from May 1, 2012 to April 30, 2013. A spin-up phase from January 1 to April 30, 2012 was conducted with an initial condition of constant pressure in -2.0 m. The simulations were performed on the high performance computer JUROPA of the Jülich Supercomputing Centre. More information on the model setup is presented in Fang et al. [2015].

3.4.3 Upscaling of saturated hydraulic conductivity using the entropy concept

In this study, we used the same soil hydraulic parameters θ_r, α and n for the litter and soil layers as Fang et al. [2015] based on HYDRUS-1D inverse modelling (Table 3.1). We used the same distributed θ_s field as Fang et al. [2015]. For the saturated hydraulic conductivity K_s, we instead used an extensive data set based on double infiltrometer measurements at 108 locations within the Wüstebach catchment [Wiekenkamp et al., 2015]. Because the double infiltrometer measurements integrate over the whole soil profile, we assumed that the local K_s is vertically homogeneous. We believe that this assumption is valid given the generally low

soil depth in the Wüstebach catchment (1.6 m on average). We interpolated the point data to the whole model domain using multilevel B-Spline Interpolation (BSI) [Lee et al., 1997] in SAGA-GIS software version 2.1.4. [Böhner et al., 2006]. (Figure 3.2).

Table 3.1: Hydraulic Parameters for the litter and soil layers (refer to Fang et al., 2015)

	θ_r	α (1/cm)	n
litter	0	0.026	1.29
5cm	0.122	0.01	1.26
20cm	0.148	0.01	1.19
50cm	0.12	0.01	1.21

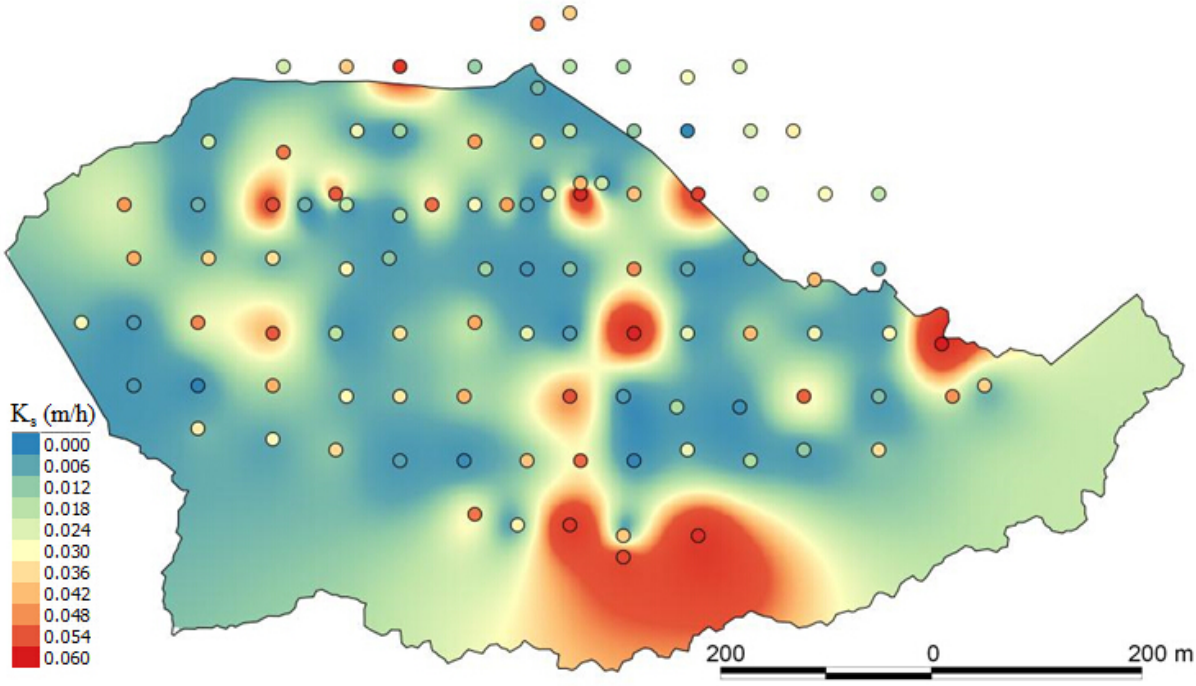

Figure 3.2: K_s distribution for 1 m resolution with multilevel B-Spline Interpolation (BSI).

The entropy concept can be used to describe the effect of spatial aggregation on terrain information [Singh, 1997]. Following Niedda [2004], we used the entropy concept based on terrain curvature information for the upscaling of the K_s fields. The terrain surface can be described as a function of horizontal coordinates, i.e. *f(x,y)* and the gradient of this surface

can be denoted as ∇f. The terrain curvature κ_p describes the rate at which the surface slope *S* changes and can be expressed in a coordinate-free form as [Peckham, 2003]:

$$\kappa_p = -S^{-1}(\nabla S \cdot \nabla f) \qquad (3.1)$$

In this study, the terrain curvature was derived from digital elevation information using SAGA-GIS software version 2.1.4 [Böhner et al., 2006]. Spatial aggregation of terrain information can lead to a reduction of local hydraulic gradients due to smoothing effects. This impact can be partially compensated by increasing local soil hydraulic conductivity using an amplification factor in order to produce the same water flow rate [Niedda, 2004]. The amplification factor can be derived from the loss of terrain curvature information described in the following. In a first step, the information content *I* is calculated using:

$$I = -\sum_{j=1}^{N} p_j \ln(p_j) \qquad (3.2)$$

where *N* is the number of bins into which the parameter range (between the minimum and maximum of profile curvature in this study) is divided and p_j is the proportion of elements in the bin *j*. We followed the approach of [Niedda, 2004] and used bins 0.001 wide for the calculation of the terrain curvature information content.

Next, the terrain curvature information is related to the amplification factor τ using the following equation [Niedda, 2004]:

$$I = I^* - ln\tau \qquad (3.3)$$

where I^* is the curvature information content at the highest resolution (in this case 1 m). In this specific case, τ equals 1 since we assume that the effective saturated hydraulic conductivity (K_s^*) equals K_s. Thus, at 1 m resolution I^* can be equated with I and I^* and thus can be used to determine values for τ for the lower resolution cases. Finally, K_s^* fields for each aggregation level can be derived using:

$$K_s^* = \tau K_s \qquad (3.4)$$

Consequently, the hydraulic conductivity of all grid cells of the model domain will be increased by the same factor without considering the impact of locally varying information loss, because of spatially varying relief. However, it would be more useful to apply the localized amplification factor only to aggregated regions that exhibit information loss (i.e. decrease in hydraulic gradient). Therefore, we developed two types of selection strategies to ensure that only those grid cells are considered that are prone to significant information loss. The first selection strategy uses the standard deviation (STD) of slope values at 1 m resolution as indicator for the variations in hydraulic gradient. The second selection strategy involves the calculation of the partitioning parameter γ using equation 3.5:

$$\gamma = \frac{S_{low}}{S_{high,max}} \qquad (3.5)$$

where S_{low} is the slope of a grid cell of the low-resolution DEM and $S_{high,max}$ is the maximum slope of the high-resolution DEM for the same area. High values of STD and γ indicate grids cells, which are prone to information loss due to spatial aggregation, while smaller values of

STD and γ indicate grid cells of lower scale dependence. The values of γ are in the range between 0 and 1, where $\gamma = 0$ indicates a flat surface and $\gamma = 1$ indicates no information loss. We then conducted a statistical analysis to determine the threshold values for STD and γ based on slope information because curvature values tend to be both positive and negative and thus cannot be used as threshold criteria. Since slope values are always positive, they can be used for this purpose.

3.4.4 Scenario analysis

Using the derived amplification factors we calculated K_s^* fields for different spatial resolutions. We then used these K_s^* fields in the ParFlow-CLM simulation of the Wüstebach catchment and compared the simulated with observed SWC and runoff time series. Furthermore, we conducted and compared four simulation scenarios using the 10 m resolution model that are based on the heterogeneous K_s^* fields as described in section 3.4.3:

- Scenario 1 (S1): No amplification factor is applied to the K_s field.
- Scenario 2 (S2): A global amplification factor is applied to all grid cells of the computational domain.
- Scenario 3 (S3): A localized amplification factor is applied only to grid cells that exceed the STD threshold value.
- Scenario 4 (S4): A localized amplification factor is applied only to grid cells that fall below the threshold value of γ.

The purpose of using scenario S1 is to illustrate the negative effect of terrain information loss on simulated soil moisture and runoff in the Wüstebach catchment. With S2 we investigate how well model estimates can be improved by directly applying the amplification factor approach of [Niedda, 2004]. The latter two model scenarios S3 and S4 are performed to

evaluate whether localized application of the amplification factor will led to better simulation results in terms of soil moisture and runoff compared to the first two scenarios S1 and S2.

S1 and S3 were also applied to simulations using the 20 m resolution for purpose of comparison between different resolutions (Scenarios S1_20m and S3_20m). The results are presented and discussed in the following section. Unfortunately, due to the limitation of computational time and convergence problem, the simulation results of 5 m and 1 m resolution are not available at this present. Figure 3.3 shows an organigram to illustrate the flowchart of our methodology.

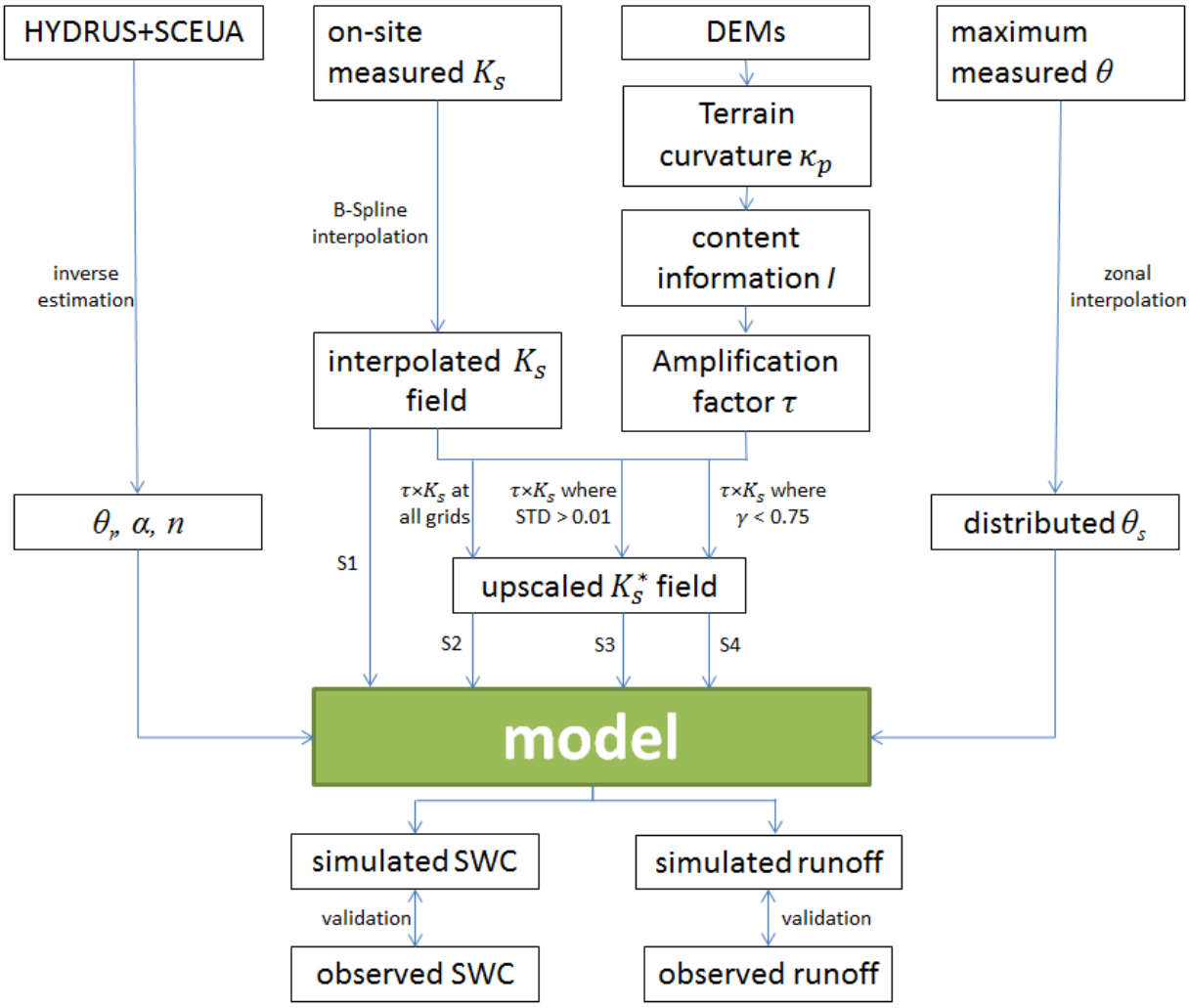

Figure 3.3: Schematic outline of the modelling process.

3.5 Results and discussions

3.5.1 Information contents and amplification factors

Figure 3.4 shows the cumulative frequency distribution of terrain curvature derived for each DEM resolution. As expected, the 1 m DEM contains the most detailed terrain curvature information and spatial aggregation resulted in significant loss of this information. The 5 and 10 m DEMs lost curvature information especially in the range of -0.01 to 0.01, whereas at 20 m resolution the curvature information is almost completely reduced to values between -0.003 and 0.003.

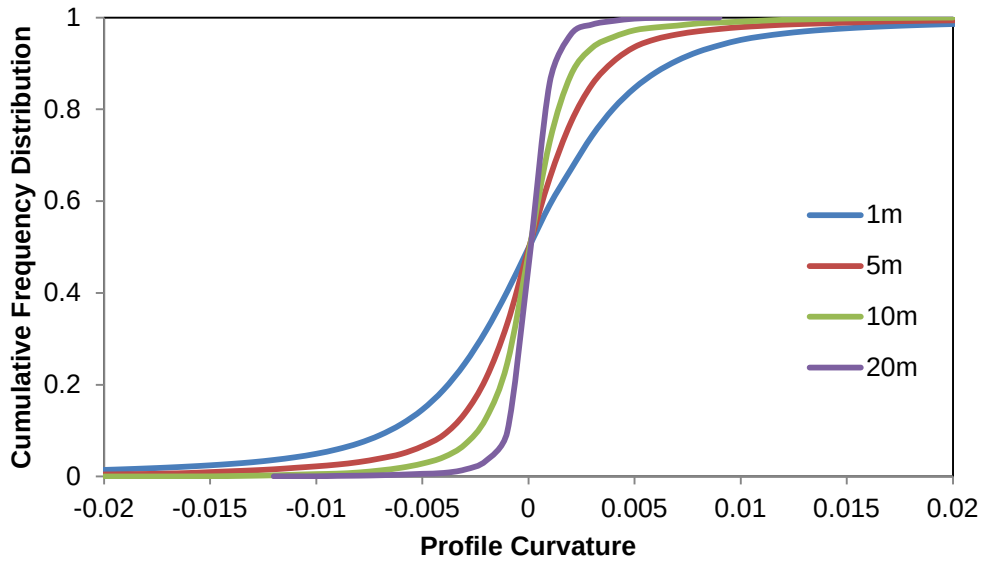

Figure 3.4: Cumulative frequency distribution of terrain curvature derived from 1m, 5m, 10m, and 20m DEMs.

The terrain curvature information content in the Wüstebach catchment decreases strongly with increasing grid size (Figure 3.5), and the first four resolutions show a highly linear

correlation (R^2 = 0.994). Such a linear relationship was also found in two forested catchments in Sardinia, Italy [Niedda, 2004] and for a catchment in central New York [Kuo et al., 1999]. At 50 and 100 m resolutions again a linear relationship was found, but with a lower slope value. The first linear relationship indicates smoothing of relatively small scale terrain features with large differences in altitude (e.g. steep slopes along the rivulet and the street), while the second linear relationship indicates smoothing of larger scale features of lower relief energy (e.g. gentle hillslopes). However, it has to be noted that the number of bins is much smaller for 50 and 100 m resolutions (10 and 5 respectively, compared to 203 of 1 m resolution), which makes the calculation of information content *I* using equation 3.2 less reliable. Thus, we restricted our analysis to the 10 and 20 m resolution cases.

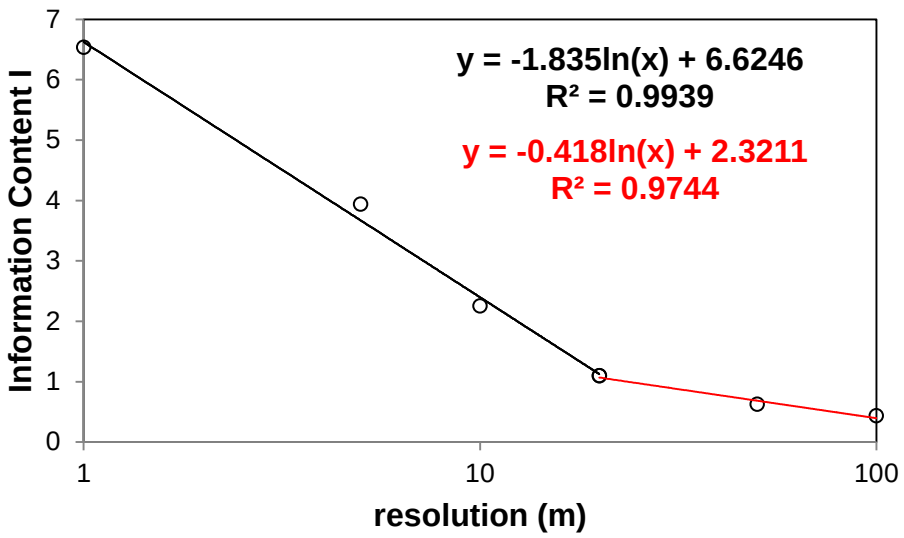

Figure 3.5: Information content of terrain curvature distribution versus spatial resolution of the DEM (black line: 1-20m resolutions, red line: 20-100m resolutions).

The calculated information contents and corresponding amplification factors for the different DEM resolutions are shown in Table 3.2. When reducing the spatial resolution from 1 to 5 m,

nearly half of the information content was lost (from 6.535 to 3.938) resulting in an amplification factor of 10. Further aggregation to 10 and 20 m resulted in amplification factors of 72.5 and 230, respectively. Thus, spatial aggregation requires an over-proportionate increase of the amplification factor to compensate for the loss of terrain curvature information.

Table 3.2: Calculated information content *I* and amplification factor τ for 1, 5, 10, 20, 50, and 100 m resolutions.

resolution (m)	I	ΔI	amp factor τ
1	6.535	0	1
5	3.938	2.597	13.42340735
10	2.251	4.284	72.52998046
20	1.096	5.439	230.2118565
50	0.623	5.912	369.4443056
100	0.432	6.103	447.1973518

Figure 3.6 shows the distribution of STD and γ in the Wüstebach catchment at 10 m resolution based on the 1 m DEM. High values of STD indicate areas of high slope variability and which are more prone to information loss due to spatial aggregation. The highest STD values can be found along the river and the street due the presence of distinct slopes. Figure 3.7a shows that the STD values exhibit a log-normal frequency distribution with a maximum at 0.015, whereas γ is almost normally distributed (Figure 3.7b). We then conducted a sensitivity analysis using different threshold values in that range between 0.005 and 0.025 for STD and between 0.6 and 0.8 for γ, respectively. The threshold values that gave the best model performance were 0.01 for STD and 0.75 for γ (RMSE of 0.0168 and 0.0178, respectively) (Table 3.3) and thus were used in the model scenario analysis.

Table 3.3: Sensitivity analysis of threshold value of STD and γ for 10 and 20 m resolutions

10m				20m			
STD	RMSE SWC	γ	RMSE SWC	STD	RMSE SWC	γ	RMSE SWC
0.005	0.0172	0.6	0.0312	0.005	0.0392	0.6	0.056
0.01	0.0168	0.65	0.0221	0.01	0.0376	0.65	0.0477
0.015	0.0169	0.7	0.0196	0.015	0.0394	0.7	0.0424
0.02	0.0183	0.75	0.0178	0.02	0.0402	0.75	0.0447
0.025	0.0208	0.8	0.0204	0.025	0.0432	0.8	0.0491

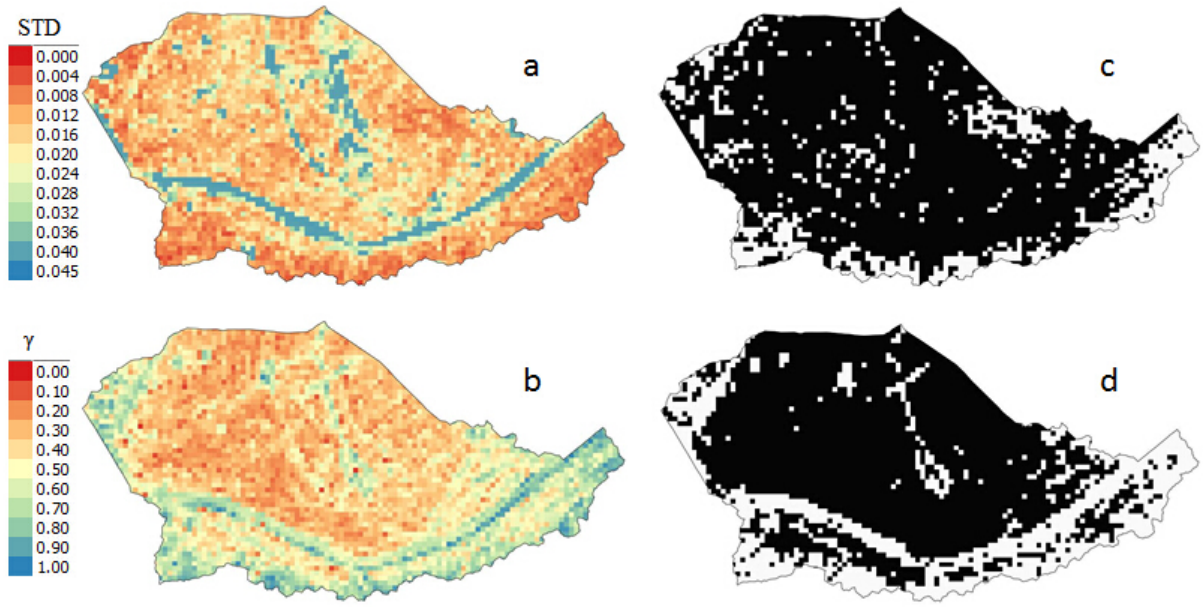

Figure 3.6: Distribution of STD (a) and γ (b) of slope in 10 m resolution, the black grid cells in c and d indicate where the amplification factor was applied respectively.

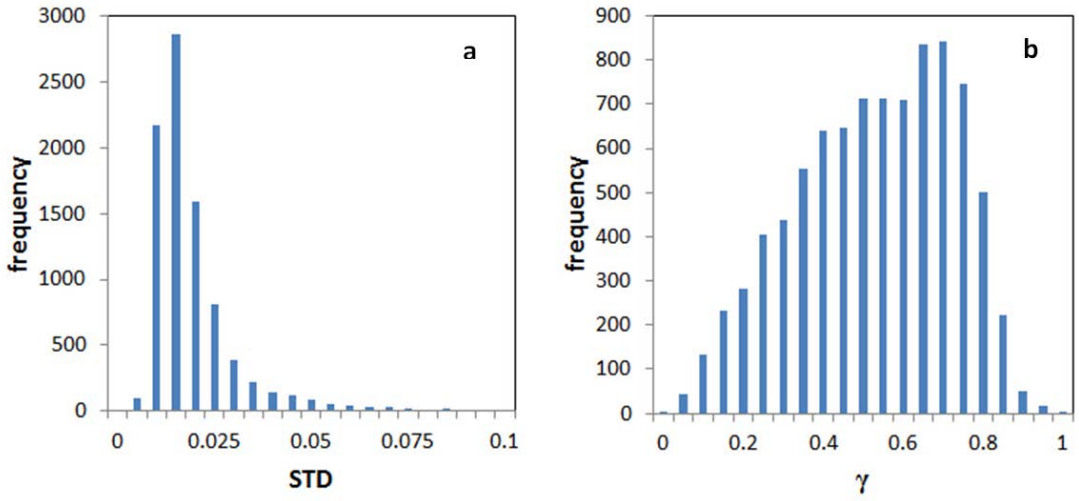

Figure 3.7: Frequency distributions of STD (a) and γ (b) in the Wüstebach catchment at 10 m resolution.

3.5.2 Comparison of the model scenarios

3.5.2.1 Results of model Scenarios 1 and 2

Table 3.4 shows the model performances of the four scenarios in terms of root mean square error (RMSE) and Nash-Sutcliffe Efficiency (NSE) of simulated vertical-averaged SWC and runoff, respectively. The results indicate that omitting the amplification factor produced the worst model performance for all four criteria. The results are especially poor for the soil water content simulation (NSE: -11.6). On the other hand, the area-wide application of the global amplification factor (scenario 2) produced better model performance, both in terms of SWC and runoff simulation (RMSE of SWC reduced from 0.0677 to 0.0277, and RMSE of runoff reduced from 0.302 to 0.092). This finding suggests that the loss of topographical information can be effectively compensated by increasing K_s using appropriate amplification factors.

Table 3.4: Model performances of the four model scenarios of SWC and runoff time series.

Model scenario	RMSE		NSE	
	Runoff	SWC	Runoff	SWC
1	0.302	0.0677	-1.640	-11.600
2	0.092	0.0277	0.554	-1.264
3	0.077	0.0168	0.682	0.463
4	0.081	0.0178	0.649	0.117

Figure 3.8 and 3.9 show simulated SWC and runoff time series of the different model scenarios. Clearly, applying the amplification factor considerably improved the low model performance of scenario 1, which is especially poor in runoff estimation (Figure 3.9, red curve). However, we notice that the model often underestimated SWC dynamics in 20 and 50 cm layers (Figure 3.8 blue curve), and led to a negative NSE (-1.264), indicating over-compensation of the soil hydraulic conductivity. Therefore, we investigated two further Scenarios 3 and 4 introducing threshold values for the application of amplification factors as described in section 3.4.3.

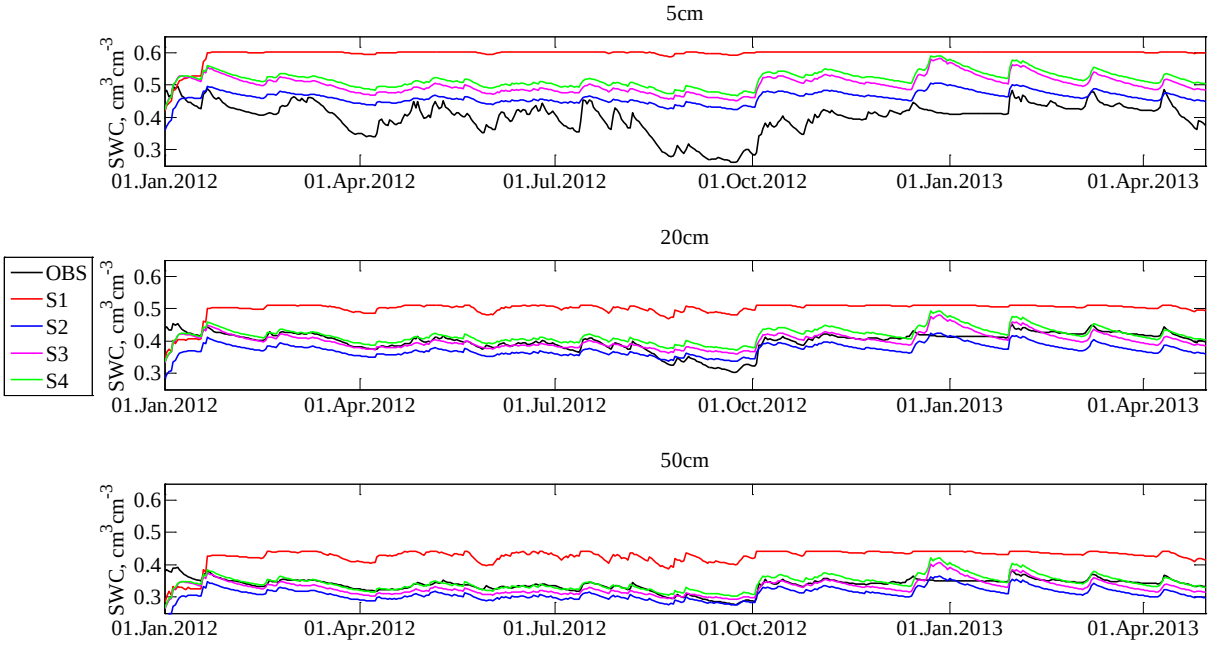

Figure 3.8: Time series of SWC of observation and simulation scenarios from January 1, 2012 to April 30, 2013.

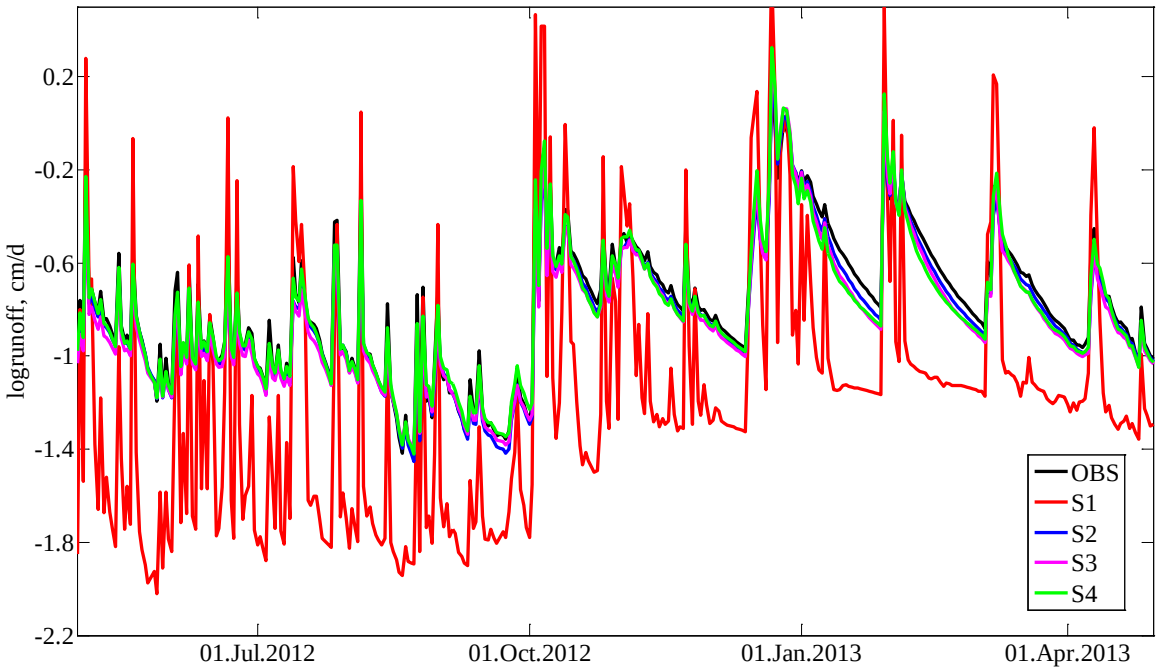

Figure 3.9: Time series of log-transformed observed runoff and simulated runoff from model scenarios with 10 m spatial resolution (S1 – S4) from May 1, 2012 to April 30, 2013.

3.5.2.2 Results of model Scenarios 3 and 4

In model Scenarios 3 and 4, we applied the localized amplification factor only to those grid cells of the computational domain with 10 m resolution where STD is larger than 0.01 and where γ is lower than 0.75, respectively (Figure 3.6). As shown in Table 3.3, application of the STD threshold further reduces RMSE of SWC time series from 0.0277 to 0.0168, and RMSE of runoff time series from 0.092 to 0.081. The NSE of SWC and runoff time series are significantly improved (from -1.264 to 0.463 and from 0.554 to 0.682, respectively). Using γ instead of STD (S4) also greatly improves model performance in all the four criteria, but is slightly poorer than Scenario 3 (Table 3.4). Figures 3.8 and 3.9 show much better agreement between observed and simulated SWC and log-transformed runoff (S3: pink curve, S4: green curve). Scenarios 3 and 4 led to a better reproduction of soil water content pattern, especially in the western part of the catchment (Figure 3.10c and 3.10d), where the difference of SWC

patterns are consistent with the different application of amplification factor in these two Scenarios (Figure 3.6c and 3.6d). This is also supported by the scatter plot shown in Figure 3.11: Although S1 provides high correlation coefficient between simulated and observed SWC (R: 0.737), SWC estimates are strongly overestimated (bias: -0.103, RMSD: 0.085) indicating excessive soil water retardation.S2, with the global amplification factor applied, effectively reduces bias from -0.103 to -0.039. With the strategily application of localized amplification factor, S3 provides the best estimate of vertically averaged 1-year-average SWC pattern at the 104 monitoring locations with lowest bias and root mean square deviation of all model scenarios (bias: -0.002, RMSD: 0.061) and S4 provides the second best simulation results. Therefore, we can conclude that using STD as threshold for the localized amplification factor application reduced the over-compensation of K_s^* most effectively.

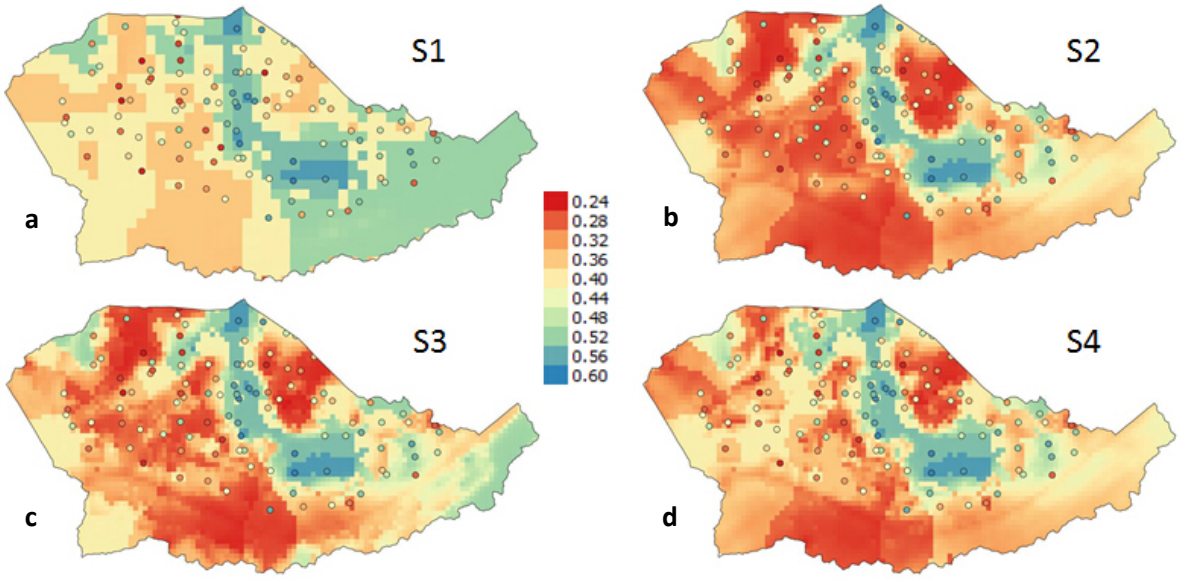

Figure 3.10: Observed and simulated soil moisture pattern at 20 cm depth (one year average between May 1, 2012 and April 30, 2013) of the four model scenarios (a: S1, b: S2, c: S3, d: S4).

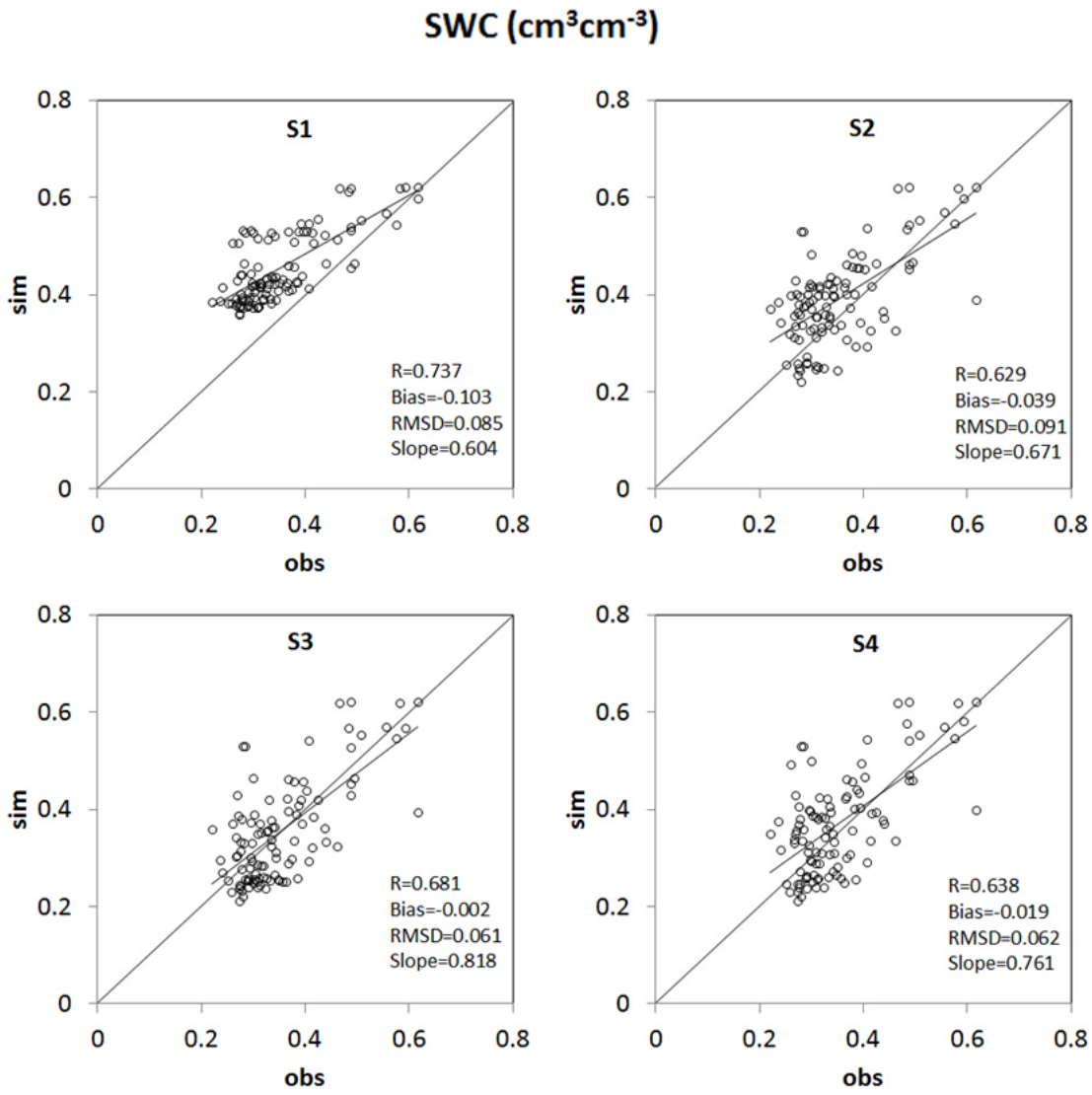

Figure 3.11: Scatter plot of observed and simulated one year vertical averaged soil moisture (May 1, 2012 - April 30, 2013) of the four scenarios with 10 m resolution (S1 – S4) at 104 SWC observation locations.

3.5.3 Comparison of different model resolutions

In order to investigate the effects of spatial resolution on our scale dependent parameterization strategy, we performed model Scenarios 1 and 3 also at 20 m resolution (S1_20m and S3_20m). In general, we found that the simulation results of the 10 m model resolution are better compared to the 20 m resolution (Table 3.5). This finding suggests the

information lost due the spatial aggregation to 20 m cannot be fully compensated by the application of an amplification factor. Besides, these results provide some very interesting insights. Inspecting the simulation results of runoff of model scenario S1, it gets apparent that the 10 m model produced a much lower RMSE (~0.302) and a much higher NSE (~-1.640) compared to the 20 m model (Table 3.5). This indicates that whether we compensated the information loss or not, the grid size plays a very significant role in runoff simulation.

Table 3.5: Statistical results of model scenarios 1 and 3 for 10 and 20 m resolutions of SWC and runoff time series.

Model scenario	Spatial resolution	RMSE		NSE	
		Runoff	SWC	Runoff	SWC
1	10m	0.302	0.0677	-1.640	-11.600
1	20m	0.550	0.0680	-7.733	-11.757
3	10m	0.077	0.0168	0.682	0.463
3	20m	0.166	0.0376	0.203	-2.114

In terms of SWC time series, 10 m resolution produced a much lower RMSE (~0.0168) and a much higher NSE (0.463) compared to 20 m resolution (~0.0376 and -2.114). On the other hand, for S1 the two model resolutions produced similar RMSE (~0.0677 and 0.0686). This finding is also supported by the simulated SWC distributions shown in Figure 3.12: S1 and S1_20m show very similar SWC pattern (Figure 3.12a and 3.12c) and statistical results (Figure 3.13a and 3.13b). This indicates that with the information loss of terrain curvature, simulated SWC is less sensitive to the resolution of the numerical model. However, in case of upscaled K_s field, the spatial resolution again plays an important role in SWC estimation. With the application of the amplification factor in S3, the 10 m resolution case is much better than the 20 m case in terms of all the four criteria of R, bias, RMSD, and slope (Figure 3.13c

and 3.13d). This indicates that water flow is retarded due to the reduction of the hydraulic gradient.

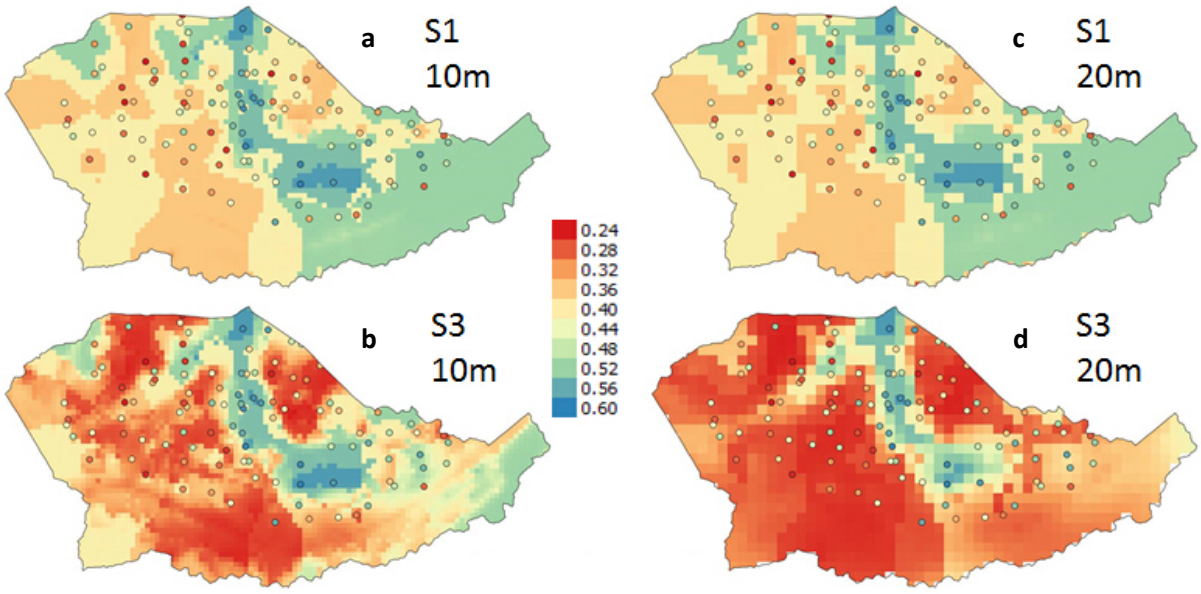

Figure 3.12: Observed and simulated soil moisture pattern at 20 cm depth (one year average between May 1, 2012 and April 30, 2013) using 10 m (a: S1, b: S3) and 20 m resolutions (c: S1_20m, d: S3_20m).

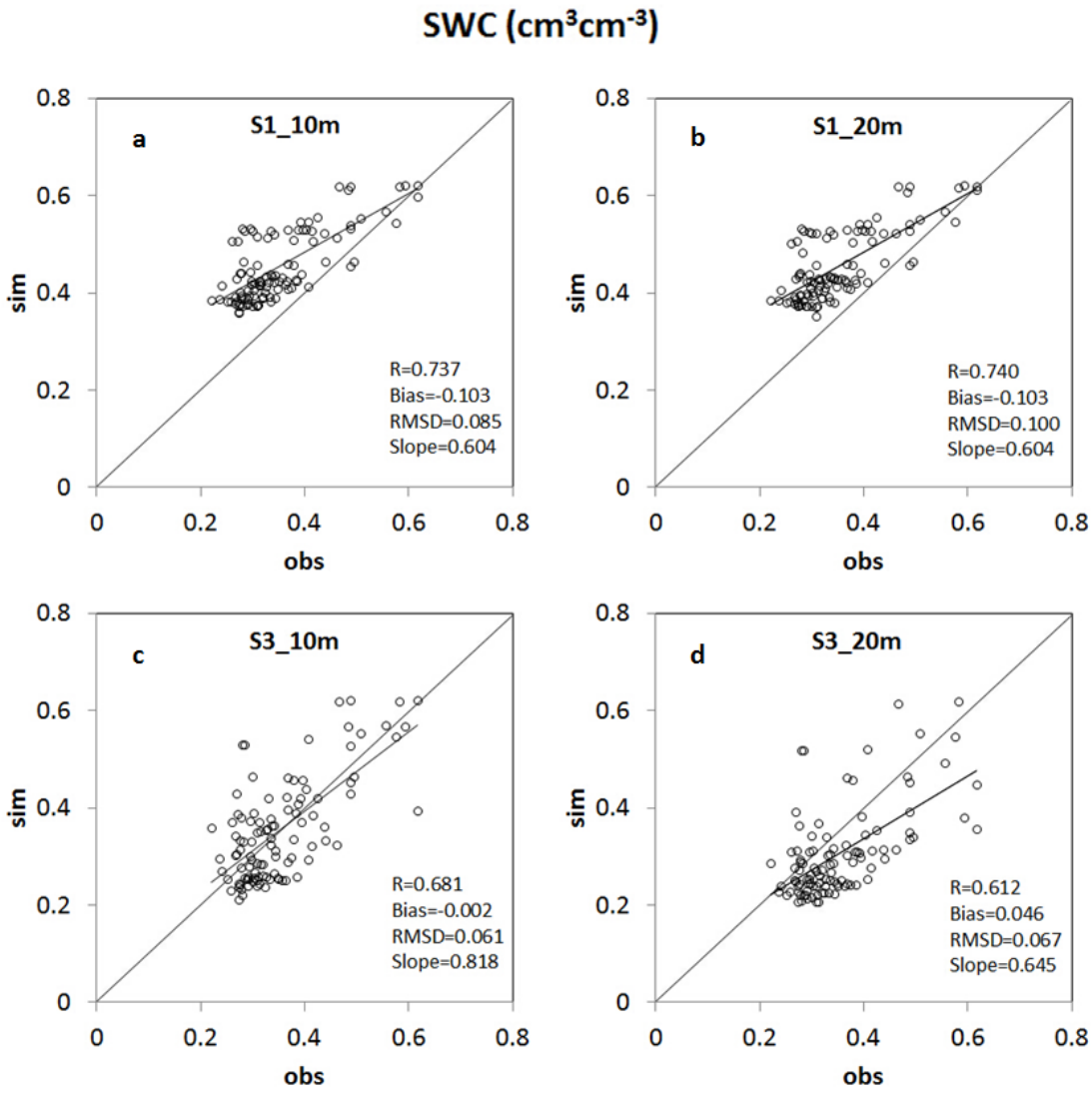

Figure 3.13: Scatter plot of observed and simulated vertical averaged 1-year-average soil moisture at 104 SWC observation locations: a) S1 10 m, b) S1 20 m, c) S3 10 m, and d) S3 20 m resolution.

We also notice that S3_20m with K_s scaling gave better results than S1 without scaling (see Table 3.5). Thus, in our case appropriate K_s scaling is more important than model resolution. This finding is supported by the distributed yearly-averaged SWC distributions (Figure 3.12). For instance, Figure 3.12d shows that the simulation result of S3_20m agrees well with the observed dry zone at the northwest corner of the Wüstebach catchment and the eastern hillslope of the Wüstebach creek. On the other hand, S1 overestimates SWC in the hillslope zone and failed to show the spatial variation, especially with respect to the dry zones. Figure

3.13 also shows that S3_20m (Figure 3.13d) provides better statistical results than S1 (Figure 3.13a). This finding suggests that for the Wüstebach catchment applying an effective K_s upscaling strategy is more important than to increase model resolution.

3.6 Conclusions

We conducted extensive soil water content and runoff simulation using ParFlow-CLM in a forested catchment Wüstebach site based on a similar setup of a previous study. To have further improved estimates of soil water content and runoff, an interpolated 2-D K_s field based on 108 double infiltrometer measurements was upscaled using an amplification factor based on information entropy theory. To test whether the loss in hydraulic gradients due to spatial aggregation of a three-dimensional hydrological model can be compensated by parameter upscaling using the information entropy concept we compared four different model scenarios. The results led us to the following conclusions:

The calculated amplification factor in Wüstebach catchment has log-linear correlation with model resolution (grid size), which is consistent with the findings of [Niedda, 2004].The simulation gave poor results without upscaling K_s, indicating that the loss of terrain information during spatial aggregation has a significant effect on model results. The K_s upscaling improved model results considerably. However, we evidenced overestimation of runoff and underestimate of SWC in case of area-wide application of the amplification factor. We tested two compensation strategies based on the STD and γ of the slopes and found that a threshold value of STD = 0.01 produces the best simulation results both in terms of SWC and runoff and effectively solves the problem of over-compensation of K_s. An effective K_s upscaling strategy is able to compensate for issues related to spatial aggregation.

Applying the original method of Niedda [2004] in the framework of 3D hydrological modelling, we found that a uniformly application of an amplification factor lead to local overcorrection of soil hydraulic conductivity and poor simulation results. The main innovation of our study is the introduction of two different upscaling strategies to avoid such overcompensation of hydraulic conductivity field in order to achieve better simulation results both in terms of SWC and runoff. Like for the original method of Niedda [2004], our approach is still based on basic terrain information. These proposed methods are not restricted to a specific model and can be transferred to other distributed model applications.

In future work, we will use higher resolution simulations (e.g. 5 m) and test our upscaling method in larger catchments and in different environmental settings with different terrain characteristics to strengthen our conclusion. We anticipate that our proposed scaling approach is useful for the application of next-generation hyper-resolution global land surface models [Wood et al., 2011].

4 Evaluation of 3D model parameterizations using water transit time distributions

This chapter will be submitted to Journal of Hydrology as: Fang, Z., Stockinger, M., Vereecken, H., Bogena, H., 2016. Evaluation of 3D model parameterizations using water transit time distributions.

4.1 Abstract

High reliability simulation of soil water content using various kinds of numerical modeling tools has been studied in recent years. Multiple methods have been applied for more accurate parameterizations. We followed a recently developed hydraulic parameter upscaling schemes based on terrain information entropy of Fang et al. [2016] and used the output of simulated pressure to put into a particle tracking simulation platform SLIM-FAST to investigate the water particle migration and transit time distribution (TTD) at a forested headwater catchment Wüstebach testing site. We conducted different model scenarios to investigate the effect of number of initial particles, dispersion parameters and hydraulic parameter upscaling schemes. A stable isotope tracer model TRANSEP was used in simulation of TTD for comparison purpose. Our results indicate that: 1) the initial number of water particles has no effect on TTD, unless the initial number exceeds a very high amount. 2) Higher α_L leads to higher TTD, a 0.002 m α_L gives best agreement with model TRANSEP. 3) Unlike the soil water content estimation, the scenario S2 of Fang et al. [2016] with global upscaling scheme has the best agreement with TRANSEP results, however, it fails to represent vertical movement of the water particles. On the other hand, the localized upscaling schemes S3 and S4, which have better SWC estimates, represent the vertical movement well. TTD estimation using particle tracking codes like SLIM-FAST can support the evaluation of 3D hydrological models like Parflow-CLM with respect to the correct parametrization of hydrological properties and the representation of water flow pathways.

4.2 Introduction

In recent times numerical hydrological models for the prediction of fluid transport are increasingly used to support the management of surface and ground water [Wood et al., 2011]. To this end, parallel simulation platforms have been developed in the past decade to enable detailed estimations of long-term dynamics of hydrological fluxes and storages (e.g. soil moisture, runoff discharge, evapotranspiration), e.g. STOMP [White and Oostrom, 2006], PFLOTRAN [Lichtner et al., 2015], MODFLOW [Harbaugh, 2005], HYDRUS [Simunek et al., 2012], HydroGeoSphere (HGS) [Therrien et al., 2010], and PARFLOW [Maxwell et al., 2014]. Soil moisture is a significant variable in the soil-vegetation-atmosphere continuum due to its important role in the exchange of water and energy at the soil surface [Vereecken et al., 2008]. Therefore, the accurate simulation of soil moisture dynamics in space and time is of key important to achieve reliable hydrological predictions. In order to enable realistic distributed soil moisture simulations, the model domain of numerical models needs to be informed with appropriate soil hydraulic parameters. Numerous methods have been applied in recent studies to obtain appropriate model parameterizations, including inverse calibration [Burbey and Zhang, 2015; Simunek and van Genuchten, 1996], linear regression [Arshad et al., 2013], pedotransfer functions (PTFs) [Schaap et al., 2001], upscaling techniques [Zhu and Mohanty, 2002; Zhang et al., 2004] to name a few. Recently, also terrain information entropy was introduced for soil hydraulic parameters estimation [Niedda, 2004; Fang et al., 2016]. Another challenge is the appropriate validation of distributed hydrological models. Recently, Fang et al. [2015] and Koch et al. [2016] used data from a soil moisture sensor network to validate 3D numerical water transport models with respect to correct simulation soil moisture pattern. However, even if the models are accurately reproducing the spatial soil moisture pattern, this no guarantee for the correct representation of water particles movement in the

catchment. An effective way to evaluate the model performance with respect to water transport is the analysis of water transit time distribution (TTD). Typically, TTD are estimated from stable isotope data using simple model assumption [Kirchner, 2016]. For instance, Stockinger et al. [2014] used the tracer-aided conceptual model TRANSEP and continuous measurements of stable isotope of water as tracers to estimate the spatial heterogeneity of TTDs of the Wüstebach catchment. In addition, TTD analysis were also performed in the framework of 2D and 3D modeling studies using particle tracking, e.g. Marçais et al., [2015]; Green et al., [2014]; Woolfenden and Ginn, [2009]. Such particle tracking schemes were commonly applied with physically-based models in the framework of groundwater flow and contaminant transport study, e.g. Suk, [2012]; Cadini et al., [2012]; Salamon et al., [2006]; Goode, [1990]; Binning and Celia, [2002]. Recently, the particle tracking code SLIM-FAST in conjunction with the Parflow-CLM numerical model was successfully applied to different catchment and with varying spatial resolutions [Kollet and Maxwell, 2008; de Rooij et al., 2013]. As one of the most significant factors of particle migration in soil and aquifers, longitude and transverse dispersivity were widely studied in recent studies by either experimental methods or numerical modeling [Gelhar et al., 1992; Vanderborght and Vereecken, 2007; Kollet and Maxwell, 2008; Chou and Wyseure, 2009; Perfect et al., 2002]. The correct dispersivity estimation is an important requisite to achieve realistic estimates of TTDs using particle transport modelling. However, different researches based on different testing methods and materials often revealed quite different longitude dispersivity for aquifers and soils [Schulze-Makuch, 2005].

In this study, we used the particle tracking code SLIM-FAST for an in-depth evaluation of the Parflow-CLM model performance with respect to water transport within a headwater catchment. To this end we used the same parameterization and simulation results obtained by Fang et al. [2016] for the Wüstebach catchment. The output simulated pressure of four

Parflow-CLM model scenarios (Table 4.1) was used as input to SLIM-FAST to evaluate the four upscaling schemes and explore the soil and aquifer dispersion parameterization in term of water particle migration. The recently estimated TTD for this catchment (Stockinger et al., 2014) was used for comparison. More specifically we wanted to give answers the following research questions:

1) How many particles are needed to achieve reliable estimates of TTD in a forested headwater catchment?

2) How strong is the TTD estimation influenced by the dispersivity parametrization?

3) How well compare TTD estimated from stable isotopes as tracers with those derived from 3D hydrological modelling?

4) Which parameterization scheme for the 3D numerical model provides the best possible representation of water particles movement and flow pathways in the Wüstebach catchment?

Table 4.1: Four model scenarios (Fang et al., 2016)

Scenarios	description
S1	No K_s upscaling
S2	Global K_s amplification by 72.53 in all grid cells
S3	Localized K_s amplification based on STD distribution
S4	Localized K_s amplification based on partition parameter λ distribution

4.3 Experimental setup

4.3.1 The experimental test site Wüstebach

This research was conducted at the Wüstebach test site, which is a 38.5 ha large experimental catchment of the TERENO Eifel/Lower Rhine Valley Observatory [Zacharias et al., 2011] and the Collaborative Research Centre TR32 [Vereecken et al., 2010; Simmer et al., 2015]

located in western Germany. In recent times several studies have been conducted at the Wüstebach test site to characterize the dynamics of soil water content, runoff and evapotranspiration using both field measurements and numerical modeling [Bogena et al., 2010, 2015; Fang et al., 2015, 2016; Koch et al., 2016; Cornelissen et al., 2015; Graf et al., 2014; Simmer et al., 2015; Wiekenkamp et al., 2016]. The altitude ranges from 595 m in the North to 628 m in the South and the average slope is 3.6 % with maximum values near the riparian zone. The bedrock is mainly composed of fractured Devonian shales exhibiting very low hydraulic conductivity (10^{-9} to 10^{-7} m/s) [Graf et al, 2014]. The bedrock that assumed impermeable is overlain by a periglacial solifluction layer with an average thickness of 1.6 m. Cambisols and Planosols are mainly located on hillslopes, whereas Gleysols and half-bogs developed in the riparian zone under the influence of groundwater [Bogena et al., 2015]. The prevailing soil texture is silty clay loam with a medium to high fraction of coarse material. The litter layer has a thickness of about 5 cm [Richter, 2008]. More than 90% of the forest is comprised of Norway spruce trees planted in 1946 [Etmann, 2009], with a typical canopy height of about 25 m [Bogena et al., 2015]. The test site belongs to the temperate climate zone with a mean temperature of about 7°C and exhibits a long-term mean annual precipitation amount of 1310 mm for the period 1981 to 2013.

4.3.2 Hydrology data collections

Long-term soil moisture data from a wireless senor network installed in the Wüstebach catchment consisting of 150 sensor nodes [Bogena et al., 2010] and discharge data measured at the catchment outlet using a runoff station equipped with a combination of a V-notch weir for low flow [Bogena et al., 2015] was used in Parflow-CLM simulation. Stable isotopes data of water was collected at Wüstebach site and used in the tracer-based black-box model TRANSEP. The outlet's TTD derived from TRANSEP [Stockinger et al., 2014] was used

instead as a comparison with the SLIM-FAST generated ones. See Section 4.4.3 for more details about TRANSEP model.

4.4 Model and methods

4.4.1 The SLIM-FAST model

SLIM-FAST is a newly-developed numerical model designed to simulate the migration of dissolved, non-reactive and reactive chemical species in saturated and unsaturated groundwater systems [Maxwell, 2010]. It simulates transient mass transport processes within porous or fractured rock media. Steady state or transient groundwater flow fields, as derived from other numerical or analytic models, need to be supplied externally. In this study, we used the 3D pressure fields simulated using the Parflow-CLM model directly into SLIM-FAST model, as the two models are well related.

SLIM-FAST makes these simplified assumptions:

1) The collection of species is neutrally buoyant
2) Sorption (ion exchange/surface complexation) reactions are assumed to be in instantaneous equilibrium, and
3) Aqueous complexing reactions are not considered.

Under these assumptions, the mass balance for species *j* takes the form:

$$\frac{\partial}{\partial t}\left(\emptyset\left(c_j + c_j^{im}\right)\right) + \nabla\cdot\left(\emptyset\mathbf{v}c_j\right) - \nabla\cdot\left(\emptyset\mathbf{D}\cdot\nabla c_j\right) = -\lambda_j\emptyset\left(c_j + c_j^{im}\right) + \lambda_k\emptyset\left(c_k + c_k^{im}\right) - R_j^{min} - s_j^{fm} - c_j\sum_w Q_w\delta(x - x_w)\,\delta(y - y_w)\delta(z - z_w) \quad (4.1)$$

where

c_j represents the aqueous concentration of primary species j in solution (Maqueous/L^3-aqueous)

c_j^{im} represents the immobile concentration of primary species j sorbed onto the solid phase (M-sorbed/L^3-aqueous)

$c_j^T = \emptyset\left(c_j + c_j^{im}\right)$ represents the total (bulk) concentration (M-aqueous plus Msorbed/L^3-bulk) of species j

$\emptyset$ and $\mathbf{v}$ represent the meduim porosity (-) and groundwater flow velocity (L/T)

$\mathbf{D}(\mathbf{x}) = (\alpha_T V + D_e)\mathbf{I} + (\alpha_L - \alpha_T)\frac{\mathbf{vv}}{V}$ is the hydrodynamic dispersion tensor (L2/T)

where α_L and α_T are longitudinal and transverse medium dispersivities (L) and D_e is an effective molecular diffusivity (L^2/T) for the porous medium

λ_j is the (radioactive) decay rate of species j (1/T)

R_j^{min} is the rate of loss or gain of aqueous mass from mineral dissolution or precipitation reactions (M/T)

s_j^{fm} is the rate of loss or gain of aqueous mass in a fracture regime to and from the matrix regime from matrix diffusion (M/T)

Q_w is the volumetric rate of pumping (fluid loss, L^3/T) from a well at location (x_w, y_w, z_w).

In the current particle approach, the spatial distribution of total species mass, as represented by the total concentration c_j^T , is approximated by a finite system of N_j particles,

$$c_j^T(\mathbf{x}, t) = \sum_{p=1}^{N_j} m_p \delta(\mathbf{x} - \mathbf{X}_p(t)) \qquad (4.2)$$

where δ is a Dirac function. The particles may carry, or be associated with, different species attributes such as mass (m_p), position ($\mathbf{X}_p$), type (j), age ($t - t_0$), or even its regime or phase of existence (e.g., fracture, matrix).

4.4.2 Parflow-CLM and SLIM-FAST model setup

For the Parflow-CLM application we used the model setup and parameterization as described in Fang et al. [2016]. The model domain used for the Wüstebach catchment has a total size of 1180 m × 740 m and a uniform depth of 1.6 m, which corresponds to the averaged measured soil depth. In addition, following Bogena et al. [2013] a litter layer was considered with a uniform depth of 0.05 m. The vertical resolution of the model domain was set to 0.025m. The soil profile was differentiated into four different soil horizons with specific hydraulic properties following Bogena et al. [2013] to represent the vertical heterogeneity: a soil covering litter layer (+0.05-0 m), a top A horizon (0-0.1 m), an intermediate B horizon (0.1-0-4 m), and a C horizon (0.4-1.6 m) overlaying the bedrock. Soil hydraulic properties were parameterized using the van Genuchten - Mualem model [van Genuchten, 1980].

The simulation was conducted on hourly time steps for 365 days from May 1, 2012 to April 30, 2013. A spin-up phase from January 1 to April 30, 2012 was conducted with an initial condition of constant pressure in -2.0 m. The simulations were performed on the high performance computer JUROPA of the Jülich Supercomputing Centre. More information on the Parflow-CLM model setup is presented in Fang et al. [2015, 2016].

For the SLIM-FAST application, we set the soil hydraulic parameters the same as in Fang et al. [2016]. We put the output of all the four model scenarios in Fang et al., [2016] into SLIM-FAST model for comparison purpose. We used water particles as the tracking particles and we assumed no reactions happened during simulation period. We used “forward” simulation mode that track the movement of particles from the surface to the stream. The locations of initial particles were set to be at the top 5 cm of the soil layer. Such setup allows us to simulate stable isotope tracer experiment to estimate the migration of water particles and for

comparison purpose. We did not put the initial particles near domain boundary to avoid mass loss of water particles.

4.4.3 Streamwater TTD estimate using TRANSEP

The TTD derived from the conceptual model TRANSEP by Stockinger et al. [2014] was compared to the different TTDs derived from the individual ParFlow-CLM setups. Stockinger et al. [2014] inversely simulated the stable isotope $\delta^{18}O$ time series of the Wüstebach's outlet streamflow to calibrate the outlet's TTD using the convolution integral:

$$C(t) = \frac{\int_0^t C_{in}(t-\tau_T)p_{eff}(t-\tau_T)h(\tau_T)d\tau_T}{\int_0^t p_{eff}(t-\tau_T)h(\tau_T)d\tau_T} \quad (4.3)$$

where $C(t)$ is the stream water isotope concentration at time t, $C_{in}(t-\tau_T)$ is the precipitation isotope concentration at time t with travel time τ_T and $h(\tau_T)$ is the TTD.

The chosen model for the TTD was two parallel linear reservoirs:

$$h(\tau_T) = \frac{\phi}{\tau_f}\exp\left(-\frac{\tau_T}{\tau_f}\right) + \frac{1-\phi}{\tau_s}\exp\left(-\frac{\tau_T}{\tau_s}\right) \quad (4.4)$$

where ϕ is a partitioning factor (between 0 and 1) and τ_f and τ_s are the mean transit times of the fast and slow reservoir, respectively.

The parameter space was searched using the Ant Colony Optimization algorithm [Abbaspour et al., 2001] with the Nash-Sutcliffe Efficiency as the objective function [Nash and Sutcliffe, 1970].

The observed and simulated isotope data in model TRANSEP is shown in Figure 4.1. The estimated TTD from Stockinger et al. [2014] and the calibrated one with spin-up phase were

treated as two models output P1 and P1+, respectively. In this study, we compared SLIM-FAST estimated TTDs with both P1 and P1+.

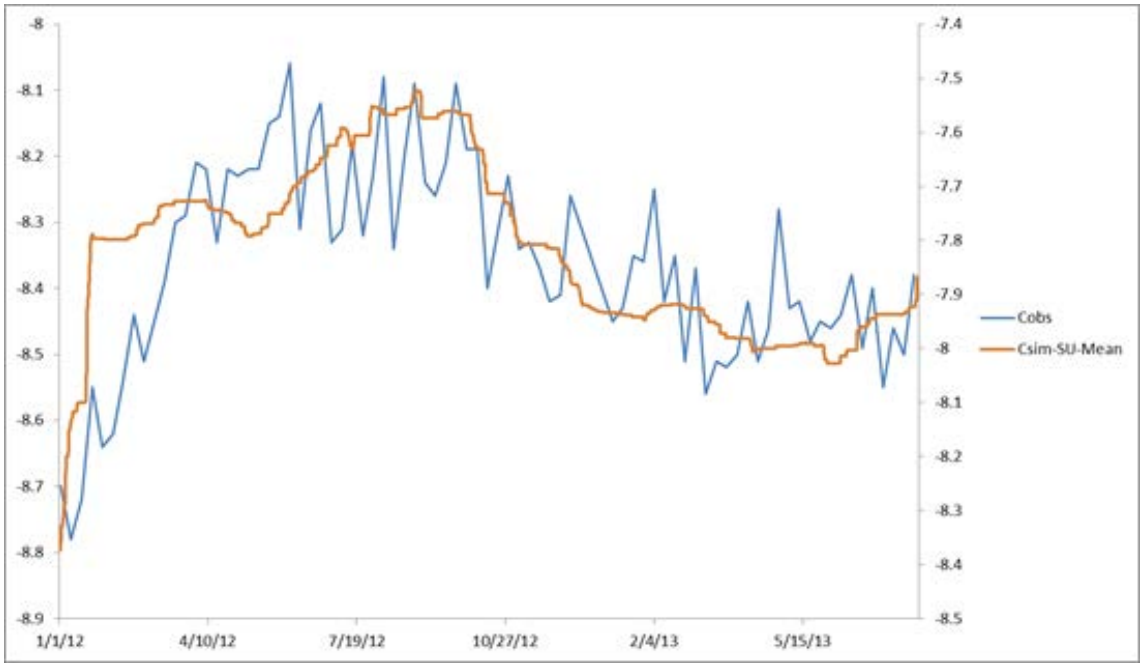

Figure 4.1: Observed and simulated isotope data in TRANSEP.

4.4.4 Scenario analysis

We conducted several different groups of scenarios to investigate the effect of dispersion parameters, different effective K_s fields, and number of particles on transit time distribution estimates.

- Scenario group 1 (SG1): different number of initial input particles in the model domain.
- Scenario group 2 (SG2): different longitude dispersivity α_L from zero (no dispersion) to 0.1 m (high dispersion), the transverse dispersivity α_T was set as 1/10 of the longitude dispersivity for each scenario.
- Scenario group 3 (SG3): the four model scenarios of Fang et al. [2016] with different upscaling schemes for K_s.

The model scenarios SG1 are performed to evaluate if the number of initial particles impacts TTD estimation. The purpose of using scenario SG2 is to find the optimized dispersion parameters α_L and α_T. With SG3 we validate how well TTD estimates can be improved by applying the global and localized amplification factor.

4.5 Results and discussions

4.5.1 Comparison of different number of initial particles

To investigate the effect of initial number of particles, we conducted a sensitive analysis from 100 (very sparse) to 1000000 (very dense) particles uniformly distributed in the top 5 cm soil layer. Figure 4.2 shows the results TTD curves that within a range between 1000 to 500000 initial particles the simulated results almost have no difference. If the number is less than 100, the TTD curve features some step shape, which is due to that for some blocks there is only one particle in it. When the number is as dense is 1000000, the simulated TTD curve becomes unreasonable because that immediate after the start of simulation, many particles move out of the domain due to the high amount of existing particles at the top of soil. In general, a wide range of number of initial particles from 1000 to 500000 actually has no effect on the estimated TTD. This scenarios group SG1 was tested with different upscaling schemes and dispersion parameters, the conclusions are the same.

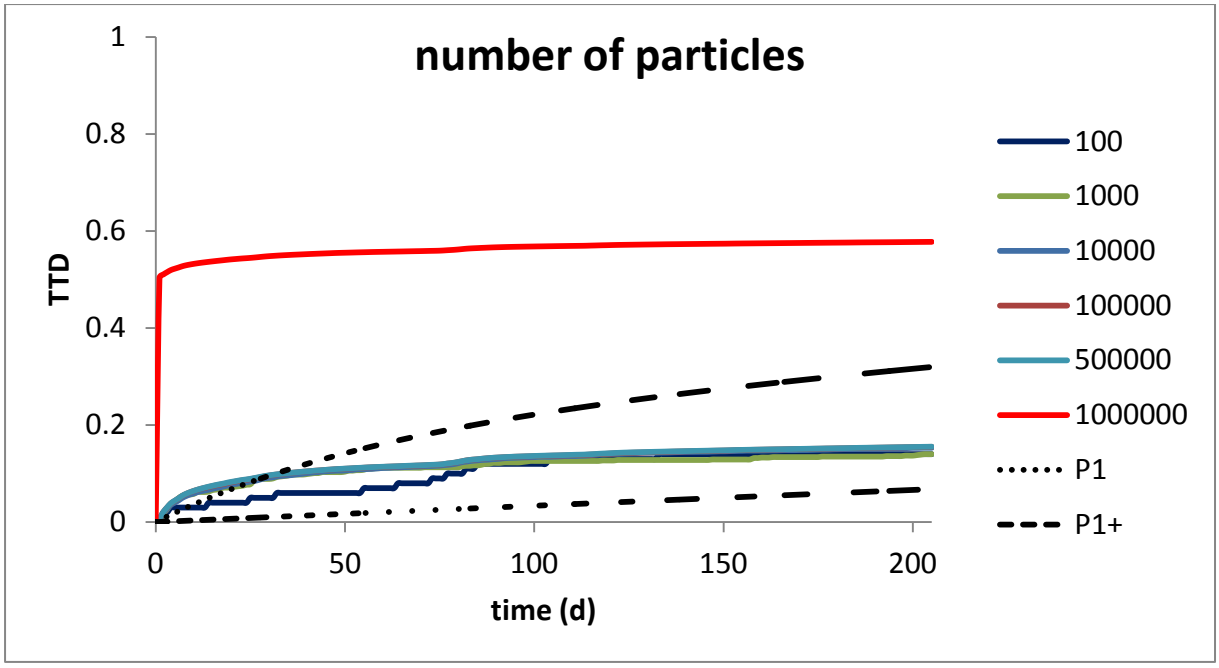

Figure 4.2: Time series of TTD simulation scenarios of number of initial particles with comparison to TRANSEP model P1 and P1+.

4.5.2 Effect of dispersion parameters

Before we validate the different model scenarios of parameter upscaling schemes, appropriate values for the longitude and transverse dispersivity (α_L and α_T) need to be determined. Due to the usually unavailable of measured dispersivity data, α_L and α_T were often assumed to be zero for the water particles [de Rooij et al., 2012]. Previous study of the effect of different range of α_L indicates 0 – 0.01 m longitude dispersivity is an accepted range for water particles [Gelhar et al., 1992; Vanderborght and Vereecken, 2007; Kollet and Maxwell, 2008]. In this study, we tested six different levels of longitude dispersivity, 0 (no dispersivity), 0.001m, 0.002m, 0.005m, 0.01m, and 0.1m (very high dispersivity,) [Schulze-Makuch, 2005; Vanderborght and Vereecken, 2007]. The estimated transit time distributions are shown in Figure 4.3. Unlike the SWC data, due to lack of actual observations of TTDs at Wüstebach site, we assumed the TTDs estimated based on TRANSEP model P1 and the calibrated model

P1+ represent uncertainty range of TTD for comparison purpose with SLIM-FAST model. Estimated TTDs lower than P1 and higher than P1+ are treated as good agreement. Figure 4.3 indicates that with α_L less than 0.005 m, estimated TTDs agree well with the TRANSEP models. When α_L is less than 0.002 m, the shapes of TTD curves are quite similar. When α_L is larger than 0.005 m, the TTD curves deviate from the uncertainty range (Table 2). To quantify the variation of TTDS based on different α_L, we calculated the differences between SLIM-FAST estimated TTD and TRANSEP estimated TTDs in terms of RMSE, as shown in Table 4.2 suggest that the 0.002 m α_L gives the best model performance (RMSE = 0.026). Therefore in the following three scenario groups we used α_L = 0.002 m to investigate the effect of other factors on TTD estimation.

Table 4.2: RMSE of TTD with different dispersion parameters

dispersivity (m)	0	0.001	0.002	0.005	0.01	0.1
RMSE	0.146	0.068	0.026	0.192	0.286	0.653

Figure 4.3 also indicates an important difference between SLIM-FAST estimated TTD and isotope tracer model estimated TTD. The SLIM-FAST estimated TTD show a faster increase during the first ten days, meaning that more water particles move out of the domain during this period. After 20 – 40 days, the TTD curve tends to be flat and the particles become more stable. In the isotope tracer model P1 and P1+, the TTD curve has a relative uniform slope through the whole model period.

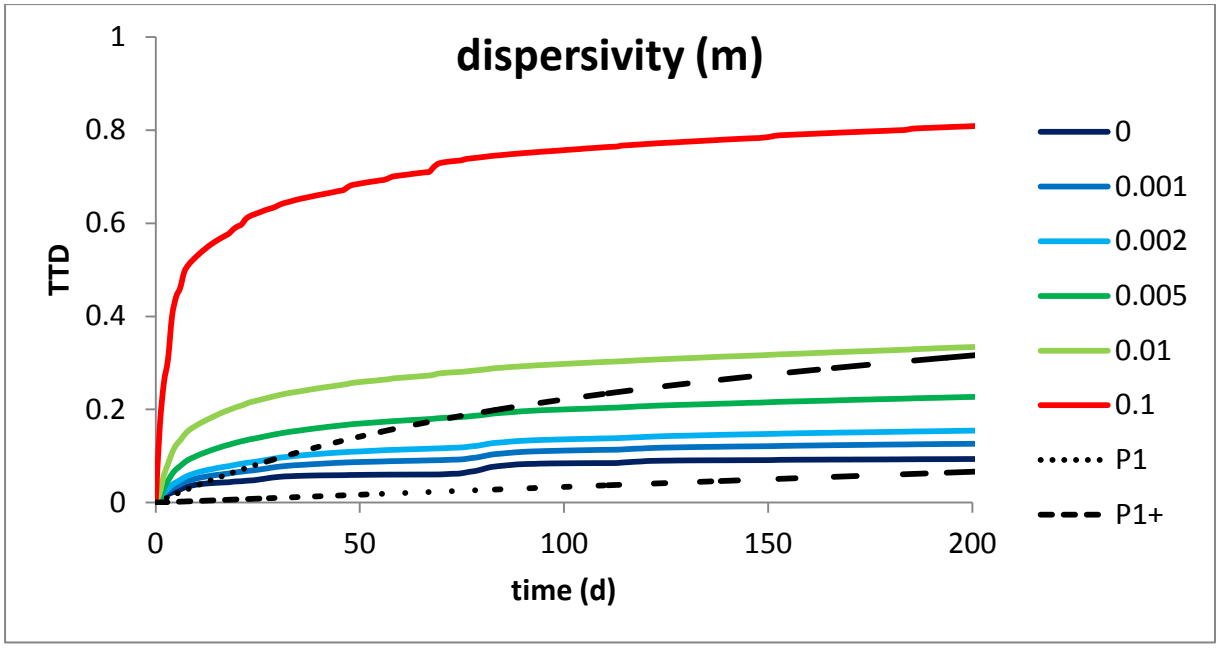

Figure 4.3: Time series of TTD simulation scenarios of longitude dispersivity with comparison to TRANSEP model P1 and P1+.

4.5.3 Comparison of upscaling schemes

We tested the outputs of four model scenarios from Fang et al. [2016] in SLIM-FAST model to validate how the different effective K_s fields affect the water particles migration in subsurface. The results in Figure 4.4 show that all the four schemes estimated TTD located well within uncertainty range. The two localized K_s upscaling schemes have very similar TTD curves. One important finding in this study is that the global K_s upscaling scheme gives the most similar shape of TTD curve as the P1 and P1+ models and has the minimum RMSE of 0.011. This finding indicates that although the localized upscaling strategies led to better estimation of soil moisture content variation, the actual movement of each particle was not well captured. The reason is that the localized upscaling schemes only applied amplification factor to the grid cells where we considered "significant" terrain information loss but did not applied to those considered "insignificant" grids. When represented in term of water particle movements, such distinction made the particles in the amplified blocks move extreme faster

to compensate the nearby relatively immobility of particles in the non-amplified blocks to form a reasonable velocity. This fast movement caused faster transit time in the early period within 20 days since simulation started. On the other hand, with the global amplification scheme, there is no such significant distinction and the particles in all the blocks move smoothly, making a relatively flat TTD curve.

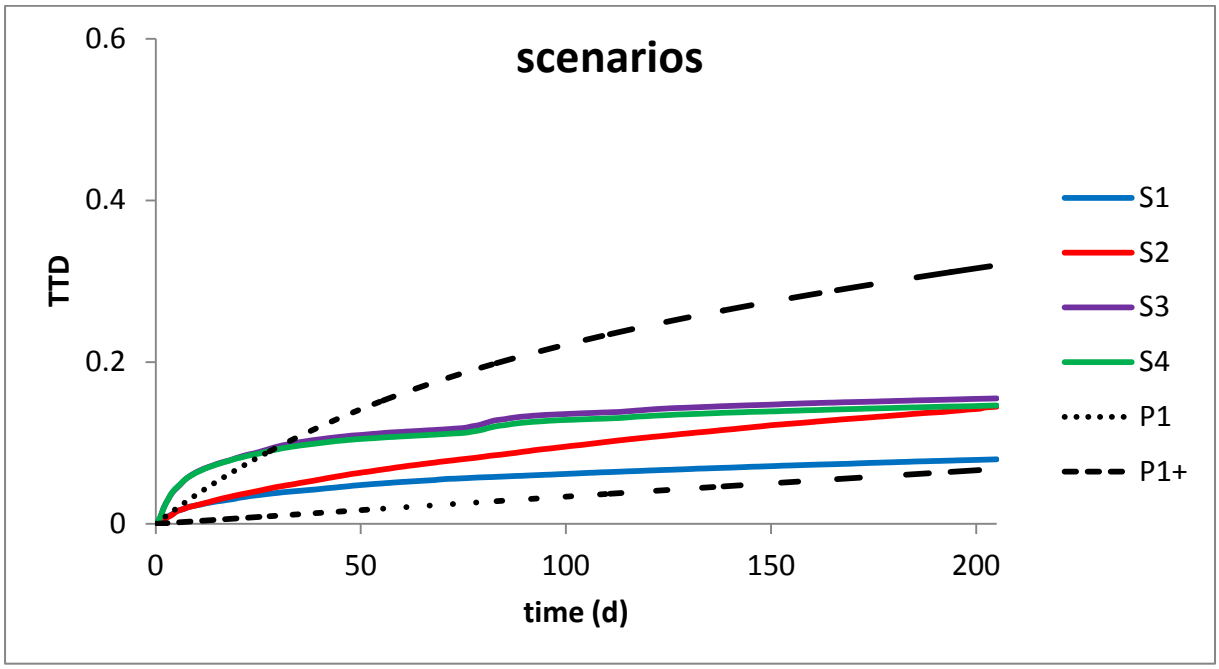

Figure 4.4: Time series of TTD simulation scenarios of K_s upscaling schemes with comparison to TRANSEP model P1 and P1+.

However, figure 4.5 shows the effectivity of localized upscaling schemes in vertical movement of particles. Both S1 and S3 failed to move the particles vertically. In scenario S1, the K_s is too low so water cannot effectively move downward. In scenario S2, the over-compensation of K_s caused the water flow too fast in horizontal direction to the outlet. The localized amplification factors in S3 and S4 gave appropriate K_s fields for the water particles to transport reasonably in vertical direction.

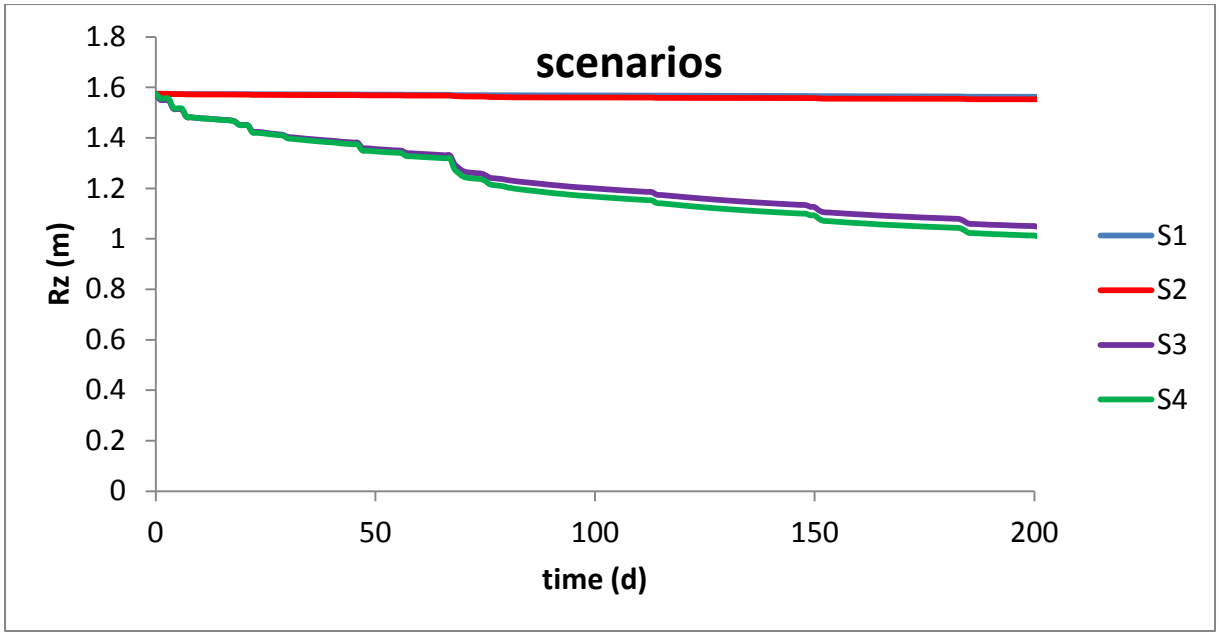

Figure 4.5: Time series of average central location of particles in vertical direction z of different K_s upscaling schemes.

4.6 Conclusions

We used particle-tracking code SLIM-FAST to validate four model scenarios of soil hydraulic parameters upscaling schemes of Fang et al. [2016] and investigated the effect of dispersion parameters in soil and aquifers on water particle migrations and transit time distributions at the Wüstebach headwater catchment. Our results indicate that: 1) Generally, the initial number of water particles has no effect on TTD, unless the initial number exceeds a very high amount like 1000000. 2) Higher α_L leads to higher TTD, a 0.002 m α_L gives best agreement with a black-box model TRANSEP. 3) Unlike the soil water content estimation, the scenario S2 of Fang et al. [2016] with global upscaling scheme has the best agreement with TRANSEP results, however, it fails to represent vertical movement of the water particles. On the other hand, the localized upscaling schemes S3 and S4, which have better SWC estimates, represent the vertical movement well. In future studies, an inverse calibration

of dispersion parameters could be included. Nevertheless, we can conclude that analysis of TTD estimated using particle tracking codes like SLIM-FAST can support the evaluation of 3D hydrological models like Parflow-CLM with respect to the correct parametrization of hydrological properties and the representation of water flow pathways. An inverse calibration of dispersion parameters could also be included in future studies to better understand how water and other tracing particles migrate in pathways in soil and fracture medium. More transit time distribution estimates from various models are needed for comparison purpose.

5 Synthesis

We estimated soil hydraulic parameters using inverse calibration HYDRUS and SCE-UA and conducted large-scale long-term, high-resolution simulation of soil water content, runoff, and evapotranspiration of a headwater forested Wüstebach catchment in Western Germany using an integrated parallel 3D simulation platform ParFlow-CLM. Water budget gap was well closed with comparison of observed precipitation, discharge and actual evapotranspiration. We investigated the effect of heterogeneity and anisotropy on soil moisture distribution variation using EOF and wavelet coherence analysis. To further improve model performance, we introduced information entropy concept to represent the loss of terrain curvature information due to spatial aggregation, calculated the amplification factors applied to hydraulic conductivity field to compensate the information loss for different model resolutions. Four model scenarios reflecting different upscaling schemes of amplification factor application were simulated and compared with observation soil moisture data collected from SoilNET sensors. A particle-tracking program SLIM-FAST was used to estimate water transit time distribution and compared with results of an isotope tracer black-box model to further illustrate how well the upscaling schemes work and how initial number of water particles in the domain and dispersion parameters impact on TTD estimation.

5.1 Final Conclusions

We found that scaling factor of 20 for the horizontal K_s of the soil layer that overlies the impermeable bedrock increased the model performance in terms of runoff and soil moisture dynamics, but not for ET. This indicates that the interflow process plays an important role for the generation of runoff in the Wüstebach catchment. Furthermore, we could show that

spatial information on porosity can significantly improve the simulation of spatial pattern of soil moisture using a 3D hydrological model.

Our EOF analysis showed that the spatial pattern of observed soil moisture content is better reproduced by the ParFlow-CLM model with distributed soil porosity information used. However, given the limited heterogeneity in the input parameters, the spatial variability of simulated soil moisture was clearly lower compared to the observations. Nevertheless, the EOF analysis indicated the ParFlow-CLM model was able to reproduce a characteristic turning point θ_t as already found in the study by Graf et al. [2014], suggesting different spatial soil moisture pattern for mean soil moisture below and above θ_t.

Using the cross-wavelet coherence analysis we were able to analyze the model results in more detail. For instance, the analyses revealed that the ParFlow-CLM model can reproduce the soil moisture observations better during wet seasons. Dry seasons were suffered from delays of correlation and even anti-correlation between simulated and observed soil moisture.

Our detailed analysis of the ParFlow-CLM model results reveals a general overestimation of soil moisture content during dry seasons. We attribute this shortcoming to the low topographic gradients of the riparian zone that may have led to an underestimation of lateral drainage and thus overestimation of riparian zone wetness. Another possible reason is the presence of fast vertical bypass flow during strong precipitation events at the Wüstebach catchment, which cannot be considered by ParFlow-CLM.

The calculated amplification factor in Wüstebach catchment has log-linear correlation with model resolution (grid size), which is consistent with the findings of [Niedda, 2004]. The

simulation gave poor results without upscaling K_s, indicating that the loss of terrain information during spatial aggregation has a significant effect on model results. The K_s upscaling improved model results considerably. However, we evidenced overestimation of runoff and underestimate of SWC in case of area-wide application of the amplification factor. We tested two compensation strategies based on the STD and γ of the slopes and found that a threshold value of STD = 0.01 produces the best simulation results both in terms of SWC and runoff and effectively solves the problem of over-compensation of K_s. An effective K_s upscaling strategy is able to compensate for issues related to spatial aggregation.

Our results of SLIM-FAST simulation indicate that: 1) Generally, the initial number of water particles has no effect on TTD, unless the initial number exceeds a very high amount like 1000000. 2) Higher α_L leads to higher TTD, a 0.002 m α_L gives best agreement with a black-box model TRANSEP. 3) Unlike the soil water content estimation, the scenario S2 of Fang et al. [2016] with global upscaling scheme has the best agreement with TRANSEP results, however, it fails to represent vertical movement of the water particles. On the other hand, the localized upscaling schemes S3 and S4, which have better SWC estimates, represent the vertical movement well. We can conclude that analysis TTD estimated using particle tracking codes like SLIM-FAST can support the evaluation of 3D hydrological models like Parflow-CLM with respect to the correct parametrization of hydrological properties and the representation of water flow pathways.

5.2 Outlook

Future studies should consider that, in addition to θ_s and K_s studied in this research, heterogeneous hydraulic parameters θ_r, van Genuchten α and n, need to be included in the

analysis in order to increase the model performance. Such information could be generated by 3-D inverse calibration, with availability of computational ability, or other indirect estimation methods such like pedotransfer functions. More measured data of the hydraulic parameters collected at Wüstebach site would also contribute to improve the models. Heterogeneity in meteorological forcing data and land surface parameters such like different types of vegetation is well worth investigating using ParFlow-CLM modeling system to explore the spatio-temporal variation of distribution of simulated actual evapotranspiration. More information of the fast lateral subsurface flow is needed to collect for a better understanding of water dynamic at Wüstebach catchment, which can help enhance the ParFlow-CLM to consider by-pass flow during infiltration, then a better agreement of the soil moisture simulation during dry periods could be achieved.

Higher resolution simulations (e.g. 1 m, 5 m) are also needed in future research to test our upscaling method in larger catchments and in different environmental settings with different terrain characteristics to strengthen our conclusion. In addition to EOFs and wavelet coherence analysis, development of other innovative validation methods are needed to provide better understanding of the spatio-temporal distribution of variation of estimated soil moisture and evapotranspiration.

An inverse calibration of dispersion parameters could also be included in future studies to better understand how water and other tracing particles migrate in pathways in soil and fracture medium. Large scale tracer experiments as well as transit time distribution estimates from other models are needed for comparison purpose.

With the realization of the above future work, we can build a comprehensive modeling system of monitoring, parametrization, simulation, and validation. This model system can be widely applied to different scales and resolutions of catchments, and different types of land surface, and to provide insight of a whole picture of atmospheric, surface and subsurface water dynamics and balance prediction.

Acknowledgements

This research was supported by Projects MIKLIP and TERENO. First I would like to thank Dr. Bogena, Dr. Kollet and Dr. Vereecken for funding me to work at Forschungszentrum Jülich and pursue my PhD degree at University of Bonn.

Here I would like to express my appreciation to my supervisor, Dr. Vereecken, and Dr. Bogena, who grants me the great opportunity to study and work with. Also they gives a lot of directs, advices and inspirations throughout my research, from the very beginning I entered the gate of Agrosphere Institute IBG-3, Forschungszentrum Jülich to the completion of this PhD dissertation.

Second I thank to Dr. Kollet who provides me the key simulation tool Parflow-CLM platform and a lot of guidance of modeling work. And I thank to all the experiment colleagues for their hard field work and kindly offer me all the data obtained from Wüstebach and Rur catchments I have used in my research. I also thank the Centre for High-Performance Scientific Computing in Terrestrial System, Geoverbund ABC/J for access of high performance supercomputer system JUROPA, JUQUEEN, and the clusters to run high resolution, large scale and long term simulations using Parflow-CLM model and the related post-processing scripts.This makes a perfect combination of modelling and observation data for me to work with throughout my three-year research at Forschungszentrum Jülich.

Then I want to say thanks to my colleagues and friends Wei, Sebastian, Alex, Michael, and Inge, who always give me kind helps to solve problems and confusions. I also want to thank my coauthors Julian, Bernd, Thomas, and Simon for the kind help and collaborate in my publications of high-quality papers in top research journal Journal of Hydrology.

Also I thank to my family and friends, especially my wife Nan Li, who always accompanies me in my three-year living and adventure in Europe. They give me the most important support and encouragement to me to face, pass and conquer failures and fractures.

Finally I thank to Professors Vereecken, Diekkrüger, Zumbroich, and Peterseim to become my PhD defense committee members and give me huge help on revising my writing and plenty of suggestions.

Without any of you I cannot complete this Dissertation, a billion of thanks!

References

Abbaspour, K.C., Schulin, R., van Genuchten, M.T., 2001. Estimating unsaturated soil parameters using ant colony optimization. Adv Water Resour, 24(8):827–841.

Allen, R.G., Pereira, L.S., Raes, D., Smith., M., 1998. Crop evapotranspiration: guidelines for computing crop water requirements Food and Agriculture Organization of the United Nations, Rome.

Ashby, S.F., Falgout, R.D., 1996. A parallel miltugrid preconditioned conjugate gradient algorithm for groundwater flow simulations. Nuclear Science and Engineering. 124(1), 145-159.

Bachmair, S., Weiler, M., 2012. Hillslope characteristics as controls of subsurface flow variability. Hydrol. Earth Syst. Sci. 16, 3699-3715.

Beier, C., Hansen, K., Gundersen, P., 1993. Spatial variability of through fall fluxes in a spruce forest. Environ. Pollut. 81, 257–267.

Bierkens, M.F.P., van den Hurk, B.J.J.M., 2007. Groundwater convergence as a possible mechanism for multi-year persistence in rainfall. Geophysical Research Letters. 34, L02402.

Binning, P., Celia, M.A., 2002. A forward particle tracking Eulerian–Lagrangian localized adjoint method for solution of the contaminant transport equation in three dimensions. Advances in Water Resources 25, 147–157.

Blume, T., Zehe, E., Bronstert, A., 2009. Use of soil moisture dynamics and patterns at different spatio-temporal scales for investigation of subsurface flow processes. Hydrol. Earth Syst. Sci. 13, 1215–1234.

Bogena, H.R., Diekkrüger, B., 2002. Modelling solute and sediment transport at different spatial and temporal scales. Earth Surface Processes and Landforms, 27 (13): 1475-1489.

Bogena, H.R., Huisman, J.A., Oberdörster, C., Vereecken, H., 2007. Evaluation of a low-cost soil moisture sensor for wireless network applications. J. Hydrol. 344, 32–42.

Bogena, H.R., Huisman, J.A., Meier, H., Rosenbaum, U., Weuthen A., 2009. Hybrid wireless underground sensor networks. Quantification of signal attenuation in soil. Vadose Zone J., 8(3), 755–761.

Bogena, H.R., Herbst, M., Huisman, J.A., Rosenbaum, U., Weuthen, A., Vereecken H., 2010. Potential of wireless sensor networks for measuring soil moisture variability. Vadose Zone J. 9(4), 1002–1013.

Bogena, H.R., Huisman, J.A., Baatz, R., Hendricks-Franssen, H.-J.,Vereecken, H., 2013. Accuracy of the cosmic-ray soil moisture probe in humid forest ecosystems: The worst case scenario. Water Resource Research. 49, 1-14.

Bogena, H.R., Bol, R., Borchard, N., Brüggemann, N., Diekkrüger, B., Drüe, C., Groh, J., Gottselig, N., Huisman, S.J., Lücke, A., Missong, A., Neuwirth, B., Pütz, T., Schmidt, M., Stockinger, M., Tappe, W., Weihermüller, L., Wiekenkamp I., Vereecken, H., 2015. A terrestrial observatory approach for the integrated investigation of the effects of deforestation on water, energy, and matter fluxes. Science China: Earth Sciences 58(1): 61-75.

Böhner, J., McCloy, K.R., Strobl, J., 2006. SAGA – Analysis and Modelling Applications. Göttinger Geographische Abhandlungen. Vol.115, 130pp.

Bonan G.B., et al., 2003. A dynamic global vegetation model for use with climate models: concepts and description of simulated vegetation dynamics. Global Change Biology 9: 1543–1566.

Bouten, W., Heimovaara, T.J., Tiktak, A., 1992. Spatial patterns of throughfall and soil water dynamics in a Douglas fir stand. Water Resour. Res. 28(12), 3227–3233.

Burbey, T.J., Zhang, M., 2015. Inverse modeling using PS-InSAR for improved calibration of hydraulic parameters and prediction of future subsidence for Las Vegas Valley, USA. Proc. IAHS, 372, 411–416.

Cadini, F., Bertoli, I., De Sanctis, J. Zio, E., 2012. A novel particle tracking scheme for modeling contaminant transport in a dual-continua fractured medium. Water Resour. Res., 48, W10517.

Castillo, V.M., Gomez-Plaza, A., Martinez-Mena, M., 2003. The role of antecedent soil water content in the runoff response of semiarid catchments: A simulation approach. Journal of Hydrology, 284, no. 1-4, 114-130.

Clark, M.P., Fan, Y., Lawrence, D.M., Adam, J.C., Bolster, D., Gochis, D.J., Hooper, R.P., Kumar, M., Leung, L.R., Mackay, D.S., Maxwell, R.M., Shen, C., Swenson, S.C., Zeng, ., 2015. Improving the representation of hydrologic processes in Earth System Models. Water Resour. Res. 51, doi:10.1002/2015WR017096.

Cornelissen, T., Diekkrüger, B., Bogena, H.R., 2014. Importance of a bedrock aquifer in the 3D simulation of discharge and soil moisture patterns at different spatial and temporal scales - The Wüstebach case study. J. Hydrol. 516: 140-153.

Dai, Y., Zeng, X., Dickinson, R.E., Baker, I., Bonan, G.B., Bosilovich, M.G., Denning, A.S., Dirmeyer, P.A., Houser, P.R., Niu, G., Oleson, K.W., Schlosser, C.A., Yang, Z.L. 2003. The Common Land Model. Bull. Amer. Meteor. Soc. 84:1013-1023.

de Rooij, R., Graham, W., Maxwell, R.M., 2013. A particle-tracking scheme for simulating pathlines in coupled surface-subsurface flows. Advances in Water Resources 52, 7–18.

Duan Q., Sorooshian, S., Gupta, V.K., 1994. Optimal use of the SCE-UA global optimization method for calibrating watershed models. Journal of Hydrology. 158, 265-284.

Etmann, M., 2009. Dendrologische Aufnahmen im Wassereinzugsgebiet Oberer Wüstebach anhand verschiedener Mess- und Schätzverfahren. Master thesis, 80 pp. Univ. of Münster.

Fang, Z., Bogena, H.R., Kollet, S.J., Koch, J., Vereecken, H., 2015. Spatio-temporal validation of long-term 3D hydrological simulations of a forested catchment using orthogonal functions and wavelet coherence analysis. Journal of Hydrology. 533, 234-249.

Fang, Z., Bogena, H.R., Kollet, S.J., Vereecken, H., 2016. Scale Dependent Parameterization of Soil Hydraulic Conductivity in 3D Simulation of Hydrological Processes in a Forested Headwater Catchment. Journal of Hydrology. 529, 1754-1767.

Feddes, R.A., Kowalik, P., Kolinska-Malinka, K., Zaradny, H., 1976. Simulation of field water uptake by plants using a soil water dependent root extraction function. J. Hydrol. 31, 13–26.

Gelhar, L.W., Welty, C., Rehfeldt, K.R., 1992. A Critical review of data on field-scale dispersion in aquifers. WATER RESOURCES RESEARCH, VOL.28, NO.7, 1955-1974.

Geza, M., McCray, J.E., 2008. Effects of soil data resolution on SWAT model stream flow and water quality predictions. Journal of Environmental Management. 88(3), 393–406.

Ghasemizade M., Schirmer, M., 2013. Subsurface flow contribution in the hydrological cycle: lessons learned and challenges ahead—a review. Environ Earth Sci. 69, 707–718.

Goode, D.J., 1990. Particle velocity interpolation in block-centered finite difference groundwater flow models. WATER RESOURCES RESEARCH, VOL. 26, NO. 5, 925-940.

Graf, A., Bogena, H.R., Drüe, C., Hardelauf, H., Pütz, T., Heinemann, G., Vereecken H., 2014. Spatiotemporal relations between water budget components and soil moisture in a forested tributary catchment. Water Resour. Res. 50, 4837-4854.

Grayson, R.B., Blöschl, G., 2000. Spatial Patterns in Catchment Hydrology. Observations and Modelling. Cambridge Univ. Press, Cambridge, pp. 406.

Grayson, R.B., Western, A.W., Chiew, F., Blöschl, G., 1997. Preferred states in spatial soil moisture patterns: Local and nonlocal controls. Water Resour. Res. 33(12), 2897–2908.

Green, C.T., Zhang, Y., Jurgens, B.C., Starn, J.J., Landon, M.K., 2014. Accuracy of travel time distribution (TTD) models as affected by TTD complexity, observation errors, and model and tracer selection. Water Resour. Res., 50, 6191–6213.

Groffman, P.M., Williams, C.O., Pouyat, R.V., Band, L.E., Yesilonis, I., 2009. Nitrate leaching and nitrous oxide flux in urban forests and grasslands. Journal of Environmental Quality. 38, 1848-1860.

Gulden, L.E. et al., 2007. Improving land-surface model hydrology: Is an explicit aquifer model better than a deeper soil profile? Geophysical Research Letters. 34(9).

Hannachi, A., Jolliffe, I.T., Stephenson, D.B., 2007, Empirical orthogonal functions and related techniques in atmospheric science: A review, Int. J. Climatol., 27, 1119–1152.

Harbaugh, A.W., 2005, MODFLOW-2005, the U.S. Geological Survey modular ground-water model -- the Ground-Water Flow Process: U.S. Geological Survey Techniques and Methods 6-A16.

Herbst, M. Diekkrüger, B., 2003. Modelling the spatial variability of soil moisture in a micro-scale catchment and comparison with field data using geostatistics. Phys. Chem. Earth. 28, 239–245.

Hopp, L., McDonnell, J.J., 2009. Connectivity at the hillslope scale: Identifying interactions between storm size, bedrock permeability, slope angle and soil depth. Journal of Hydrology, 376(3–4), 378-391.

Hopp, L., McDonnell, J., Condon, P., 2011. Lateral Subsurface Flow in a Soil Cover over Waste Rock in a Humid Temperate Environment. Vadose Zone J. 10 doi:10.2136/vzj2010.0094.

Hughson, D.L., Yeh T.-C.J., 2000. An iterative model for three dimensional flow in variably saturated porous media. Water Resour. Res., 36(4), 829– 840.

Jawson, S.D., Niemann, J.D., 2007, Spatial patterns from EOF analysis of soil moisture at a large scale and their dependence on soil, land-use, and topographic properties, Adv. Water Resour., 30, 366–381.

Jost, G., Heuvelink, G.B.M., Papritz, A., 2005. Analysing the space-time distribution of soil water storage of a forest ecosystemusing spatio-temporal kriging. Geoderma. 128, 258–273.

Kim, G., Barros, A.P., 2002, Space–time characterization of soil moisture from passive microwave remotely sensed imagery and ancillary data, Remote Sens. Environ., 81, 93–403.

Koch, J., Jensen, K.H., Stisen, S., 2015. Toward a true spatial model evaluation in distributed hydrological modeling: Kappa statistics, Fuzzy theory, and EOF-analysis benchmarked by the human perception and evaluated against a modeling case study. Water Resources Research.

Kollet, S. Maxwell, R.M., 2008. Capturing the influence of groundwater dynamics on land surface processes using an integrated, distributed watershed model. Water Resources Research. 44, W02402.

Kollet, S.J., Maxwell, R.M., 2008. Demonstrating fractal scaling of baseflow residence time distributions using a fully-coupled groundwater and land surface model. GEOPHYSICAL RESEARCH LETTERS, VOL. 35, L07402.

Kollet, S.J., Maxwell, R.M., Woodward, C.S., Smith, S., Vanderborght, J., Vereecken, H., Simmer, C., 2010. Proof-of-concept of regional scale hydrologic simulations at hydrologic resolution utilizing massively parallel computer resources. Water Resour. Res. 46, W04201.

Krebs, P., Stocker, M., Pezzatti, G.B., Conedera, M., 2015, An alternative approach to transverse and profile terrain curvature, International Journal of Geographical Information Science, 643-666.

Krzeminska, D., Bogaard, T.A., van Asch, T.W., van Beek, L.P.H., 2012. A conceptual model of the hydrological influence of fissures on landslide activity. Hydrol. Earth Syst. Sci. 16, 1561–1576.

Kuo, W.L., Steenhuis, T.S., McCulloch, C.E., Mohler, C.L., Weinstein, D.A., DeGloria, S.D., Swaney, D.P., 1999. Effect of grid size on runoff and soil moisture for a variable-source-area hydrology model. Water Resour. Res. 35, 3419– 3428.

Lawrence, J. E., Hornberger, G.M., 2007. Soil moisture variability across climate zones, Geophys. Res. Lett. 34, L20402.

Lauzon, N., Anctil, F., Petrinovic, J., 2004. Characterization of soil moisture conditions at temporal scales from a few days to annual. Hydrol. Processes. 18, 3235–3254.

Lee, S., Wolberg, G., Shin, S.Y., 1997. Scattered data interpolation with multilevel B-Splines. IEEE Transactions on Visualisation and Computer Graphics. Vol.3, No.3.

Li, B., Yeh, T.-C.J, 1999. Cokriging estimation of the conductivity field under variably saturated flow conditions. Water Resour. Res., 35 (12), 3663-3674.

Lichtner, P.C., Hammond, G.E., Lu, C., Karra, S., Bisht, G., Andre, B., Mills, R., Kumar J., 2015. PFLOTRAN User Manual.

Lin, H., 2006. Temporal stability of soil moisture spatial pattern and subsurface preferential flow pathways in the Shale Hills Catchment. Vadose Zone J. 5, 317–340.

Liu, S.Y., Yeh, T.-C.J., 2004. An integrative approach for monitoring water movement in the vadose zone. Vadose Zone Journal, Vol. 3(2), p 681-692.

Liu, Y., 2003, Spatial patterns of soil moisture connected to monthly-seasonal precipitation variability in a monsoon region, J. Geophys. Res., 108(D22), 8856, doi:10.1029/2002JD003124.

Manzoni, S., Katul, G.G., Porporato, A., 2009. Analysis of soil carbon transit times and age distributions using network theories. JOURNAL OF GEOPHYSICAL RESEARCH, VOL. 114, G04025.

Mascaro, G., Vivoni, E.R., Méndez-Barroso, L.A., 2015, Hyperresolution hydrologic modeling in a regional watershed and its interpretation using empirical orthogonal functions,

Advances in Water Resources, ISSN 0309-1708, http://dx.doi.org/10.1016/j.advwatres.2015.05.023.

Mauder, M., Desjardins, R.L., Oncley, S.P., MacPherson, I., 2007.Atmospheric response to a partial solar eclipse over a cotton field in central California. J. Appl. Meteorol. Climatol. 46, 1792–1803.

Maxwell, R.M., Kollet, S.J., 2008. Interdependence of groundwater dynamics and land-energy feedbacks under climate change. Nature Geoscience. 1(10), 665-669.

Maxwell, R.M., Kollet, S.J., 2008. Quantifying the effects of three-dimensional subsurface heterogeneity on Hortonian runoff processes using a coupled numerical, stochastic approach. Adv. Water Resour. 31, 807–817.

Maxwell, R.M., 2010. SLIM-FAST: A User's Manual V.4. GWMI 2010-01, 49 p.Chou, P.Y., Wyseure, G., 2009. Hydrodynamic dispersion characteristics of lateral inflow into a river tested by a laboratory model. Hydrol. Earth Syst. Sci., 13, 217–228, 2009.

Maxwell, R.M., Kollet, S.J., Smith, S.G., Woodward, C.S., Falgout, R.D., Ferguson, I.M., Engdahl, N., Condon, L.E., Lopez, S.R., Gilbert, J., Bearup, L., Jefferson, J., Prubilick, C., Baldwin, C., Bosl, W.J., Hornung, R., Ashby, S., 2014. ParFlow User's Manual. Integrated GroundWater Modeling Center Report GWMI 2014-01, 159p.

Mendicino, G., Sole, A., 1997. The information content theory for the estimation of the topographic index distribution used in TOPMODEL. Hydrol. Processes. 11, 1099– 1114.

Nash, J.E., Sutcliffe, J.V., 1970. River flow forecasting through conceptual models. Part I: A discussion of principles. J. Hydrol, 125, 277-291.

Niedda, M., 2004. Upscaling hydraulic conductivity by means of entropy of terrain curvature representation. Water Resources Research. 40, W04206.

Niu, G.Y., Yang, Z.L., Dickinson, R.E., Gulden, L.E., Su, H., 2007. Development of a simple groundwater model for use in climate models and evaluation with Gravity Recovery and Climate Experiment data. Journal of Geophysical Research-Atmospheres. 112(D7).

Parent, A.C., Anctil, F.,Parent, L.E., 2006. Characterization of temporal variability in near-surface soil moisture at scales from 1 h to 2 weeks. J. Hydrol. 325, 56–66.

Peckham, S.D., 2003. Mathematical modeling of landforms: Optimality and steady-state solutions. In: Concepts and Modelling in Geomorphology: International Perspectives, Eds. Evans, I.S., Dikau, R., Tokunaga, E., Ohmori, H. and Hirano, M., 167-182.

Perfect, E., Sukop, M.C., Haszler, G.R., 2002. Prediction of dispersivity for undisturbed soil columns from water retention parameters. Soil Sci. Soc. Am. J. 66:696–701.

Perry, M.A., Niemann, J.D., 2008. Generation of soil moisture patterns at the catchment scale by EOF interpolation. Hydrol. Earth Syst. Sci. 12, 39-53.

Qu, W., Bogena, H.R., Huisman, J.A., Martinez, G., Pachepsky, Y.A., Vereecken, H., 2014. Effects of soil hydraulic properties on the spatial variability of soil moisture: evidence from sensor network data and inverse modeling. Vadose Zone J. doi:10.2136/vzj2014.07.0099.

Rahman, M., Sulis, M., Kollet, S.J., 2014. The concept of dual-boundary forcing in land surface-subsurface interactions of the terrestrial hydrological and energy cycles. Water Resources Research. doi:10.1002/2014WR015738.

Rezaei Arshad, R., Sayyad, G., Mosaddeghi, M., Gharabaghi, B., 2013. Predicting saturated hydraulic conductivity by artificial intelligence and regression models. ISRN Soil Science, vol. Article ID 308159.

Richter, D.,1995. Ergebnisse methodischer Untersuchungen zur Korrektur des systematische Mesfehlers des Hellmann-Niederschlagmessers. in Berichte des Deutschen Wetterdienstes. 194, Lysimeter Research Group, Selbstverlag des Deutschen Wetterdienstes, Offenbach am Main, Germany. pp. 93.

Richter, F., 2008. Bodenkarte zur Standorterkundung. Verfahren Quellgebiet Wüstebachtal (Forst), Geol. Dienst Nordrhein-Westfalen, Krefeld, Germany.

Rosenbaum, U., Huisman, J.A., Weuthen, A., Vereecken, H., Bogena, H.R., 2010. Sensor-to-sensor variability of the ECH2O EC-5, TE, and 5TE sensors in dielectric liquids. Vadose Zone J. 9, 181–186.

Rosenbaum, U., Huisman, J.A., Vrba, J., Vereecken, H., Bogena, H.R., 2011. Correction of temperature and electrical conductivity effects on dielectric permittivity measurements with ECH2O sensors. Vadose Zone J. 10, 582–593.

Rosenbaum, U., Bogena, H.R., Herbst, M., Huisman, J.A., Peterson, T.J., Weuthen, A., Western, A.W., Vereecken, H., 2012. Seasonal and event dynamics of spatial soil moisture patterns at the small catchment scale. Water Resour. Res. 48, W10544.

Salamon, P., Fernandez-Garcia, D., Gomez-Hernandez, J.J., 2006. A numerical assessment of the random walk particle tracking method for heterogeneous aquifers. IAHS Publ. 304.

Schaap, M., Bouten, W., Verstraten, J.,1997. Forest floor moisture dynamics in a Douglas fir stand. Journal of hydrology. 201, 367-383.

Schaap, M.G., Leij, F.J., van Genuchten, M.T., 2001. ROSETTA: a computer program for estimating soil hydraulic parameters with hierarchical pedotransfer functions. Journal of Hydrology, Volume 251, Issues 3–4, 1, 163–176.

Schaefli, B., Zehe, E., 2009. Hydrological model performance and parameter estimation in the wavelet-domain. Hydrol. Earth Syst. Sci. 13, 1921-1936.

Schulze-Makuch, D., 2005. Longitudinal dispersivity data and implications for scaling behavior. GROUND WATER 43, no. 3: 443–456.

Schmidt, R., Petrovic, S., Güntner, A., Barthelmes, F., Wünsch, J., Kusche, J., 2008,Periodic components of water storage changes from GRACE and global hydrology models, J. Geophys. Res., 113, B08419, doi:10.1029/2007JB005363.

Schöniger, M., Sommerhäuser, M., Herrmann, A., 1997. Modeling flow and transport process in fracture rock groundwater system in a mall basin scale, Hard Rock Hydrosystems. IAHS Publ. No. 241.

Seneviratne, S.I., Corti, T., Davin, E.L., Hirschi, M., Jaeger, E.B., Lehner, I., Orlowsky, B., Teuling, A.J., 2010. Investigating soil moisture-climate interactions in a changing climate: A review. Earth-Science Reviews, v. 99, no. 3-4, p. 125-161.

Si, B.C. 2008. Spatial scaling analyses of soil physical properties: A review of spectral and wavelet methods. Vadose Zone J. 7, 547–562.

Simmer, C., Thiele-Eich, I., Masbou, M., Amelung, W., Bogena, H.R., Crewell, S., Diekkrüger, B., Ewert, F., Hendricks Franssen, H.-J., Huisman, J.A., Kemna, A., Klitzsch, N., Kollet, S., Langensiepen, M., Löhnert, U., Rahman, A.S.M.M., Rascher, U., Schneider, K., Schween, J., Shao, Y., Shrestha, P., Stiebler, M., Sulis, M., Vanderborght, J., Vereecken, H., Kruk, J., Waldhoff, G., Zerenner, T., 2015. Monitoring and Modeling the Terrestrial System from Pores to Catchments - the Transregional Collaborative Research Center on Patterns in the Soil-Vegetation-Atmosphere System. Bull. Amer. Meteor. Soc. 96: 1765-1787.

Simunek, J., van Genuchten, M.T., 1996. Parameter estimation of soil hydraulic properties from the tension disc infiltrometer experiment by numerical inversion. Water Resour. Res. 32 [9], 2683-2696.

Simunek, J., Jarvis, N.J., van Genuchten, M.T., Gardenas, A., 2003. Review and comparison of models for describing non-equilibrium and preferential flow and transport in the vadose zone. J. Hydrol. 272, 14–35.

Simunek J., van Genuchten M.T., 2008. Modeling nonequilibrium flow and transport processes using HYDRUS. Vadose Zone Journal.7(2), 782-797.

Simunek, J., van Genuchten, M.T., Sejna, M., 2012. The HYDRUS software package for simulating the two- and three-dimensional movement of water, heat, and multiple solutes in variably-saturated porous media technical manual version 2.0.

Singh, V.P., 1997. The use of entropy in hydrology and water resources. Hydrol. Processes. 11, 587– 626.

Smith, S.K., Franti, T.G., Comfort, S.D., 2002. Impact of initial soil water content, crop residue cover, and post-herbicide irrigation on herbicide runoff. Transactions of the ASAE, v. 45, no. 6, p. 1817-1824.

Stockinger, M.P., Bogena, H.R., Lücke, A., Diekkrüger, D., Weiler, M., Vereecken, H., 2014. Seasonal soil moisture patterns: controlling transit time distributions in a forested headwater catchment, Water Resour. Res., 50, 5270–5289.

Sudduth, K.A., Drummond, S.T., and Kitchen, N.R., 2001. Accuracy issues in electromagnetic induction sensing of soil electrical conductivity for precision agriculture. Computers and Electronics in Agriculture, v. 31, no. 3, p. 239-264.

Suk, H., 2012. Practical implementation of new particle tracking method to the real field of groundwater flow and transport. ENVIRONMENTAL ENGINEERING SCIENCE, Volume 29, Number 1.

Syed, T.H., Lakshmi, V., Paleologos, E., Lohmann, D., Mitchell, K., Famiglietti, J.S.,2004, Analysis of process controls in land surface hydrological cycle over the continental United States, J. Geophys. Res., 109, D22105.

Tang, K.M., McGinnis, D.F., Frindte, K., Brüchert, V., Grossart, H.P., 2014. Paradox reconsidered: Methane oversaturation in well-oxygenated lake waters. Limnol. Oceanogr. 59, 275–284.

Therrien, R., McLaren, R.G., Sudicky, E.A., Panday, S.M., 2010. HydroGeoSphere. A Three-dimensional Numerical Model Describing Fully-integrated Subsurface and Surface Flow and Solute Transport. Waterloo, ON, Canada.

Torrence, C., Compo, G.P., 1998. A practical guide to wavelet analysis, Bull. Am. Meteorol. Soc. 79, 61–78.

TERENO, 2011. Forschungszentrum Jülich, Jülich, Germny. Available at http://teodoor.icg.kfa-juelich.de/, verified 9 Oct. 2012.

Teuling, A.J., Troch, P.A., 2005 Improved understanding of soil moisture variability dynamics. Geophys. Res. Lett. 32, L05404.

Teuling, A.J., Hupet, F., Uilenhoet, R., Troch, P., 2007. Climate variability effects on spatial soil moisture dynamics, Geophys. Res. Lett. 34, L06406.

Tromp-van Meerveld, H.J., McDonnell, J.J., 2006. Threshold relations in subsurface stormflow 2: The fill and spill hypothesis. Water Resources Research 42, W02411.

Uchida, T., Tromp-van Meerveld, I., McDonnell, J.J., 2005. The role of lateral pipe flow in hillslope runoff response: an intercomparison of non-linear hillslope response. Journal of Hydrology. 311(1–4), 117-133.

van Genuchten, M.T., 1980. A closed-form equation for predicting the hydraulic conductivity of unsaturated soils. Soil Sci. Soc. Am. J. 44: 892–898.

Vanderborght, J., Vereecken, H., 2007. Review of dispersivities for transport modeling in soils. Vadose Zone Journal 6:29–52.

Vargas, R., Detto, M., Baldocchi, D.D., Allen, M.F., 2010. Multiscale analysis of temporal variability of soil CO2 production as influenced by weather and vegetation. Glob. Change Biol. 16, 1589–1605.

Venema, V., Schomburg, A., Ament, F., Simmer, C., 2007. Two adaptive radiative transfer schemes for numerical weather prediction models. Atmospheric Chemistry and Physics. 7, 5659-5674.

Vereecken, H., Kamai, T., Harter, T., Kasteel, R., Hopmans, J., Vanderborght, J., 2007. Explaining soil moisture variability as a function of mean soil moisture, A stochastic unsaturated flow perspective. Geophys. Res. Lett. 34, L22402.

Vereecken, H., Huisman, J.A., Bogena, H.R., Vanderborght, J., Vrugt, J.A., Hopmans, J.W., 2008. On the value of soil moisture measurements in vadose zone hydrology. A review. Water Resour. Res. 44, W00D06.

Vereecken, H., Kollet S.J., Simmer C., 2010. Patterns in soil vegetation atmosphere systems: monitoring, modeling, and data assimilation. Vadose Zone J. 9, 821-827.

Vieux, B.E., 1993. Aggregation and smoothing effects on surface runoff modeling. J. Comput. Civ. Eng. 7, 310– 338.

Vivoni, E.R., Rodriguez, J.C., Watts, C.J., 2010. On the spatiotemporal variability of soil moisture and evapotranspiration in a mountainous basin within the North American monsoon region. Water Resour. Res. 46, W02509.

Vrugt, J.A., Gupta, H.V., Bouten, W., Sorooshian, S., 2003. A Shuffled Complex Evolution Metropolis algorithm for optimization and uncertainty assessment of hydrologic model parameters. Water Resour. Res. 39(8), 1201.

Wang, W., Neuman, S.P., Yao, T., Wierenga, P. J., 2003. Simulation of large-scale field infiltration experiments using a hierarchy of models based on public, generic, and site data. Vadose Zone J., 2, 297-312.

Ward, A.L., Conrad, M.E., Keller, M.J., Daily, W.D., Majer, E.L., Fink, J.B., Murray, C.J., Freedman, V.L., White, M.D., Gee, G.W., Yabusaki, S.B., Hoverston, G.M., Zhang, Z.F.,

2006. Vadose zone transport field study summary report. PNNL-15543, Pacific Northwest National Laboratory, Richland, WA.

Ward, A.L., Zhang, Z.F., Gee, G.W, 2006. Upscaling unsaturated hydraulic parameters for flow through heterogeneous, anisotropic sediments. Adv. Water Resour., 29 (2), 268-280.

Weiler, M., 2005. An infiltration model based on flow variability in macropores: Development, sensitivity analysis and applications. J. Hydrol. 310, 294–315.

Weiler, M., McDonnell, J.J., 2007. Conceptualizing lateral preferential flow and flow networks and simulating the effects on gauged and ungauged hillslopes. Water Resources Research. 43, W03403.

Western, A.W., Blöschl, G., 1999. On spatial scaling of soil moisture. J. Hydrol. 217, 203–224.

White, M.D., Oostrom, M., 2006. STOMP Subsurface Transport Over Multiple Phases Version 4.0 User's Guide.

Wiekenkamp, I., Huisman, J.A., Bogena, H., Lin, H., Vereecken, H., 2016. Spatial and temporal occurrence of preferential flow at the catchment scale. J. Hydrol. 534, 139–149.

Wood, E.F., et al., 2011. Hyper-resolution global land surface modeling: Meeting a grand challenge for monitoring Earth's terrestrial water. Water Resour. Res. 47, W05301.

Ye, X., Zhang, Q., Viney, N.R., 2010. The effect of soil data resolution on hydrological processes modelling in a large humid watershed. Hydrological Processes. 130–140.

Yu, X., Duffy, C., Baldwin, D.C., Lin, H., 2014. The role of macropores and multi-resolution soil survey datasets for distributed surface–subsurface flow modeling. J. Hydrol. 516, 97–106.

Zacharias, S., Bogena, H., Samaniego, L., Mauder, M., Fuß, R., Pütz, T., Frenzel, M., Schwank, M., Baessler, C., Butterbach-Bahl, K., Bens, O., Borg, E., Brauer, A., Dietrich, P., Hajnsek, I., Helle, G., Kiese, R., Kunstmann, H., Klotz, S., Munch, J. C., Papen, H., Priesack, E., Schmid, H. P., Steinbrecher, R., Rosenbaum, U., Teutsch, G., Vereecken, H., 2011. A

network of terrestrial environmental observatories in Germany. Vadose Zone Journal. 10(3), 955-973.

Zhang, B., Tang, J., Gao, C., Zepp, H., 2011. Subsurface lateral flow from hillslope and its contribution to nitrate loading in streams through an agricultural catchment during subtropical rainstorm events. Hydrol. Earth Syst. Sci. 15, 3153–3170.

Zhang, N.Q., Wang, M.H., Wang, N., 2002. Precision agriculture - a worldwide overview. Computers and Electronics in Agriculture, v. 36, no. 2-3, p. 113-132.

Zhang, Z.F., Ward, A.L., Gee, G.W., 2004. A combined parameter scaling and inverse technique to upscale the unsaturated hydraulic parameters for heterogeneous soils. Water Resour. Res. W08306.

Zhu, J., Mohanty, B.P., 2002. Upscaling of soil hydraulic properties for steady state evaporation and infiltration. Water Resour. Res., 38(9), 1178,Woolfenden, L.R., Ginn, T.R,, 2009. Modeled ground water age distributions. GROUND WATER, Vol. 47, No. 4, 547–557.

Publications

Fang, Z., Stockinger, M., Vereecken, H., Bogena, H., 2016. Evaluation of 3D Model Parameterizations Using Water Transit Time Distributions. Journal of Hydrology.

Wiekenkamp, I., **Fang, Z.**, Koch, J., Bogena, H., Huisman, J.A., Kollet, S., Vereecken, H., 2016. Exploring Effects of Deforestation on Wüstebach Catchment Using Large-scale Long-term 3D Simulation. Journal of Hydrology.

Fang, Z., Bogena, H., Kollet, S., Vereecken, H., 2016. Scale Dependent Parameterization of Soil Hydraulic Conductivity in 3D Simulation of Hydrological Processes in a Forested Headwater Catchment. Journal of Hydrology. 536, 365-375.

Koch, J., Cornelissen, T., **Fang, Z.**, Bogena, H., Diekkrüger, B., Kollet, S., Stisen, S., 2016. Inter-comparison of Three Distributed Hydrological Models with Respect to the Seasonal Variability of Soil Moisture Patterns at a Small Forested Catchment. Journal of Hydrology. 533, 234-249.

Fang, Z., Bogena, H., Kollet, S., Koch, J., Vereecken, H., 2015. Spatio-temporal Validation of Long-term 3D Hydrological Simulations of a Forested Catchment Using Orthogonal Functions and Wavelet Coherence Analysis. Journal of Hydrology. 529, 1754-1767.

Hou, Z., Bacon, D., Engel, D., Lin, G., Fang, Y., Ren, H., **Fang, Z.**, 2014. Uncertainty Analyses of CO2 Plume Expansion Subsequent to Wellbore CO2 Leakage into Aquifers. International Journal of Greenhouse Gas Control. 27: 69–80.

Fang, Z., Hou, Z., Lin, G., Engel, D., Fang, Y., Eslinger, P., 2014. Exploring Effects of Data Quality, Data Worth, and Redundancy of CO2 Saturation Data on Injection Reservoir Characterization through PEST Inversion. Environmental Earth Sciences. 71(7):3025-3037.

Huang, M., Hou, Z., Leung, R., Ke, Y., Liu, Y., **Fang, Z.**, Sun, Y., 2013. Uncertainty Analysis of Runoff Simulations and Parameter Identifiability in the Community Land Model - Evidence from MOPEX Basins. Journal of Hydrometeorology. 14, 1754–1772.

Hou, Z., Engel, D., Lin, G., Fang, Y., **Fang, Z.**, 2013. An Uncertainty Quantification Framework for Studying the Effect of Spatial Heterogeneity in Reservoir Permeability on CO2 Sequestration. Mathematical Geosciences. 45(7):799-817.

Yao, T., Wierenga, P., Neuman, S., Post, D., **Fang, Z.**, Hovland, L., 2009. NSF Report of project Data Source and Data Quality Effects on Vadose Zone Transport Modeling. Award ID: 0440311